

2007

LIBRARY
Michigan State
University

This is to certify that the
thesis entitled

MODELING TRAVEL TIME IN URBAN ARTERIAL
NETWORKS WITH TIME-VARIANT TURNING MOVEMENTS
USING STATE-SPACE NEURAL NETWORKS

presented by

Timothy Joseph Likens

has been accepted towards fulfillment
of the requirements for the

M.S. degree in Civil Engineering



Major Professor's Signature

8/3/2007

Date

PLACE IN RETURN BOX to remove this checkout from your record.
TO AVOID FINES return on or before date due.
MAY BE RECALLED with earlier due date if requested.

DATE DUE	DATE DUE	DATE DUE

**MODELING TRAVEL TIME IN URBAN ARTERIAL NETWORKS WITH TIME-
VARIANT TURNING MOVEMENTS USING STATE-SPACE NEURAL
NETWORKS**

By

Timothy Joseph Likens

A THESIS

**Submitted to
Michigan State University
in partial fulfillment of the requirements
for the degree of**

MASTER OF SCIENCE

Department of Civil Engineering

2007

ABSTRACT

MODELING TRAVEL TIME IN URBAN ARTERIAL NETWORKS WITH TIME-VARIANT TURNING MOVEMENTS USING STATE-SPACE NEURAL NETWORKS

By

Timothy Joseph Likens

Advanced Traffic Management Systems (ATMS) and Advanced Traveler Information Systems (ATIS) have become integral components in congestion mitigation strategies, and are dependent on the ability to reliably estimate and predict travel time. Urban arterial networks are highly complex and dynamic systems for which travel time has been difficult to accurately model. This is in part due to the impact of turning movements at signalized intersections on traffic flow, and thus travel time. State-Space Neural Network (SSNN) models are developed in this thesis to estimate and predict travel time on arterial links and routes within an arterial network. Separate models are developed respective to through, right-turn, and left-turn vehicle movements. The data used to model travel time include variables that are easily collected in the field using existing surveillance infrastructure such as queue length, flow rate, and average speed. The inclusion of variable turning movements in the modeling procedure is observed to have a significant impact on the accuracy of SSNN models developed to estimate and predict travel time, especially for the right-turn movement.

Keywords: Travel Time Prediction, State-Space Neural Networks, Turning Movements, Urban Arterial Networks.

Dedicated to Grandma Hojnowski and Grandma Likens, who could not be here to read
the final page.

ACKNOWLEDGEMENTS

I must first thank my fiancée Rebecca Peters for her love and devotion despite the countless number of days I had to spend away from her in pursuit of my Master's Degree. Her support carried me through some long nights, and motivated me to leap hurdles along the way. I am also forever gracious to my parents Terry and Jean Likens. The endless sacrifices they have made for my brother Jeff and I have enabled us to do achieve great things. May the work we do now pay our debts to them in the form of pride and joy.

I would also like to thank my advisor, Dr. Ghassan Abu-Lebdeh. His continuing guidance helped me not only to complete this thesis, but also to challenge myself in terms of my career aspirations. As my goals evolved throughout the course of the Master's program, Dr. Abu-Lebdeh was consistently supportive. I wish to also acknowledge Dr. François Dion for the education he provided in the classroom. He taught me a great deal about modeling and simulation that I will carry with me into my professional career.

Finally, I am greatly appreciative of the support Dr. Rick Lyles gave in bringing me back to Michigan State University. He has been my mentor at MSU, and his class gave me my first interest in Transportation Engineering. Dr. Lyles recognized my desire to teach, and I cannot thank him enough for having me as his Teaching Assistant. I thank him for placing trust in me to be a part of his classroom, and I will miss being able to drop by his office for what was always an interesting conversation.

Timothy J. Likens

Michigan State University, 2007

TABLE OF CONTENTS

LIST OF TABLES	vii
LIST OF FIGURES	viii
INTRODUCTION	1
CHAPTER 1 – LITERATURE REVIEW	5
1.1 Travel Time Estimation and Prediction	6
1.2 Travel Time Reliability	7
1.3 State-Space Neural Network Application	8
1.4 Conclusions Based on Related Literature	9
CHAPTER 2 – PROBLEM STATEMENT AND RESEARCH OBJECTIVE	10
2.1 Background and Definitions	11
2.2 Average Travel Time Estimation versus Prediction	14
2.3 Formulation for Average Travel Time Estimation and Short-Term Prediction Models	16
2.4 Factors Impacting Average Travel Time Estimation and Short-Term Prediction	22
2.5 Modeling Approach for Travel Time Estimation and Short-Term Prediction	24
CHAPTER 3 – EXPERIMENTAL SET-UP	27
3.1 Overview of VISSIM Microscopic Simulation	28
3.2 Static Network Elements	29
3.3 Stochastic Network Elements	31
3.4 Time-Dependent Network Elements	32
3.5 Signalized Intersection Control Design Using Synchro	36
3.6 Data Collection from VISSIM Simulation	37
3.7 VISSIM Simulation Runs and Model Validation	39
CHAPTER 4 – MULTIVARIATE LINEAR REGRESSION FOR AVERAGE LINK SPEED ESTIMATION	40
4.1 Multivariate Linear Regression Methodology	40
4.2 Linear Regression Models for Link Speed Estimation	44
4.3 Average Speed Estimation for Major Arterials	45
4.4 Average Speed Estimation for Minor Arterials	52

CHAPTER 5 – STATE-SPACE NEURAL NETWORK MODELING METHODOLOGY	59
5.1 State-Space Neural Networks	60
5.2 State-Space Neural Network Topology	61
5.2.1 SSNN Topology for Travel Time Estimation	62
5.2.2 SSNN Topology for Travel Time Prediction	62
5.3 State-Space Neural Network Training and Testing	65
5.4 Application of State-Space Neural Network Models to Travel Time Estimation and Prediction for Arterial Routes	68
CHAPTER 6 – RESULTS AND DISCUSSION	70
6.1 Measures of Effectiveness	70
6.2 Travel Time Estimation on Arterial Links	73
6.2.1 Results of SSNN Travel Time Estimation Model for Through Movement	74
6.2.2 Results of SSNN Travel Time Estimation Model for Left-Turn Movement	76
6.2.3 Results of SSNN Travel Time Estimation Model for Right-Turn Movement	79
6.3 Travel Time Prediction on Arterial Links	83
6.3.1 Results of SSNN Travel Time Prediction Model for Through Movement	84
6.3.2 Results of SSNN Travel Time Prediction Model for Left-Turn Movement	97
6.3.3 Results of SSNN Travel Time Prediction Model for Right-Turn Movement	109
6.4 Travel Time Prediction on Arterial Routes	121
6.4.1 Results of SSNN Travel Time Prediction Models for Arterial Route 16-25	122
6.4.2 Results of SSNN Travel Time Prediction Models for Arterial Route 16-3	125
6.4.3 Results of SSNN Travel Time Prediction Models for Arterial Route 15-2	128
CHAPTER 7 – CONCLUSIONS AND FUTURE RESEARCH	132
7.1 Key Findings and Conclusions	132
7.2 Limitations	135
7.3 Scope of Future Research	136
APPENDIX	137
REFERENCES	141

LIST OF TABLES

Table 2.1 – Variables Considered for Travel Time Estimation and Short-Term Prediction	24
Table 4.1 – Candidate Independent Variables for Multivariate Linear Regression	42
Table 5.1 – Input and Output Variables for SSNN Travel Time Estimation Models.....	66
Table 5.2 – Input and Output Variables for SSNN Travel Time Prediction Models	67
Table 6.1 – Travel Time Estimation Error Statistics for the Through Movement	76
Table 6.2 – Travel Time Estimation Error Statistics for the Left-Turn Movement	78
Table 6.3 – Travel Time Estimation Error Statistics for the Right-Turn Movement	81
Table 6.4 – Mean Absolute Percentage Error Comparison Under Constant and Variable Turning Movement Percentage Conditions	82
Table 6.5 – Travel Time Prediction Error Statistics for the Through Movement	86
Table 6.6 – Mean Absolute Percentage Error Comparison for Through Movement Under Constant and Variable Turning Movement Percentage Conditions	96
Table 6.7 – Travel Time Prediction Error Statistics for the Left-Turn Movement	99
Table 6.8 – Mean Absolute Percentage Error Comparison for Left-Turn Movement Under Constant and Variable Turning Movement Percentage Conditions	108
Table 6.9 – Travel Time Prediction Error Statistics for the Right-Turn Movement	111
Table 6.10 – Mean Absolute Percentage Error Comparison for Right-Turn Movement Under Constant and Variable Turning Movement Percentage Conditions	120

LIST OF FIGURES

Figure 2.1 – Time-Space Domain for the Formulation of Average Travel Time Estimation and Short-term Prediction	21
Figure 2.2 – Flowchart of Modeling Approach for Travel Time Estimation and Short-Term Prediction	26
Figure 3.1 – Urban Arterial Network Designed in VISSIM for Travel Time Estimation and Prediction	30
Figure 3.2 – Average Flow Rate Distributions at Entry Points of Arterials	33
Figure 3.3 – Left-Turn Profiles for Signalized Intersection Approaches	35
Figure 3.4 – Right-Turn Profiles for Signalized Intersection Approaches	35
Figure 3.5 – Typical Signal Timing Plan for Signalized Intersections	37
Figure 4.1 – Training Plot for Normalized Actual Average Speed versus Normalized Estimated Average Speed for Through Movement on Major Arterials	47
Figure 4.2 – Testing Plot for Normalized Actual Average Speed versus Normalized Estimated Average Speed for Through Movement on Major Arterials	47
Figure 4.3 – Training Plot for Normalized Actual Average Speed versus Normalized Estimated Average Speed for Left-Turn Movement on Major Arterials	48
Figure 4.4 – Testing Plot for Normalized Actual Average Speed versus Normalized Estimated Average Speed for Left-Turn Movement on Major Arterials	48
Figure 4.5 – Normalized Average Through Speed versus Normalized Average Right-Turn Speed on Major Arterials	50
Figure 4.6 – Training Plot for Normalized Actual Average Speed versus Normalized Estimated Average Speed for Right-Turn Movement on Major Arterials	51
Figure 4.7 – Testing Plot for Normalized Actual Average Speed versus Normalized Estimated Average Speed for Right-Turn Movement on Major Arterials	52
Figure 4.8 – Training Plot for Normalized Actual Average Speed versus Normalized Estimated Average Speed for Through Movement on Minor Arterials	53

Figure 4.9 – Testing Plot for Normalized Actual Average Speed versus Normalized Estimated Average Speed for Through Movement on Minor Arterials	54
Figure 4.10 – Training Plot for Normalized Actual Average Speed versus Normalized Estimated Average Speed for Left-Turn Movement on Minor Arterials	55
Figure 4.11 – Testing Plot for Normalized Actual Average Speed versus Normalized Estimated Average Speed for Left-Turn Movement on Minor Arterials	55
Figure 4.12 – Training Plot for Normalized Actual Average Speed versus Normalized Estimated Average Speed for Right-Turn Movement on Minor Arterials	57
Figure 4.13 – Testing Plot for Normalized Actual Average Speed versus Normalized Estimated Average Speed for Right-Turn Movement on Minor Arterials	58
Figure 5.1 – Simple Neural Network Framework	61
Figure 5.2 – State-Space Neural Network Topology for Travel Time Estimation	63
Figure 5.3 – State-Space Neural Network Topology for Travel Time Prediction	64
Figure 5.4 – Sample MATLAB Graphical Output for SSNN Training	67
Figure 5.5 – Study Routes for the Evaluation of SSNN Model Performance	69
Figure 6.1 – Training Scatter Plot of Actual versus Estimated Travel Time for the Through Movement	74
Figure 6.2 – Testing Scatter Plot of Actual versus Estimated Travel Time for the Through Movement	75
Figure 6.3 – Training Scatter Plot of Actual versus Estimated Travel Time for the Left-Turn Movement	77
Figure 6.4 – Testing Scatter Plot of Actual versus Estimated Travel Time for the Left-Turn Movement	78
Figure 6.5 – Training Scatter Plot of Actual versus Estimated Travel Time for the Right-Turn Movement	79
Figure 6.6 – Testing Scatter Plot of Actual versus Estimated Travel Time for the Right-Turn Movement	80
Figure 6.7 – Training Scatter Plot of Actual versus Predicted Travel Time for the Through Movement	84

Figure 6.8 – Testing Scatter Plot of Actual versus Predicted Travel Time for the Through Movement	85
Figure 6.9 – Absolute Percentage Error of Through Movement Travel Time Prediction for Training Set Arterial 6-10	87
Figure 6.10 – Absolute Percentage Error of Through Movement Travel Time Prediction for Testing Set Arterial 6-10	87
Figure 6.11 – Absolute Percentage Error of Through Movement Travel Time Prediction for Training Set Arterial 16-20	89
Figure 6.12 – Absolute Percentage Error of Through Movement Travel Time Prediction for Testing Set Arterial 16-20	89
Figure 6.13 – Absolute Percentage Error of Through Movement Travel Time Prediction for Training Set Arterial 21-25	91
Figure 6.14 – Absolute Percentage Error of Through Movement Travel Time Prediction for Testing Set Arterial 21-25	91
Figure 6.15 – Absolute Percentage Error of Through Movement Travel Time Prediction for Training Set Arterial 3-23	92
Figure 6.16 – Absolute Percentage Error of Through Movement Travel Time Prediction for Testing Set Arterial 3-23	92
Figure 6.17 – Pattern of Actual versus Predicted Travel Time for Through Movement on Testing Set Arterial 6-10	94
Figure 6.18 – Pattern of Actual versus Predicted Travel Time for Through Movement on Testing Set Arterial 16-20	94
Figure 6.19 – Pattern of Actual versus Predicted Travel Time for Through Movement on Testing Set Arterial 21-25	95
Figure 6.20 – Pattern of Actual versus Predicted Travel Time for Through Movement on Testing Set Arterial 3-23	95
Figure 6.21 – Training Scatter Plot of Actual versus Predicted Travel Time for the Left-Turn Movement	97
Figure 6.22 – Testing Scatter Plot of Actual versus Predicted Travel Time for the Left-Turn Movement	98

Figure 6.23 – Absolute Percentage Error of Left-Turn Movement Travel Time Prediction for Training Set Arterial 6-10	100
Figure 6.24 – Absolute Percentage Error of Left-Turn Movement Travel Time Prediction for Testing Set Arterial 6-10	101
Figure 6.25 – Absolute Percentage Error of Left-Turn Movement Travel Time Prediction for Training Set Arterial 16-20	102
Figure 6.26 – Absolute Percentage Error of Left-Turn Movement Travel Time Prediction for Testing Set Arterial 16-20	102
Figure 6.27 – Absolute Percentage Error of Left-Turn Movement Travel Time Prediction for Training Set Arterial 21-25	103
Figure 6.28 – Absolute Percentage Error of Left-Turn Movement Travel Time Prediction for Testing Set Arterial 21-25	103
Figure 6.29 – Absolute Percentage Error of Left-Turn Movement Travel Time Prediction for Training Set Arterial 3-23	104
Figure 6.30 – Absolute Percentage Error of Left-Turn Movement Travel Time Prediction for Testing Set Arterial 3-23	104
Figure 6.31 – Pattern of Actual versus Predicted Travel Time for Left-Turn Movement on Testing Set Arterial 6-10	105
Figure 6.32 – Pattern of Actual versus Predicted Travel Time for Left-Turn Movement on Testing Set Arterial 16-20	106
Figure 6.33 – Pattern of Actual versus Predicted Travel Time for Left-Turn Movement on Testing Set Arterial 21-25	106
Figure 6.34 – Pattern of Actual versus Predicted Travel Time for Left-Turn Movement on Testing Set Arterial 3-23	107
Figure 6.35 – Training Scatter Plot of Actual versus Predicted Travel Time for the Right-Turn Movement	109
Figure 6.36 – Testing Scatter Plot of Actual versus Predicted Travel Time for the Right-Turn Movement	110
Figure 6.37 – Absolute Percentage Error of Right-Turn Movement Travel Time Prediction for Training Set Arterial 6-10	112

Figure 6.38 – Absolute Percentage Error of Right-Turn Movement Travel Time Prediction for Testing Set Arterial 6-10	113
Figure 6.39 – Absolute Percentage Error of Right-Turn Movement Travel Time Prediction for Training Set Arterial 16-20	114
Figure 6.40 – Absolute Percentage Error of Right-Turn Movement Travel Time Prediction for Testing Set Arterial 16-20	114
Figure 6.41 – Absolute Percentage Error of Right-Turn Movement Travel Time Prediction for Training Set Arterial 21-25	115
Figure 6.42 – Absolute Percentage Error of Right-Turn Movement Travel Time Prediction for Testing Set Arterial 21-25	115
Figure 6.43 – Absolute Percentage Error of Right-Turn Movement Travel Time Prediction for Training Set Arterial 3-23	116
Figure 6.44 – Absolute Percentage Error of Right-Turn Movement Travel Time Prediction for Testing Set Arterial 3-23	116
Figure 6.45 – Pattern of Actual versus Predicted Travel Time for Right-Turn Movement on Testing Set Arterial 6-10	117
Figure 6.46 – Pattern of Actual versus Predicted Travel Time for Right-Turn Movement on Testing Set Arterial 16-20	118
Figure 6.47 – Pattern of Actual versus Predicted Travel Time for Right-Turn Movement on Testing Set Arterial 21-25	118
Figure 6.48 – Pattern of Actual versus Predicted Travel Time for Right-Turn Movement on Testing Set Arterial 3-23	119
Figure 6.49 – Pattern of Actual versus Predicted Travel Time for Arterial Route 16-25	123
Figure 6.50 – Pattern of Actual versus Predicted Travel Time for Arterial Route 16-25	123
Figure 6.51 – Absolute Percentage Error of Travel Time Prediction for Arterial Route 16-25	125
Figure 6.52 – Pattern of Actual versus Predicted Travel Time for Arterial Route 16-3	126

Figure 6.53 – Pattern of Actual versus Predicted Travel Time for Arterial Route
16-3127

Figure 6.54 – Absolute Percentage Error of Travel Time Prediction for Arterial Route
16-3127

Figure 6.55 – Unique Route for the Validation of SSNN Model Performance128

Figure 6.56 – Pattern of Actual versus Predicted Travel Time for Arterial Route
15-2129

Figure 6.57 – Pattern of Actual versus Predicted Travel Time for Arterial Route
15-2130

Figure 6.58 – Absolute Percentage Error of Travel Time Prediction for Arterial Route
15-2131

Introduction

Throughout the United States, traffic congestion is a major problem that continues to plague urban areas. In 2003, Americans experienced approximately 3.7 billion total hours of delay and expended 2.3 gallons of additional fuel due to traffic congestion. Additionally, the impacts of urban traffic congestion cost Americans over 63 billion dollars (Schrank and Lomax 2005). In 2006, the United States Department of Transportation (USDOT) responded to these concerns with the *National Strategy to Reduce Congestion on America's Transportation Network* (Mineta 2006). The Federal Highway Administration (FHWA) has supported this plan through a number of congestion relief strategies that incorporate Intelligent Transportation Systems (ITS).

ITS has become an integral component of congestion mitigation in recent years, especially in urban areas. Typically in urban highway networks, physical capacity cannot be easily increased to reduce congestion due to right-of-way and financial restrictions. ITS can help to reduce congestion by improving the use of existing physical capacity through the use of technology and the communication of data within the existing infrastructure.

Parallel with matters related to ITS and highway congestion, the FHWA has given attention to issues associated with travel reliability. Due to fluctuating traffic demands, incidents, weather, and other variable factors, congestion is often dynamic and unpredictable. This creates an environment where congestion can occur at any time due to a number of factors. ITS applications must be able to function reliably in this dynamic environment in order to effectively reduce congestion (Cambridge Systematics 2005).

In order to improve system reliability and reduce congestion, particular ITS applications such as Advanced Traffic Management Systems (ATMS) and Advanced Traveler Information Systems (ATIS) have been developed. These systems utilize traffic data to aid in the management of traffic operations and to communicate important information to the users of the system. “These tools [ATMS/ATIS] are intended to perform real-time system-wide traffic estimation and prediction, based on the existing surveillance system...these intelligent functions are predicated on the availability of reliable and robust traffic flow models capable of representing the dynamic evolution of traffic over space and time” (Qin 2006).

In order to be effective ATMS and ATIS must provide reliable information in terms of the current and future states of traffic. Additionally, system managers and users must be able to easily understand and apply this information to make informed decisions. Chen et al. (2002) established that travel time is both important to travelers and a meaningful measure of performance. For this reason, travel time has emerged as a measure that drives many ATMS and ATIS applications.

On many urban freeway segments ATMS and ATIS applications have been successfully developed and deployed. However, these systems are not readily seen on urban arterial networks. In comparison to free-flow highway systems, traffic flow on arterial networks is much more complex. Research to effectively estimate and predict travel time on arterial networks has lagged behind freeway applications due to this complexity. In order to make ATMS and ATIS applications more viable for urban arterial networks, models must be developed to estimate and predict travel time accurately and reliably.

Traffic flow on arterial networks is heavily influenced by signalized intersections. May (1990) states that, “Signalized intersections are the most critical and complicated elements of the arterial network system.” At signalized intersections traffic flow is interrupted, resulting in queue formation as vehicles stop during the red interval and platoon expansion as the green interval begins. Turning movements, signal phasing, shockwave propagation, and other variable factors further complicate arterial traffic flow. Additionally, the operation of signalized intersections is temporally dependent as the operation of a particular cycle is impacted by the previous cycle, and will impact the following cycle. This is especially true in congested conditions.

Effective travel time estimation and prediction models must incorporate the variability in these factors. In order to encourage ATMS and ATIS deployment in urban arterial networks, models must be developed that utilize existing data collection infrastructure. In 2004, 70 percent of signalized intersections in U.S. metropolitan areas were equipped with electronic surveillance (ITS Joint Program Office 2005). These forms of electronic surveillance, such as loop detectors and cameras, are capable of collecting data representing queue lengths, flow rates, and turning movement percentages. Travel time estimation and prediction models should utilize these data and corresponding traffic signal timing data, which are easily collected with existing technology and limited need for additional infrastructure.

Previous research has been conducted to develop State-Space Neural Network (SSNN) models to estimate and predict travel time for the short-term future. Singh (2007) successfully developed such models specific to right turn, left turn, and through movements on arterial links based on flow rate, queue length, geometrics, and signal

control parameters. However, these models are based a hypothetical arterial network where turning movement percentages are constant. Turning movement percentages can severely impact signalized intersection operation as turning movements impact both signal operation efficiency and saturation flow rates (Roess et al. 2004). In actual urban arterial networks, turning movement flows will vary between intersections and over time. Therefore, reliable SSNN models must be able to accurately estimate and predict travel time in an environment where turning movements vary spatially and temporally.

The purpose of this thesis is to explore the impacts of variable right and left turning movements on travel time estimation and prediction for urban signalized networks. SSNN models are developed using methodology similar to the work done by Singh, but incorporate variable turning movements in the modeling framework. The SSNN models rely on data that is easily obtained using existing surveillance technologies such as loop detectors and cameras. The successful estimation and prediction of travel time in this environment advances the work performed by Singh and proves very promising in urban arterial ATMS and ATIS applications.

Chapter 1

Literature Review

Accurate travel time estimation and prediction is dependent on the ability to understand the relationship between travel time and variables that may impact traffic flow. Intelligent Transportation System (ITS) applications such as Advanced Traffic Management Systems (ATMS) and Advanced Traveler Information Systems (ATIS) function based on the results of research to model this relationship. Much research has been done in this area for freeway applications where traffic flow is uninterrupted. As a result, ATMS and ATIS use has become more prevalent in urban freeway systems. However, in urban arterial networks where traffic signals impact the flow of traffic, research to date has not been sufficient to support widespread ATMS and ATIS deployment. The need to advance research efforts regarding travel time estimation and short-term prediction for interrupted flow systems has been documented for this reason. Stemming from ongoing research into ITS and congestion mitigation strategies, the reliability of transportation systems has received increased attention and has become a focal point of recent initiatives. ITS applications must be reliable in terms of the transportation service provided and the information presented to users and administrators of each system. In order to advance ATMS and ATIS deployment into urban arterial networks, travel time estimation and prediction models driving these systems must perform accurately and reliably in a variety of conditions. Failure to do so may cause not

only a breakdown in the functionality of the system, but also losses in public trust in future ITS endeavors.

1.1 Travel Time Estimation and Prediction

A large number of papers have been published regarding travel time estimation and prediction for urban freeway systems. As a part of the California Partners for Advanced Highways and Transit (PATH), Coifman (2002) successfully researched the relationship between spot speed and freeway link travel time. This enables the estimation of travel time from single-point dual loop detectors. Chen et al. (2003) developed a strategy to effectively determine travel times using linear regression for display on California highway variable message signs. The application of Artificial Neural Networks (ANN) has also proven successful in estimating and predicting freeway travel times in Huston, Texas (Park and Rilett 1999). Continuing research in this area serves to improve the reliability of ATMS and ATIS freeway applications, based on a variety of fundamental models. This is apparent in performing a literature search on this topic.

The same is not true for urban arterial network applications. The results of most research efforts seem to address only incremental aspects of arterial travel time estimation and prediction, and have not yet produced robust models. For example, in a paper for the 82nd Transportation Research Board Annual Meeting, Lin et al. (2003) present the use of intersection delay parameters to estimate arterial link travel time. However, the model developed fails to perform accurately in congested networks due to the breakdown of delay estimates in over-saturated conditions. The usefulness of ATMS and ATIS

applications exists in dealing with congested conditions, so this methodology does not prove promising.

In a recent paper published in the Transportation Research Record, State-Space Neural Network (SSNN) modeling is proposed to address the complex spatiotemporal problem of modeling urban arterial network behavior with respect to travel time prediction (Liu et al. 2006). This approach seems to better address the state of a link under unstable congested conditions. However, the model is based on a specific roadway segment and negates traffic control parameters. In arterial networks, traffic signals heavily influence capacity, and thus the state of link operations. Robust SSNN models should incorporate measures of capacity such as traffic signal timing to better capture the relationship between travel time and traffic states on urban arterials. The work presented in this thesis is focused on meeting this condition.

1.2 Travel Time Reliability

The Federal Highway Administration (FHWA) has recently given attention to matters related to the reliability of highway systems in response to national concerns regarding urban congestion. Growing levels of congestion have resulted in larger variations in travel time and reduction in the reliability of the system. Through advanced data collection, processing, and communication, ITS technologies may improve the correlation between the actual and expected traffic conditions, and thus improve system reliability. In order to do so, ITS technologies themselves must be reliable.

A specific example of the reliability related to traffic conditions is in ATIS systems which provide users route guidance and congestion avoidance information. Kantowitz et al. (1997) published findings on driver acceptance of travel time information in preparation for early-stage ATIS deployments. In situations where information communicated to the driver were inaccurate, drivers often lost trust in the information system and disregarded future communications. Following these findings, travel time estimation and prediction models are useless, if not detrimental, to traffic operations when unreliable.

1.3 State-Space Neural Network Application

As previously referenced, Liu et al. (2006) presented a SSNN modeling procedure to predict travel time on an arterial roadway segment. Although lacking robustness, this research proves SSNN modeling as a promising approach to travel time estimation and prediction. Studies by van Lint (2004) and van Lint et al. (2002) have also proven the SSNN modeling useful to effectively capture the dynamic spatiotemporal relationship between measurable traffic parameters such as speed and flow rate, and travel time.

In 2006 Singh developed a SSNN modeling procedure to estimate and predict travel time for an urban arterial network using traffic data easily collected using existing surveillance infrastructure. The procedure presented in this thesis involves an examination of the impacts of variable turning movements within the arterial network on the reliability of the SSNN models previously developed.

1.4 Conclusions Based on Related Literature

A review of current literature related to the estimation and prediction of travel time reveals the need for research to improve existing modeling techniques for urban arterial networks. The operation of arterial networks is complex and dynamic, and research to date has not produced reliable estimation and prediction models. However, previous research has established a foundation on which effective models can be developed. State-Space Neural Networks (SSNN) have been shown to be useful in capturing the dynamic nature of arterial traffic conditions. Furthermore, easily collectable traffic data such as average speed and flow rate have been implemented effectively to explain variations in travel time. This research is aimed to progress the results of previous findings in order to advance the prospect of future ATMS and ATIS applications to combat urban arterial congestion problems.

Chapter 2

Problem Statement and Research Objective

Congestion in urban traffic networks is a problem that continues to cost travelers time and impact economic productivity. In the absence of readily available physical space and ample financial resources, the supply of additional physical highway capacity in urban areas is often not possible. With the advancement of information and communication technologies Intelligent Transportation Systems (ITS) such as Advanced Traffic Management Systems (ATMS) and Advanced Traveler Information Systems (ATIS) are being implemented successfully in urban areas to improve the use of existing physical capacity and combat congestion.

Travel time is a key variable that describes the state of a transportation system and is easily understood by the users of the system. For this reason, travel time estimation and prediction is an essential component of ATMS and ATIS applications. These ITS solutions are particularly prevalent in urban freeway systems to aid administrators in solving traffic problems and inform users of upcoming traffic conditions. However, ATMS and ATIS deployment is not established in the urban arterial setting. In arterial networks, traffic signals interrupt the flow of traffic, creating variability in traffic conditions that is not readily understood. Advancements in research to accurately estimate and predict travel time in signalized networks is necessary to enable the successful deployment of ATMS and ATIS application in urban arterial networks.

The objective of the work presented in this thesis is to develop models that enable accurate estimation and short-term prediction of travel time in urban arterial networks for use in future ATMS and ATIS applications. Furthermore, these models are developed using input variables that are readily available in the field through existing surveillance infrastructure. Loop detectors and cameras currently deployed in urban arterial networks are capable of sensing variables such as flow rate and queue length that can be used to estimate and predict travel time.

Previous work has been done in this area, producing some promising results. Singh (2006) developed travel time estimation and short-term prediction models for right turn, left turn, and through movements in a simulated urban arterial network. This work did include assumptions that may impact the robust nature of the models developed, though. In particular, turning movement percentages were constant between intersections and over time in the simulation network used to generate data for the development of travel time estimation and prediction models. In a realistic urban arterial network, turning movements will vary spatially and temporally based on fluctuations in demand and proximity to particular origins and destinations. This thesis incorporates variable turning movements to determine the impact on reliable estimation and prediction of travel time.

2.1 Background and Definitions

The framework presented in this thesis mirrors the framework developed by Singh (2006), with the exception of turning movement simulation. This is done so that the impacts of variable turning movements can be understood in comparison with the results

previously produced assuming constant turning percentages. The purpose is not to refute the work completed, but instead to improve the reliability of the modeling technique employed, in order to advance the reliability of such models for ATMS and ATIS applications in urban arterial networks.

The framework developed by Singh (2006) and employed in this thesis is presented in this chapter. The models developed for travel time estimation and prediction are applicable to urban arterial networks, and so the elements of such networks are defined in this section. Additionally, the concept of average travel time is presented.

Definition 1: A ‘Signalized Intersection’ is the point where two arterial links meet. A signalized intersection is defined by the use of traffic control signals to manage the flow of conflicting traffic movements from one arterial link to another.

Definition 2: An ‘Arterial Link’ is a section of road between two signalized intersections. For the purpose of travel time estimation, the length of an arterial link begins at the end of one signalized intersection and extends through and includes the next downstream intersection. Arterial links may carry traffic flow in two directions.

Definition 3: An ‘Arterial’ is a sequential group of arterial links that are traversed by making only a through movement from the entry point to the terminus of the arterial within the boundaries of the arterial network.

Definition 4: An ‘Arterial Route’ consists of a set of arterial links traversed by a vehicle making any series of left turn, right turn, and through movements from origin to destination, within the boundaries of the network.

Definition 5: An ‘Arterial Network’ is comprised of the arterial links and signalized intersections within a particular area of study. An urban arterial network typically takes on a grid formation having both major and minor arterials. ‘Major’ and ‘Minor’ refer to the relative traffic flows and importance in terms of network operation.

In an arterial network individual vehicles traverse a series of links from origin to destination. Individual vehicles that travel together along a common arterial link or route in a common time interval travel in a traffic stream. ATMS and ATIS applications typically function based on characteristics of the traffic stream, which are defined by statistical measures, such as the average, of individual vehicle movements. The concept of average travel time for a traffic stream will be implemented in the model development strategy for this thesis.

Definition 6: The ‘Average Travel Time’ is the average value of the travel times experienced by individual vehicles on a particular arterial link during a specific time interval.

As defined previously, arterial links are the primary component of any arterial or arterial route. Therefore, the average travel time for an arterial or arterial route is defined by the

average travel time on each subsidiary link. The objective in developing accurate estimation and prediction models for average travel time on an arterial link is to provide the fundamental component for estimation and prediction of average travel time for higher-level network components, such as arterials and arterial routes. This framework will provide a more robust tool available for a variety of ATMS and ATIS applications.

2.2 Average Travel Time Estimation versus Prediction

Average travel time estimation and prediction are both important elements of ATMS and ATIS applications. Travel time is easily understood by transportation system users, and has been determined to be a useful measure of performance for administrators. In such ITS applications, it is useful to know not only current travel times, but also what travel times will be in the future, so that proactive measures can be taken to avoid congested conditions.

Both current travel time and travel time in the future are based on the state of the network, or in other words, the quality of traffic operations. However, there is an important difference between estimating current average travel time, and future prediction. The estimation of travel time is based on known or estimated traffic parameters, whereas traffic conditions are unknown in the future.

Definition 7: The ‘Estimated Average Travel Time’ is the travel time experienced by vehicles during a current or past time interval. Average travel time estimation is based on known or estimated traffic parameters describing the state of traffic for any arterial link.

Definition 8: The ‘Predicted Average Travel Time’ is the travel time that is expected to be experienced by vehicles during a future time interval. Average travel time prediction is based on preceding traffic conditions and temporal fluctuations in these conditions, as future traffic parameters are unknown.

The objective of this thesis is to develop accurate and reliable travel time estimation and short-term prediction models using input variables that are easily collected using existing infrastructure. The variables that describe and influence travel time in arterial networks include flow rate, queue length, arterial geometrics, and signal timing parameters. Both travel time estimation and prediction models are developed using these variables, although the methods differ from one another.

During current or past time intervals, variables describing the state of traffic operations can be measured and calculated. A static relationship can then be determined between these input variables and the output variable, average travel time. In other words, models can be developed to calculate travel time based upon the values of the input variables. This relationship is not dependent on changes in the value of each input variable over time, rather on average values during a specified time interval. The accuracy of such models depends on the strength of correlations between each input variable and actual average travel time.

Travel time prediction for a future time period is a much more complex problem, as the values of potential variables influencing travel time are not yet known. For this reason, prediction of travel time is based on understanding temporal changes in traffic conditions during previous time intervals. A relationship is then developed between changes in the

input variables over time and the resulting changes in observed travel times. In this manner, travel time prediction can be performed using data that is easily obtained using existing infrastructure. The accuracy of prediction models depends on the ability to understand how temporal fluctuations in past traffic conditions may influence future travel times. Methodologies for both estimation and short-term prediction of average travel time in urban arterial networks are provided in this thesis.

2.3 Formulation for Average Travel Time Estimation and Short-Term Prediction Models

Let an arterial route on a network consisting of n number of arterial links be represented as $X_1, X_2, X_3, \dots, X_n$. Let t_p' be the current time interval of departure for a vehicle which starts from an entry point at the beginning of link X_1 and ends its trip after clearing the intersection that ends link X_n . This time interval t_p' starts from a discrete time t_0' and ends at time t_1' , where $t_p' = [t_0', t_1']$. The time interval t_p' is impacted by prevailing traffic conditions on the arterial network. The traffic parameters that describe traffic conditions during time t_p' can be obtained in the field through traffic detection devices, or can be estimated through other already obtained traffic variables.

The assumption is made that traffic conditions are constant within each time interval if the length of such interval is very small. In many traffic engineering studies, particularly regarding short-term travel time forecasting, it is assumed that traffic conditions are constant within short time intervals of 1 to 15 minutes. A time interval of 1 minute provides high temporal resolution to the data and may be useful if cycle-by-cycle analysis

is required. On the other hand, an interval of 15 minutes offers low temporal resolution for forecasting, as changes in unstable traffic conditions during congestion and over-saturated conditions may be overlooked or aggregated. Sisiopiku et al. (1994) in a travel time estimation study assert that effects from cycle failures, short-term events, congestion built up downstream of the subject link, and so forth cannot be detected using 15-minute observation periods. Mark and Sadek (2004) recommend temporal resolution of 5 minutes for travel time forecasting and find that no statistically significant increase in performance is gained by increasing the temporal resolution from 5 minute to 1 minute intervals. Based on the results of these studies, the length of each time interval for this thesis is determined to be 5 minutes in duration. This interval is called the aggregation interval, denoted as Φ , where $\Phi = t_1 - t_0$.

Let the known traffic conditions on a link X_l in the current time interval t_p be $V(X_l, t_p)$. The vector $V(X_l, t_p)$, which contains the variables describing traffic conditions on a link X_l during time interval t_p , is called the ‘state’ of an arterial link. The ‘state’ of an arterial or arterial route is simply a vector which contains the state of each link comprising that arterial or route during a given time interval. This generic term for traffic conditions on a link is very important in the context of travel time estimation and prediction because the set of input variables such as average flow rate, average speed, queue length, etc., impact the state of the link, and therefore travel time. Following this concept, the approach is to model the function that exists between the link state and travel time on that link.

The average travel time to traverse a link X_l during time interval t_p is denoted as $TT(X_l, t_p)$. The estimation of average travel time is defined using the terminology explained in the previous paragraphs.

Definition 9 - The average travel time on arterial link X_l is estimated by approximating the underlying function between average travel time $TT(X_l, t_p')$ and the state $V(X_l, t_p')$ of link X_l during time interval t_p' .

The formulation of average travel time prediction is derived from the definition of average travel time estimation. Assume that the average travel time is to be predicted for a future time interval that is just starting when the current time interval t_p' ends at time instant t_l' . A short interval of time in the future, denoted as Δ , for which the average travel time is to be predicted is defined as the 'prediction horizon.' The future time interval is defined as $t_{p+l\Delta} = [t_0, t_l]$, where the time interval begins at t_0 and ends at t_l . This implies that the t_0 value of future time-period is the same as t_l' , the ending time instant of the current time interval. Therefore, $t_0 = t_l'$. Moreover, the length of this future time interval $t_{p+l\Delta}$ is equal to the addition of the current time interval t_p' and the prediction horizon Δ , where $t_{p+l\Delta} = t_l' + \Delta$. The future time interval $t_{p+l\Delta}$ is a single multiple of the prediction horizon Δ , and is called a one-step future time interval. The predicted value of average travel time for this one-step future time interval will be called the one-step predicted average travel time.

The prediction horizon Δ can be assumed to be equal to the aggregation interval Φ as previously defined. So, $\Delta = \Phi = 5$ minutes. This assumption is made so that the temporal scale at which the state of a link and travel time is analyzed is equal for all time intervals whether past, current, or future. The predicted average travel time to traverse a link X_l during the one-step future time-period $t_{p+l\Delta}$ is denoted as $TT(X_l, t_{p+l\Delta})$. The problem of one-step average travel time prediction is defined using this terminology.

Definition 10 - The one-step average travel time on arterial link X_l is predicted by approximating the underlying function between the one-step predicted average travel time $TT(X_l, t_{p+1\Delta})$, state $V(X_l, t_p)$, and the estimated average travel time $TT(X_l, t_p)$.

It is important to highlight that for the above definition the state of a link and the estimated average travel time for that link in the current time period are used as inputs for the one-step predicted average travel time, which is expected to occur when unseen and unknown traffic conditions transpire.

The average travel time prediction for any n^{th} step in the future can be developed on the same basis, where $n \geq 1$. Assume that the time-period in n steps is represented as $t_{p+n\Delta}$, where the n^{th} step predicted average travel time is denoted as $TT(X_l, t_{p+n\Delta})$. The determining factors for average travel time prediction for the n^{th} step are the state of the link, $V(X_l, t_p)$, and estimated travel time, $TT(X_l, t_p)$. Additionally, the predicted average travel times through the $n-1$ step are also taken as input variables for n^{th} average travel time prediction.

Definition 11 - The n^{th} step average travel time is predicted by approximating the underlying function between the n^{th} step predicted average travel time $TT(X_l, t_{p+n\Delta})$ during time interval $t_{p+n\Delta}$, state $V(X_l, t_p)$, the estimated average travel time $TT(X_l, t_p)$, and the predicted average travel time through the $n-1$ step.

Average travel time prediction for the n^{th} step in the future is referred to as multiple-step prediction. Multiple-step average travel time prediction involves incremental prediction

from the $n = 1$ step to the n^{th} step as required for the system. Each time-step prediction will result in some deviation from the actual average travel time. As a result, it is expected that the accuracy of predictions may decrease as the number of increments increases.

The formulation defined is presented in a time-space diagram in Figure 2.1. The space domain is represented as a single link X_l and the time scale includes time intervals ranging from the current time interval t_p to the n^{th} future time interval $t_{p+1\Delta}, t_{p+2\Delta}, t_{p+3\Delta}, \dots$ for which a prediction is to be made. The current time period t_p is labeled as the ‘current horizon’ and each future time period is termed as the ‘prediction horizon.’ Consistent with the terminology presented in this section, the current horizon begins at time instant t_0 and ends at time-instant t_l , forming time period t_p . The duration of time interval t_p is equal to the aggregation interval Φ . The state of link X_l representing prevailing traffic conditions is shown as $V(X_l, t_p)$ in the current horizon. The first-step prediction horizon starts from time-instant t_0 (equal to t_l) and ends at t_l , forming first step future time interval $t_{p+1\Delta}$. Similarly, second-step and third-step prediction horizons are as shown. Each future time-period is of length Δ , where $\Delta = \Phi$.

The work presented in this thesis is focused on average travel time prediction for the first-step horizon, where $n = 1$. While prediction for the $n > 1$ horizon is possible, there is an inherent level of error that can be expected to propagate through multiple prediction increments. Models useful in predicting average travel time for the $n = 1$ step must be improved first in order to reduce the probability of error propagation for multiple time intervals.

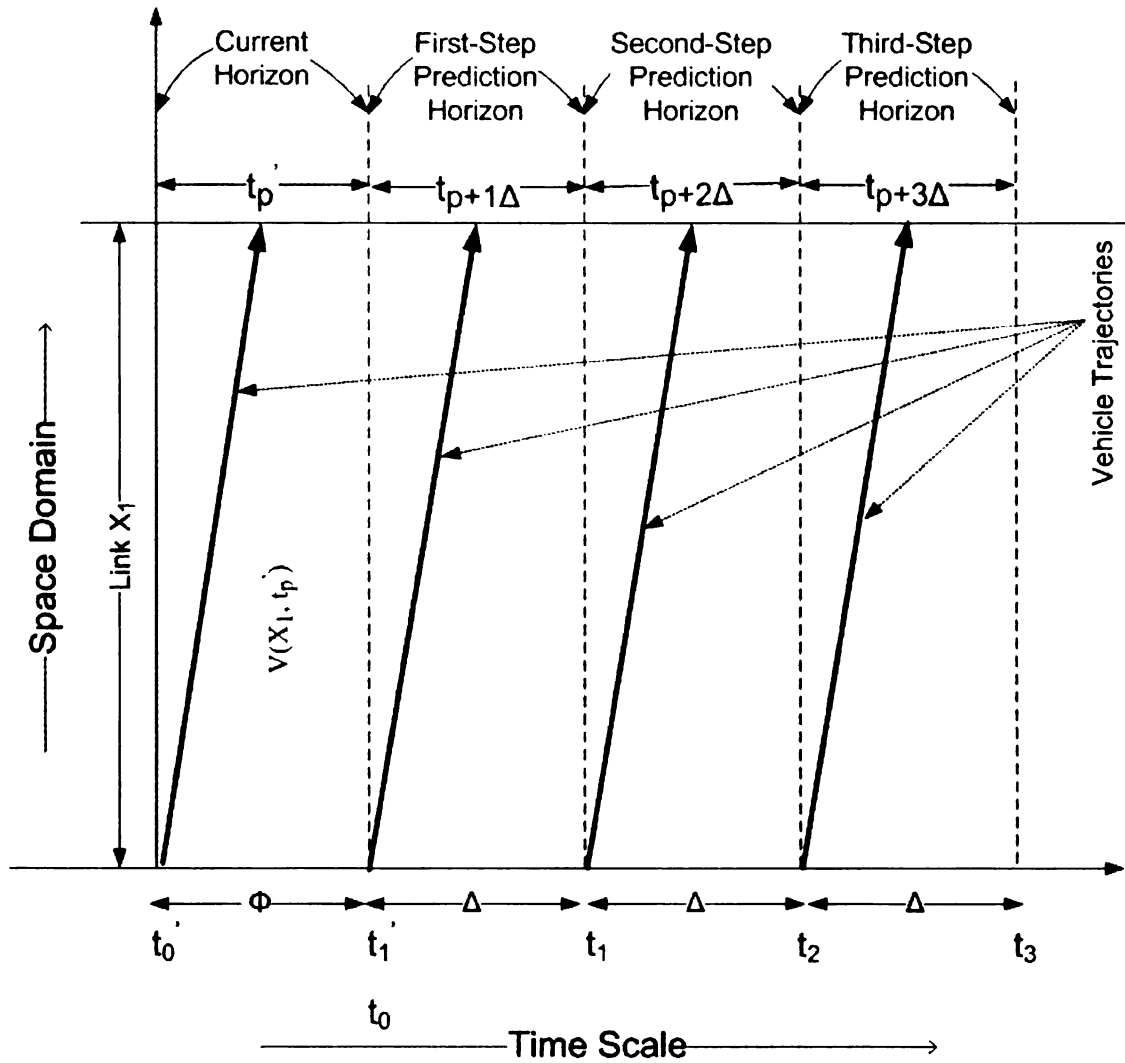


Figure 2.1 – Time-Space Domain for the Formulation of Average Travel Time Estimation and Short-term Prediction.

The intent of this work is to advance previous research regarding short-term travel time prediction for urban arterial networks and improve existing single-step prediction models. Further research is needed to progress these models to be reliable in multiple-step prediction applications.

2.4 Factors Impacting Average Travel Time Estimation and Short-Term Prediction

Travel time on arterial links can be impacted by a variety of influences. Traffic demand, roadway capacity, traffic signal operation, weather, incidents, and driver behavior can all have an effect on travel time. However, only a portion of these variable factors can be measured and used to estimate and predict travel time. For the purpose of this thesis, only variables that are easily measured using existing surveillance infrastructure such as loop detectors and cameras are considered.

The state of an arterial link is determined by the balance between traffic demand and the available supply, or capacity, of the link. Throughout a typical day, traffic demand fluctuates depending on the needs of the system users. In urban arterial networks the capacity is often insufficient to meet peak demands. As a result, vehicle spacing and average vehicle speed decreases, causing increases in average travel time. The input variables used to estimate and predict travel time should include measures of both traffic demand and link capacity for this reason.

To capture the variability in traffic demand average flow rate can be measured for a given time interval. According to the Transportation Research Board *Highway Capacity Manual* (2000), right and left-turn movements can influence flow rate as turning vehicles must reduce speed and may be restricted by conflicting movements. For this reason, average flow rate is measured for right-turn, left-turn, and through movements independently. Additionally, right-turn-on-red permission at signalized intersections can

alter arterial operation. The flow rate for the crossing approach should also be considered to better model right-turn travel time.

Traffic signal operation has a significant influence on the available capacity and resultant state of an arterial link. Conflicting traffic demands at each intersection must be serviced through the allocation of green time to each approach. Additionally, left-turning vehicles must often be accommodated by dedicating a specific signal phase for left-turns. Signal timing parameters such as duration of green and red intervals are therefore important variables that control traffic flow and thus influence travel time.

In urban arterial networks, link lengths are relatively short, and an interaction between adjacent intersections exists. The signal phasing and timing schemes must be coordinated to effectively progress vehicles from one intersection through the next. This coordination is determined by the link length, vehicle speed, and the time difference in green intervals, or offset, between adjacent intersections. In congested conditions the relative operation of adjacent intersections can be even more vital. Queues that form at intersection approaches can influence progression and travel time. Furthermore, queue length can increase in excess of the link length, and block upstream intersections.

Travel time estimation and prediction models are developed based on the above mentioned influences and the ability to collect data representing such variables using existing surveillance. In order to produce efficient models that can be implemented into a variety of ATMS and ATIS applications, models are developed for right-turn, left-turn, and through movements separately. This will allow not only for travel time estimation for arterial links, but also for arterials and arterial routes. The variables considered in the modeling procedure are defined in Table 2.1.

Table 2.1 – Variables Considered for Travel Time Estimation and Short-Term Prediction.

<i>Travel Demand</i>	V_T	Average flow rate for through movement
	V_R	Average flow rate for right-turn movement
	V_L	Average flow rate for left-turn movement
	V_X	Average flow rate for approach conflicting right-turn movement
<i>Speed</i>	S_T	Average speed for through vehicles
	S_R	Average speed for right-turning vehicles
	S_L	Average speed for left-turning vehicles
<i>Signal Control</i>	G_T	Length of green interval for through and right-turn phases
	G_L	Length of green interval for left-turn phase
	Off	Offset between adjacent signalized intersections
	R	Length of red interval for approach
<i>Queue Length</i>	Q_T	Maximum queue length for through and right-turn lanes
	Q_L	Maximum queue length for dedicated left-turn lanes
<i>Geometric</i>	LL	Link length

2.5 Modeling Approach for Travel Time Estimation and Short-Term Prediction

As acknowledged in supporting literature, there is a need for reliable a reliable modeling procedure for the estimation and prediction of travel time in urban arterial networks. In this chapter the research objectives to address this need have been identified, the elements of an arterial network have been defined, the mathematics supporting travel time estimation and prediction have been formulated, and candidate variables influencing travel time have been identified. In the following chapters of this thesis the experimental procedure and the modeling approach are detailed, along with the conclusions resulting from this research.

The overall modeling approach begins with the problem statement and identification of the need for separate models for right-turn, left-turn, and through movements in order to be robust in ATMS and ATIS applications. In order to examine the relationship between variables influencing the state of an arterial link and travel time, data are needed for the candidate input variables and average travel time. These data are generated from a sample network developed using VISSIM microscopic simulation.

Average vehicle speed has been identified as an important variable linked to average travel time. Intuitively, this is straightforward, as speed is a product of distance and time. Measuring average vehicle speed continuously along an arterial link is difficult however, as speeds fluctuate along the length of the link, and existing data surveillance devices are mainly capable of estimating vehicle speed at discrete points along the link. A multivariate linear regression model is utilized to more reliably estimate average vehicle speed along the length of a link given other more accurately obtainable data.

From the data generated using VISSIM and the average link speeds estimated from linear regression, State-Space Neural Networks (SSNN) models are introduced. Singh (2006) developed a series of SSNN models for travel time estimation and prediction in urban arterial networks. The reliability of these models is examined in this thesis under the influence of variable turning movements. The overall framework presented in this section is represented by a flow chart in Figure 2.2.

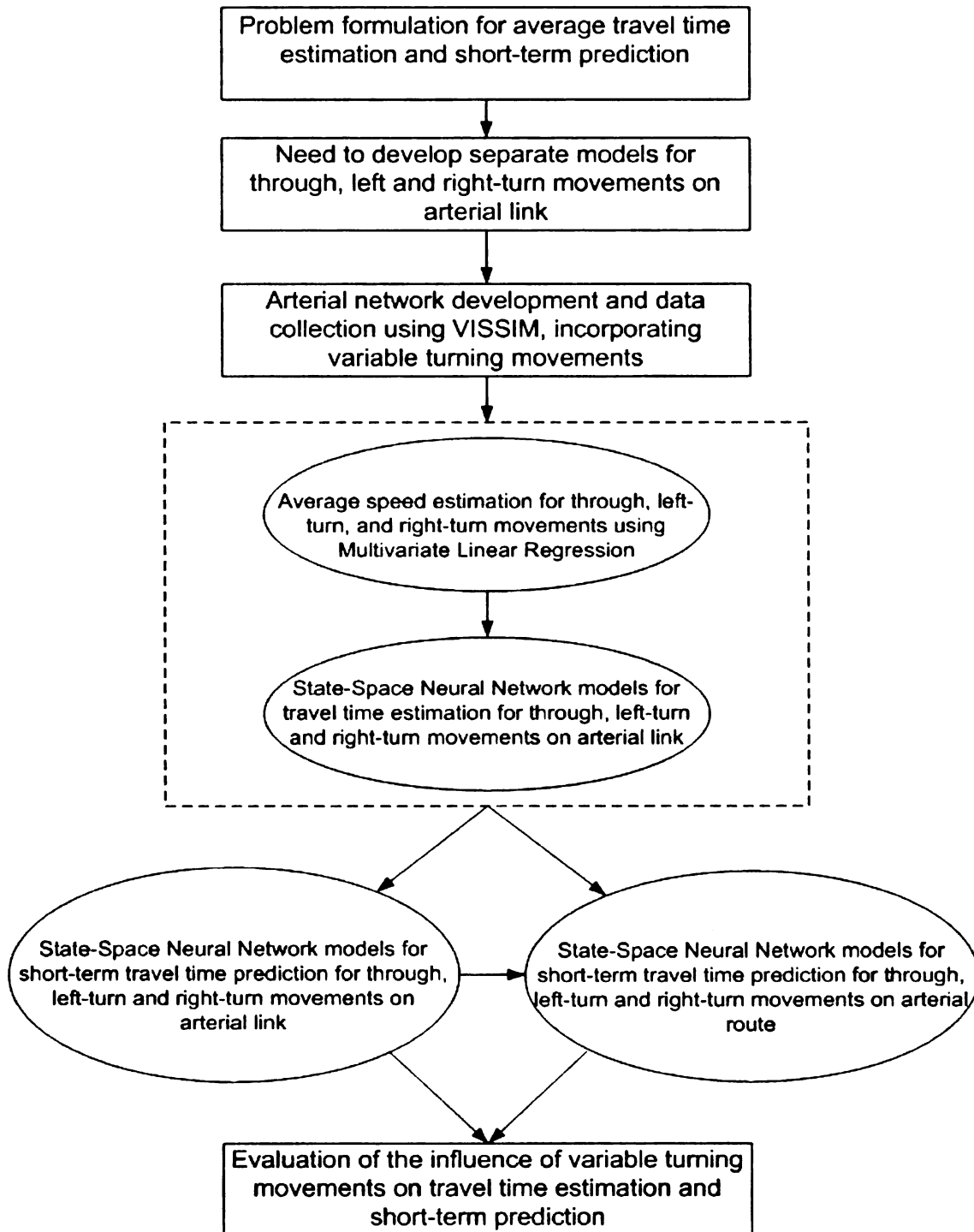


Figure 2.2 – Flowchart of Modeling Approach for Travel Time Estimation and Short-Term Prediction.

Chapter 3

Experimental Set-up

There are a wide variety of factors that influence travel time on urban arterial networks, including traffic demand, signal control operations, speed, geometrics, weather, and driver behavior. The objective of this thesis is to develop travel time estimation and prediction models based on variables describing these factors that can be easily measured in the field using existing surveillance devices such as loop detectors and cameras. Candidate variables have been identified to meet this objective and are defined in Section 2.4 of this thesis.

In order to explore the relationship between travel time and the defined set of input variables a dataset is needed containing data for each candidate variable and corresponding travel times. The intent is to develop robust models from this dataset that can be applied to future Advanced Traffic Management Systems (ATMS) and Advanced Traveler Information Systems (ATIS). Therefore, it is important that the dataset contain a large number of cases describing operations on a number of arterial links.

The use of microscopic simulation enables the collection of large amounts of data describing operations on a number of arterial links without the need for extensive field data collection procedures. Additionally, microscopic simulation allows for the variation of network parameters to study the influence of such variations on the robust nature of the models developed.

Previous work has been done to develop travel time estimation and prediction models using data from microscopic simulation. The work presented in this thesis is based on the simulation network developed by Singh (2006) and incorporates variable turning movement percentages into the experimental procedure. The influence of variable turning movements on the effectiveness of the models developed is examined. The usefulness of microscopic simulation to fulfill these objectives and the experimental procedure implemented is described in this chapter.

3.1 Overview of VISSIM Microscopic Simulation

The data used in the development of travel time estimation and prediction models are generated using VISSIM microscopic simulation software, Version 4.10. In the VISSIM environment network parameters are defined by the user, including link lengths, number of lanes, desired vehicle speeds, signal control operations, traffic compositions, flow rates, and turning movement percentages. Additionally, a variety of methods can be implemented to collect the necessary data from each simulation run.

The use of VISSIM allows wide latitude in the creation of each system element to meet the objectives of the network design. The freedom allowed in network design and data collection makes the use of VISSIM desirable for this experiment. A network is designed to replicate a realistic urban arterial environment, containing a series of arterial links and signalized intersections with spatially and temporally variable flow rates and turning movement percentages. This set-up replicates the conditions experienced in many urban arterial networks, where traffic demands change across the network throughout the day.

3.2 Static Network Elements

The urban arterial network created in VISSIM for use in this experiment consists of 10 arterials, each consisting of 4 arterial links. The arterials are aligned in a grid pattern as shown in Figure 3.1. The 5 arterials running in the east-west direction are defined as the major arterials, and the 5 arterials running in the north-south direction are defined as the minor arterials, where ‘major’ and ‘minor’ designate the level of traffic demand and relative importance with respect to signal progression and network operations. Each arterial has 2 lanes in each direction.

The point where two arterials meet represents a signalized intersection and is shown in Figure 3.1 as a solid circle. Each intersection is numbered 1 through 25, where the number of the outermost intersections designate the label for each arterial. The major arterials are referred to as arterials 1-5, 6-10, 11-15, 16-20, and 21-25. The minor arterials are referred to as arterials 1-21, 2-22, 3-23, 2-24, and 5-25. Every approach at each signalized intersection has a dedicated left-turn lane with a length of 150 feet, a through lane, and a shared through / right-turn lane.

In actual arterial networks, the length of an arterial link can be an important factor influencing travel time. In uncongested conditions link length influences travel time simply based on the free-flow speed of traffic on the link. In congested conditions though, the spacing between signalized intersections can impact traffic progression through green intervals and heighten the significance of queue formation where queue spillback can cause blockage. For this reason, link lengths are varied between 1,500 feet

and 6,000 feet in the simulation network. The link lengths for each parallel arterial are shown in Figure 3.1.

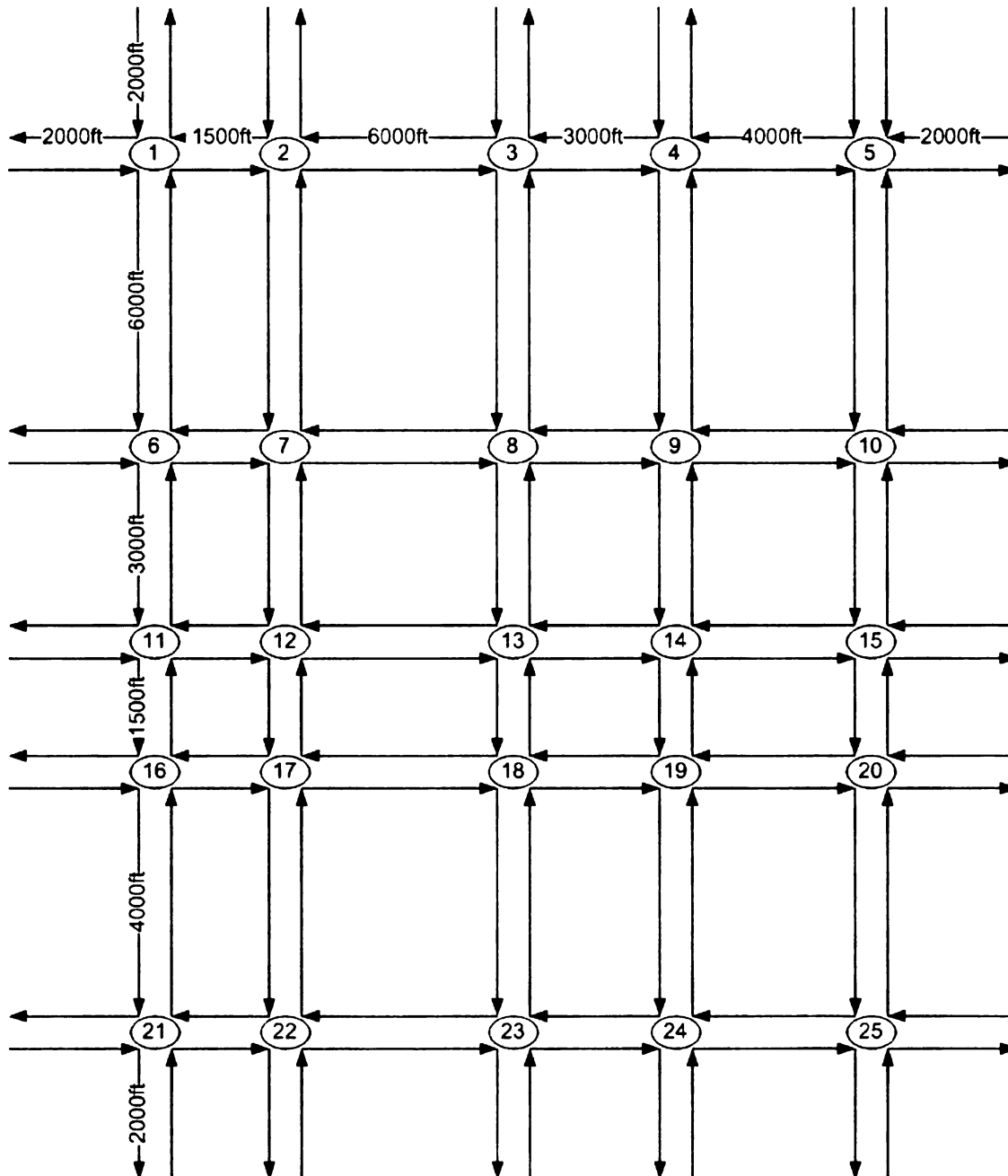


Figure 3.1 - Urban Arterial Network Designed in VISSIM for Travel Time Estimation and Prediction.

3.3 Stochastic Network Elements

In microscopic simulation, vehicle movements are controlled and tracked individually as determined by the vehicle following and lane changing logic employed by the simulation tool. The VISSIM program uses a psycho-physical driver behavior model developed by Wiedemann (1974) where vehicle acceleration and deceleration is based on individual perception thresholds to vehicles with different speeds. Stochastic distributions are used to replicate variability of individual driver characteristics. Each individual vehicle in the network is assigned specific speed, acceleration, and gap sensitivity based on the distributions determined for the system. Traffic flow is simulated through the movement of these vehicles following the Wiedemann car-following model and the defined distributions (PTV 2005).

For the simulation network developed the default distributions for vehicle following, lane changing, gap acceptance, acceleration, and deceleration are implemented. As the purpose of the simulation is to generate data, no actual field data exist whereby to further calibrate the default distributions. However, the default distributions have been calibrated over time through multiple field studies performed at the Technical University of Karlsruhe (PTV 2005), and can be used with confidence for the purpose of this thesis.

Although the majority of distributions implemented in the simulation are based on program default values, desired speed distributions must be defined for vehicles entering and traversing the network. Vehicles entering the network and traversing most links are designated a desired speed following a normal distribution with a minimum of 42.3 miles per hour (mph) and a maximum of 48.5 mph. Vehicles entering any link of length 1,500

feet are slowed to a desired speed following a normal distribution with a minimum of 28.0 mph and a maximum of 32.0 mph. This is done to remain consistent with the speed distribution defined in the network developed by Singh (2006) with an entry speed limit of 45 mph and a speed limit of 30 mph on links 1,500 feet in length. Although these distributions do not exactly match the speed limit designations in Singh's simulation, the data generated are representative of similar speed distributions for the purpose of comparison, and the variability in observed vehicle speed can be used as a continuous input variable to estimate and predict travel time.

3.4 Time-Dependent Network Elements

In a typical urban arterial network, travel demand changes across the network over time. The change in demand relative to the available capacity causes a fluctuation between uncongested and congested conditions on each arterial link. In order to reliably estimate and predict travel time, the models developed must be able to function in all network states. Therefore, it is important that the flow rate on each arterial vary over the time period of the simulation.

In the VISSIM environment, flow rate is designated at the entry point of an arterial in the simulation network. Average flow rate can be designated for particular time intervals within the simulation. For this experiment the flow rate is varied over time in 5-minute intervals between each major arterial, and a separate flow rate distribution is assigned to the set of minor arterials. The flow rate is the same for both directions at the entry points of each arterial. In general, these flow rate distributions result in a movement from an

uncongested, to congested, and back to uncongested state of the network over the course of 100 minutes. Congested conditions are observed during microscopic simulation runs where the traffic demand exceeds the supply offered by the number of lanes and signal timing operation on each arterial. This results in vehicles that can not progress through an intersection following multiple signal cycles, and queue spillback between intersections and from left-turn bays into adjacent through lanes. The time-dependent flow rate distributions for each arterial are shown in Figure 3.2.

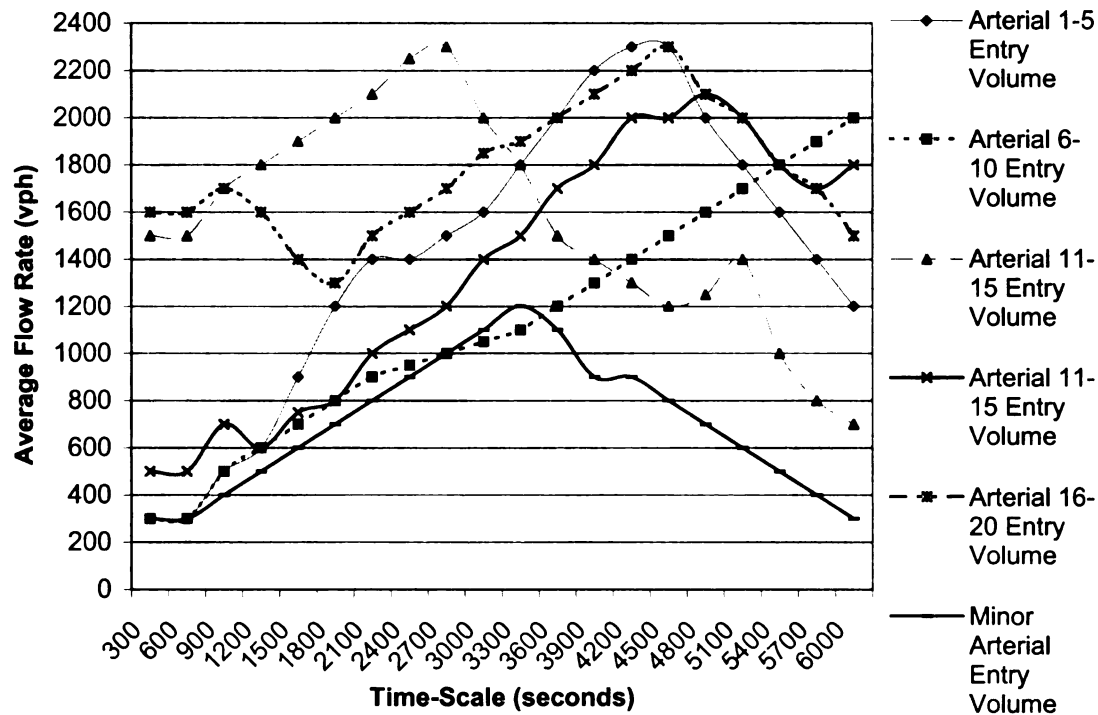


Figure 3.2 – Average Flow Rate Distributions at Entry Points of Arterials.

In addition to changes in flow rate over time across an arterial network, turning movement percentages can be expected to vary as well. Depending on the time of day and the location of particular origins and destinations within an urban arterial network,

the percentage of right-turn, left-turn, and through movements at intersection approaches will differ spatially and temporally. The impact of variable turning movements, which can be expected in a realistic urban arterial network, on the effectiveness of travel time estimation and prediction models is presented in this thesis. Therefore, such variations must be incorporated into the simulation network used to generate modeling data.

The simulation network is a generic representation of a typical urban arterial network. In this case, particular origins, destinations, and travel patterns within the network are not defined. In order to incorporate variable turning movements into the network, 4 time-varying profiles, each, for left-turn and right-turn percentages are defined. These right-turn and left-turn profiles are independently and randomly allocated to each intersection approach within the network. In this manner, both spatial and temporal variations in turning percentages are accounted for, while not causing the data generated to reflect a specific arrangement of travel patterns. The left-turn and right-turn profiles are shown in Figure 3.3 and Figure 3.4, respectively.

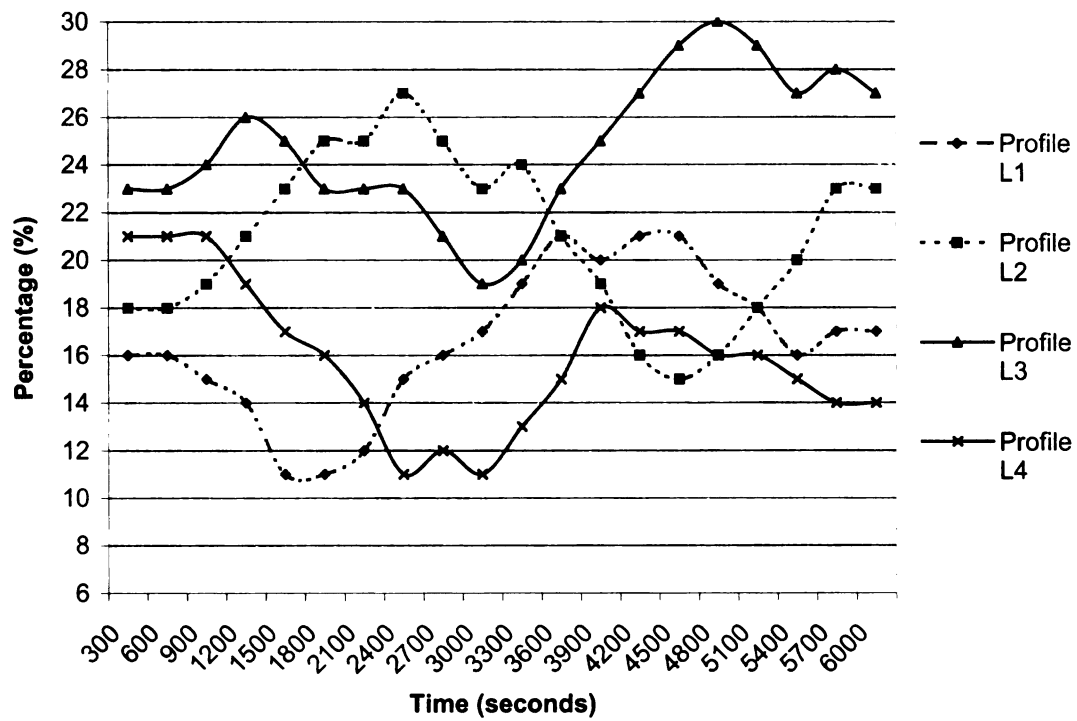


Figure 3.3 – Left-Turn Profiles for Signalized Intersection Approaches.

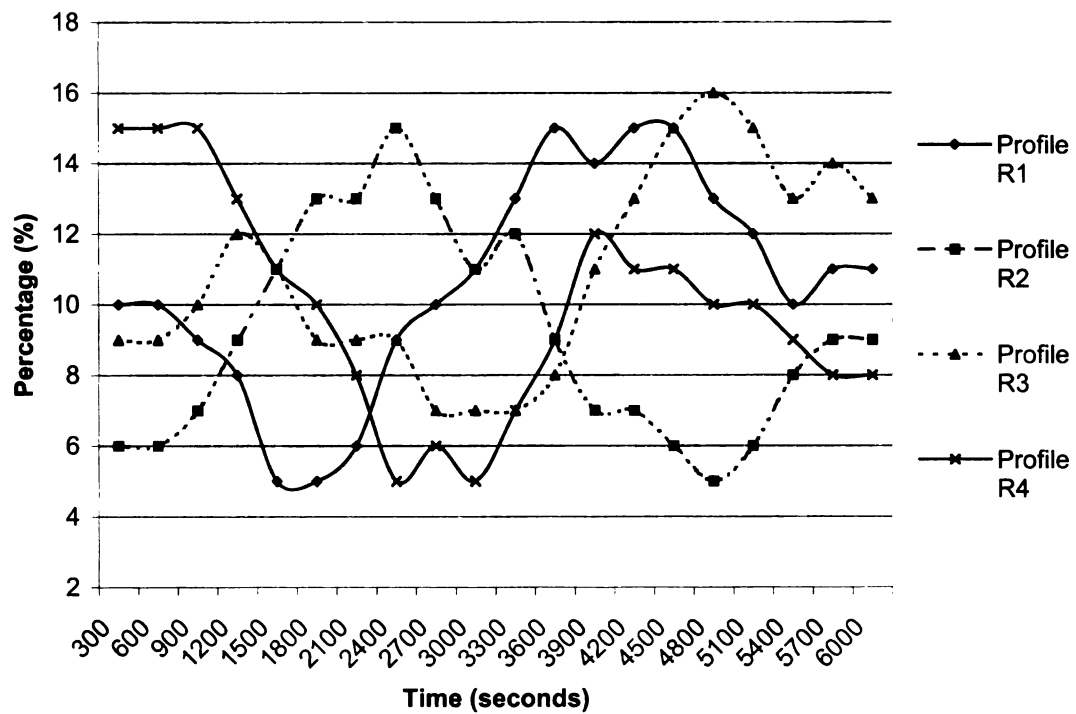


Figure 3.4 – Right-Turn Profiles for Signalized Intersection Approaches.

3.5 Signalized Intersection Control Design Using Synchro

For each intersection in the VISSIM simulation network a traffic signal timing plan must be developed to facilitate the movement of vehicles from one arterial link to another. The timing plan for each intersection designates the duration of each cycle and the allocation of green time to conflicting movements. In order to develop an appropriate signal timing plan for each intersection Synchro, Version 6, is used. Synchro is macroscopic simulation software that is used to optimize cycle lengths, green splits, signal phasing, and offsets for a traffic network.

The main input variables needed to perform signal optimization with Synchro are the flow rate for right-turn, left-turn, and through movements, and the lane configuration of each intersection approach. Additionally, the desired level and direction of progression through a series of intersections can be defined. In this experiment, the east-west arterials are considered the major arterials and carry heavier traffic volumes than the minor north-south arterials, so offsets are determined in terms of east-west progression.

The signal timing plans implemented in this experiment are fixed-time in nature. In other words, changing traffic demands do not alter the signal timing for an intersection. Under this condition, signal timing is designed based on the highest traffic volume typically experienced during a peak one-hour time period. This 'peak-hour' volume is determined for the VISSIM network based on the flow rate and turning movement profiles described in this chapter. The signal phasing, cycle length, and green intervals are optimized with Synchro and input into the VISSIM network.

The optimal signal timing plan for the signalized intersections modeled in this experiment involves a 4-phase operation, based on the geometric design and traffic demand for each intersection approach. Relatively large flow rates throughout the network during the peak-hour result in insufficient gaps to allow left-turning vehicles to progress without a protected left-turn phase in each direction. The typical phasing plan developed for each intersection is shown in Figure 3.5.

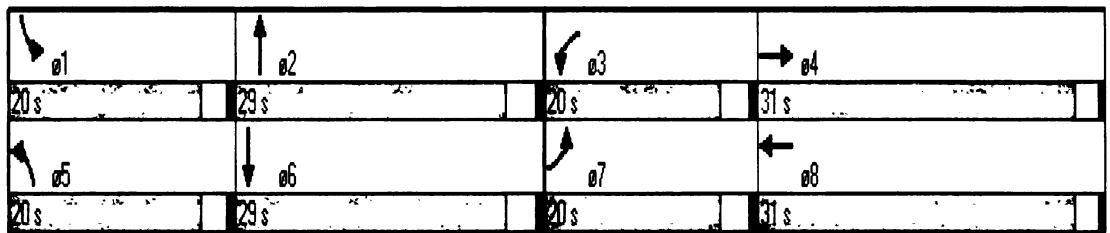


Figure 3.5 – Typical Signal Timing Plan for Signalized Intersections.

3.6 Data Collection from VISSIM Simulation

The data generated through the VISSIM microscopic simulation must be broken down into specific time intervals in order to provide both ample cases for model development, and adequate resolution in terms of changing traffic conditions. As stated in Section 2.3 of this thesis, Mark and Sadek (2004) recommend a temporal resolution of 5 minutes for travel time forecasting. The VISSIM data collection tools report a wide variety of data types that can be averaged for specific 5-minute intervals over the duration of the simulation.

During each 5-minute interval, data representing queue lengths, flow rates, and travel times are collected for each direction on each arterial link. The simulation is run over the course of 100 minutes, resulting in 20 time intervals. It is important to note that the first time interval from $t_0 = 0$ minutes to $t_1 = 5$ minutes is discarded, as at the start of the simulation the network contains no vehicles. Discarding this first interval allows vehicles to reach and fill the interior of the network and thus meaningful data is collected during the subsequent 19 time intervals.

Although VISSIM allows a wide variety of data collection options, the coding procedure to define the necessary parameters is time consuming. For this reason, three major arterials and one minor arterial are identified for this study. Data is collected for arterials 6-10, 16-20, 21-25, and 3-23. These arterials are each comprised of 4 links carrying traffic in two directions, for a total of 32 data collection points. Over the course of 19 time intervals, a total of 608 cases are generated containing data relative to queue length, flow rate, and travel time.

In addition to the data generated through VISSIM simulation, data corresponding to signal timings for each arterial link approach are determined for each of the 608 cases. Signal control data are taken from the timings input to VISSIM from the Synchro optimization for the length of green interval, red interval, and intersection offset. Additionally, link lengths are recorded for each arterial link.

The final variables defined for each data case represent average speeds for right-turn, left-turn, and through vehicle movements. In VISSIM, individual vehicle movements are tracked such that average travel time can be measured specifically for right-turn, left-turn, and through progressions from the start of an arterial link through the end of the next

downstream intersection. However, average speed can not be differentiated by movement for vehicles traversing a link. So, average observed travel times are used to compute average vehicle speed based on link length for each possible movement along an arterial link. Average speed for each case is computed in this manner.

3.7 VISSIM Simulation Runs and Model Validation

For the purpose of developing travel time estimation and prediction models, the generation of 608 data cases is determined to be sufficient to explore the relationship between travel time and the variables that impact the state of an arterial link. Each case represents spatial and temporal changes in traffic operations typical of many urban arterial networks. In total, 14 candidate variables describing link operations are identified for use in the modeling procedure.

Despite the extensive and variable dataset that is generated using VISSIM, it is important to realize that in microscopic simulation, the data generated are dependent on the random seed chosen. The random seed controls stochastic variations in the simulation such as vehicle generation patterns, and can impact the value of the simulation outcomes. The models presented in this thesis are developed based on the data generated in the initial simulation run. This dataset is referred to as the ‘training set.’ Each model is then validated using data from the second simulation run with an different independent random seed. The second dataset is referred to as the ‘testing set.’

Chapter 4

Multivariate Linear Regression for Average Link Speed Estimation

The average vehicle speed on an arterial link is an important variable linked to travel time estimation and short-term prediction. Existing surveillance devices such as loop detectors and cameras are mainly capable of estimating vehicle speeds at discrete locations on an arterial link. Furthermore, the location of surveillance devices can heavily influence the accuracy of speed estimation. For example, a camera located in proximity to an intersection approach may detect speeds that are lower than would be detected at the midpoint of the link, as vehicles slow and are often stopped with zero velocity due to traffic signal control. In order to reliably determine travel time along an arterial link, average speed must be estimated along the entire length of the link. Using other more reliable data collected using existing surveillance devices, such as queue length and flow rate, along with signal control parameters and link geometric information, multivariate linear regression models are presented in this chapter to more accurately estimate average speeds for arterial links.

4.1 Multivariate Linear Regression Methodology

Multivariate linear regression is a powerful statistical tool used to model the relationship between a dependent (response) variable and a set of independent (explanatory) variables. A linear regression equation is developed to mathematically explain this relationship.

For example, given the dependent variable Y and independent variables $X_1, X_2, X_3 \dots X_n$, the linear regression equation is expressed as:

$$Y = \beta_0 + \beta_1 X_1 + \beta_2 X_2 + \beta_3 X_3 + \dots \beta_n X_n + \delta$$

Each independent variable is assigned a parameter β_n that is known as the partial regression coefficient. The partial coefficient designates the statistical influence of each corresponding independent variable on the dependent variable while the values of the other independent variables in the model are controlled. The parameter β_0 is known as the regression constant and the error term is labeled as δ (Kutner et al. 2004). Assuming the expected value of the error coefficient $\delta = 0$, the regression equation is simplified as:

$$Y = \beta_0 + \beta_1 X_1 + \beta_2 X_2 + \beta_3 X_3 + \dots \beta_n X_n$$

The purpose of multivariate linear regression in this thesis is to accurately estimate the average value of speed on an arterial link for inclusion in State-Space Neural Network (SSNN) models to estimate and predict travel time. SSNN models are developed to estimate and predict travel time for left-turn, right-turn, and through vehicles. Therefore, three linear regression models are developed to estimate average link speed for each possible movement. The average speed value is the dependent variable and is labeled as S_L , S_R , and S_T for average left-turn, right-turn, and through speeds, respectively.

The candidate independent variables are variables that can be easily measured in the field using existing surveillance infrastructure. These variables include measures of travel

demand, traffic signal control, queue length, and link geometrics, and are shown in Table 4.1.

Table 4.1 – Candidate Independent Variables for Multivariate Linear Regression.

<i>Travel Demand</i>	V_T	Average flow rate for through movement
	V_R	Average flow rate for right-turn movement
	V_L	Average flow rate for left-turn movement
	V_X	Average flow rate for approach conflicting right-turn movement
<i>Signal Control</i>	G_T	Length of green interval for through and right-turn phases
	G_L	Length of green interval for left-turn phase
	Off	Offset between adjacent signalized intersections
	R	Length of red interval for approach
<i>Queue Length</i>	Q_T	Maximum queue length for through and right-turn lanes
	Q_L	Maximum queue length for dedicated left-turn lanes
<i>Geometric</i>	LL	Link length

In order to determine the appropriate independent variables to include in each average speed estimation linear regression model, SPSS for Windows, Version 15.0 is utilized. SPSS is a software tool used to analyze a wide variety of statistical measures and develop statistical models for a given dataset. The data generated using VISSIM microscopic simulation, including 608 individual cases as described in Chapter 3, are entered into a spreadsheet within the SPSS program. Each case contains data relative to the dependent and independent variables defined in this section. Statistical tests are performed on this dataset to develop regression models to estimate average link speed.

In general, the independent variables in a multivariate linear regression model should be independent of one another (Kutner et al. 2004). In other words, a change in one

independent variable does not correlate with changes in another independent variable. Following this logic, each independent variable in the model will explain a different portion of change in the dependent variable. The change relationship between variables is examined through correlation statistics. Using SPSS, significant correlations between candidate independent variables are identified. In the following modeling steps independent variables with strong correlations are not included in the same regression model.

Multivariate regression models can be developed in a variety of ways once the candidate independent variables are identified. A linear regression model may include all possible independent variables. However, in order to develop more accurate and efficient models that require limited data collection, it is desirable to limit each model to include only key variables that explain a significant change in the dependent variable, so long as such models are accurate. A step-wise regression procedure is used to identify the most influential explanatory variables for use in each model, and filter out those variables that do not explain a significant amount of variance in the response variable.

Step-wise regression modeling is based on the method of least squares. For the sample linear regression equation defined previously in this section, the partial coefficients $\beta_0, \beta_1, \beta_2 \dots \beta_n$ are determined by minimizing the value of the square of the regression equation, L , for the given sample of observations, as defined in the following equation:

$$L = \sum_{i=1}^n (Y_i - \beta_0 - \beta_1 X_{i1} - \beta_2 X_{i2} - \beta_3 X_{i3} - \dots - \beta_n X_{in})^2$$

In the step-wise procedure the partial coefficients are computed in stages based on the ability of each independent variable to explain additional variance in the response

variable. The independent variable with the strongest correlation to the dependent variable is included first in the model. The square of the correlation coefficient, R^2 , is calculated for each step, where the R^2 statistic ranges in value from 0.0 to 1.0. The R^2 statistic describes how well the set of independent variables explains the variance in the dependent variable, where $R^2 = 1.0$ represents a perfect linear relationship. In each step a single independent variable with the next strongest correlation to the dependent variable is added to the model, until the R^2 statistic is not significantly improved.

4.2 Linear Regression Models for Link Speed Estimation

The multivariate linear regression models to estimate average vehicle speed are derived from the training dataset generated through the initial VISSIM microscopic simulation run. This dataset consists of 608 cases representing the state of 16 arterial links. Each model is then validated by applying the model to the testing dataset generated through another independent simulation run. In Chapter 5 the modeling approach for the use of SSNN models is discussed, and the need to normalize the dataset is presented. In order to maintain consistency in the analysis for this thesis, both the training and testing datasets are normalized prior to linear regression modeling for speed estimation. The normalization of data does not alter the correlations between variables, and the results presented in this chapter will be shown in terms of normalized values.

Multiple trials of linear regression modeling are performed to increase the R^2 statistic and to improve the efficiency of the model through careful selection of candidate variables. Through the modeling procedure it is found that more accurate models are derived when

major and minor arterial links are considered separately. A total of six regression models are developed, including estimation models for left-turn, right-turn, and through movement speed for both major and minor arterial groups.

Each linear regression model is derived from the training dataset and the performance of each model is evaluated based on the resulting R^2 statistic. A plot of the actual average speed observed in simulation versus the average speed estimated using the regression model is generated to provide a visual interpretation of the performance of the model. Each model is applied to the testing dataset to validate the performance of the model with an independent source of data. Scatter plots for the training and testing datasets, including a line of best fit and resulting R^2 statistics, are presented for all six linear regression models developed.

4.3 Average Speed Estimation Models for Major Arterials

Linear regression models are developed to estimate average vehicle speed for left-turn, right-turn, and through movements for both major and minor arterials. As defined in Section 2.1, a major arterial is comprised of a series of consecutive arterial links that serve relatively large traffic flows and are more significant in terms of network operation than minor arterials. In the arterial network for this thesis, data is collected on the links comprising major arterials 6-10, 16-20, and 21-25. The data collected from these arterials in microscopic simulation include 456 cases and are used to derive the models presented in this section.

The linear regression model for through speed estimation on major arterials is:

$$S_T = .352 + .346 LL - .544 Q_T + .285 G_T + .134 Off - .070 V_L$$

The plots of actual versus estimated average through speed are shown in Figures 4.1 and 4.2 for the training and testing datasets, respectively. This model performs reasonably well, with an R^2 statistic of .807 for the training set. The performance of the model is validated in the testing set, with a similar distribution pattern and a R^2 statistic of .781. Although the model is not perfect, speed estimation is an intermediate step in the modeling procedure for this thesis, and estimated speed will be one of several variables included in the SSNN models for travel time estimation and prediction.

The linear regression model for left-turn speed estimation on major arterials is:

$$S_L = .497 + .379 LL - .461 Q_L - .149 V_T + .120 G_L - .160 V_L$$

The plots of actual versus estimated average left-turn speed are shown in Figures 4.3 and 4.4 for the training and testing datasets, respectively. This model performs reasonably well, with an R^2 statistic of .793 for the training set. The performance of the model is validated in the testing set, with a similar distribution pattern and a R^2 statistic of .777.

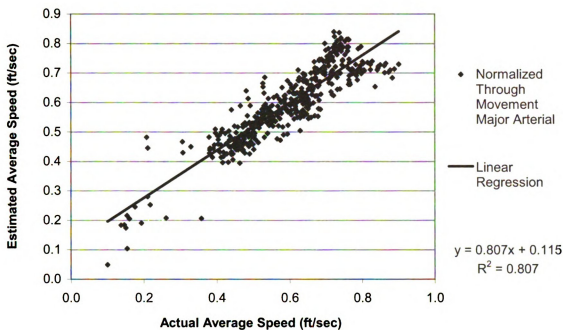


Figure 4.1 – Training Plot for Normalized Actual Average Speed versus Normalized Estimated Average Speed for Through Movement on Major Arterials.

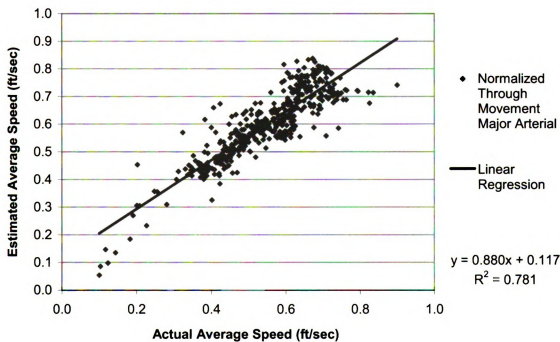


Figure 4.2 – Testing Plot for Normalized Actual Average Speed versus Normalized Estimated Average Speed for Through Movement on Major Arterials.

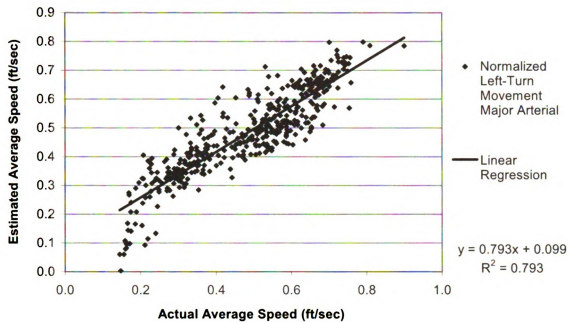


Figure 4.3 – Training Plot for Normalized Actual Average Speed versus Normalized Estimated Average Speed for Left-Turn Movement on Major Arterials.

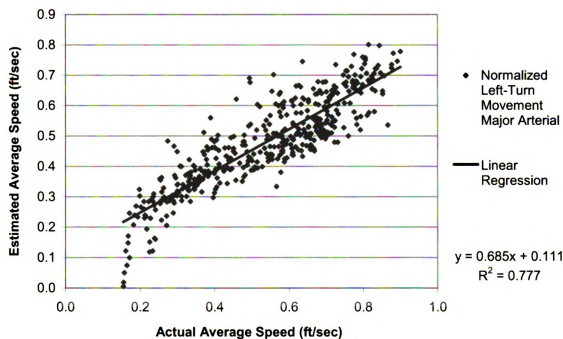


Figure 4.4 – Testing Plot for Normalized Actual Average Speed versus Normalized Estimated Average Speed for Left-Turn Movement on Major Arterials.

The derivation of the speed estimation model for right-turns requires more in-depth analysis than the modeling procedure described for through and left-turn speed estimation. Initial modeling based on the 11 independent variables defined in Table 4.1 results in poor R^2 statistics and significant derivations between the training and testing sets. Further exploration of correlation and residual statistics reveals that the candidate variables do not capture or explain the variability in right-turn speed to an acceptable level.

In order to more accurately model average right-turn speed, the relationship between right-turn speed and through speed is explored. In the VISSIM simulation model, there are no exclusive right-turn lanes. Instead, right-turning vehicles share the rightmost lane with through moving vehicles. Right-turning vehicles also share the same green interval with through vehicles at each intersection approach. Therefore, it is likely that right-turning vehicles have a similar average speed and flow in a similar manner as through vehicles on a particular link.

Figure 4.5 is a scatter plot that displays the relationship between average right-turn speeds and average through movement speeds on major arterial links. There is a linear pattern observed for the majority of the points. This line is shown in Figure 4.5 to have a nearly 1:1 slope (this line is not a regression line), signifying that right-turn and through movement average speeds are nearly the same on major arterial links. There is a secondary set of points outlined with an oval in Figure 4.5 that diverge from the typical relationship, but still appear to have a somewhat parallel linear relationship.

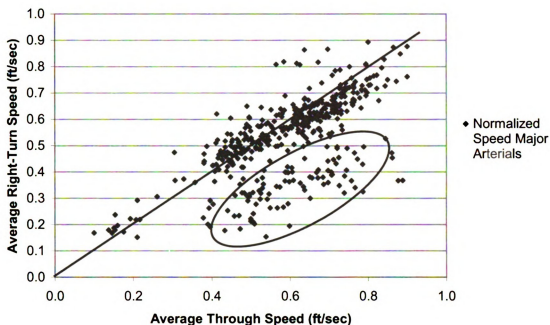


Figure 4.5 – Normalized Average Through Speed versus Normalized Average Right-Turn Speed on Major Arterials.

The linear relationship between right-turn and through speeds on major arterial links implies that average through speed is a strong predictor of right-turn speed. For this reason, the estimated average through speed for each case in the training and testing datasets is calculated based on the previously defined regression equation. The variable for estimated average through speed, S_T , is included in the step-wise regression procedure for right-turn speed estimation. In order to avoid correlations between independent variables, the independent variables included in the through speed estimation model are excluded from consideration in the right-turn speed estimation model.

The resulting linear regression model for right-turn speed estimation on major arterials is:

$$S_R = .281 + .671 S_T - .289 V_T$$

The plots of actual versus estimated average right-turn speed are shown in Figures 4.6 and 4.7 for the training and testing datasets, respectively. The performance of the model is less than desirable, with an R^2 statistic of .440 for the training set. Additional statistics are explored, including correlations between various stratifications of the candidate independent variables and right-turn speed. However, none of these measures reveal any explanatory relationships or improvements in the model. The performance of the model is validated in the testing set, with a similar distribution pattern and a R^2 statistic of .389.

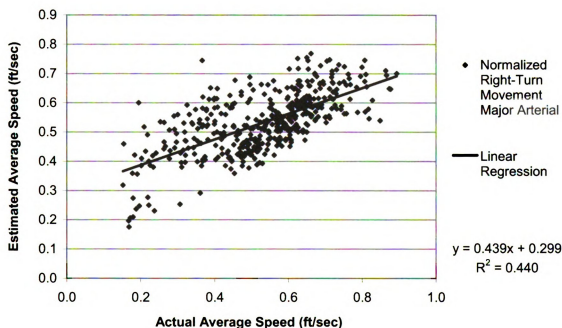


Figure 4.6 – Training Plot for Normalized Actual Average Speed versus Normalized Estimated Average Speed for Right-Turn Movement on Major Arterials.

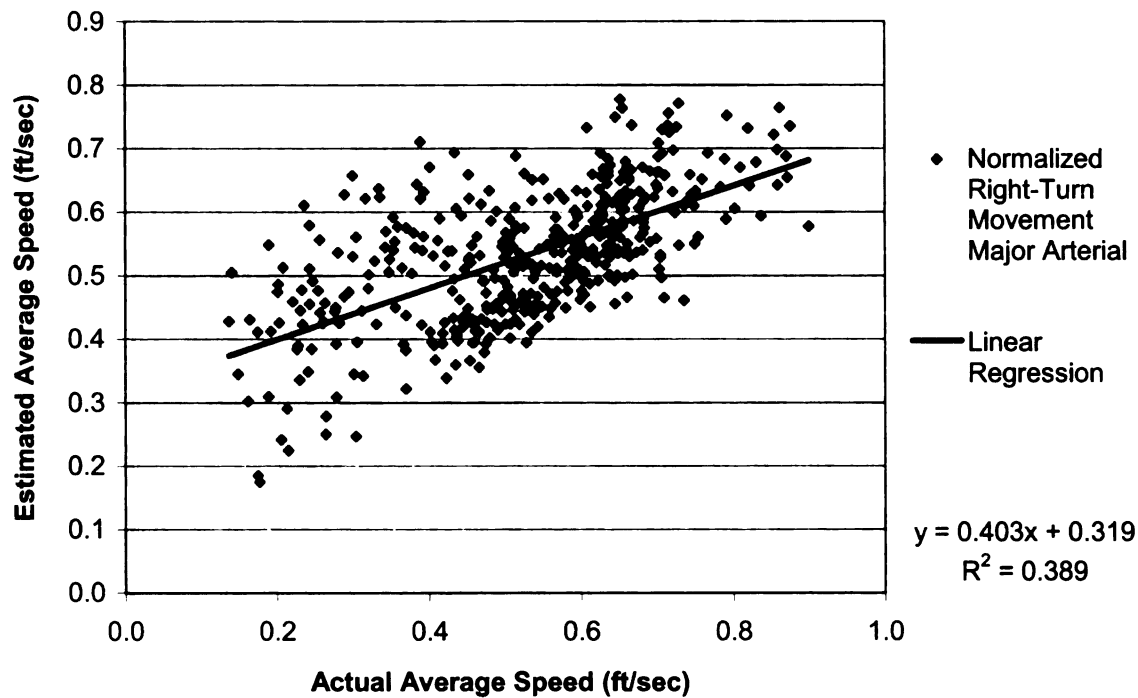


Figure 4.7 – Testing Plot for Normalized Actual Average Speed versus Normalized Estimated Average Speed for Right-Turn Movement on Major Arterials.

4.4 Average Speed Estimation Models for Minor Arterials

Minor arterials carry lesser average traffic flow than major arterials, but are important nonetheless in terms of travel time estimation and prediction for an arterial network. In the arterial network for this thesis, data is collected on the links comprising the minor arterial 3-23. The data collected on this arterial includes 114 cases and are used to derive the models presented in this section.

The linear regression model for through speed estimation on minor arterials is:

$$S_T = .615 + .323 LL - .887 Q_T$$

The plots of actual versus estimated average through speed are shown in Figures 4.8 and 4.9 for the training and testing datasets, respectively. This model performs reasonably well, with an R^2 statistic of .712 for the training set. The performance of the model is validated in the testing set, with a similar distribution pattern and a R^2 statistic of .729.

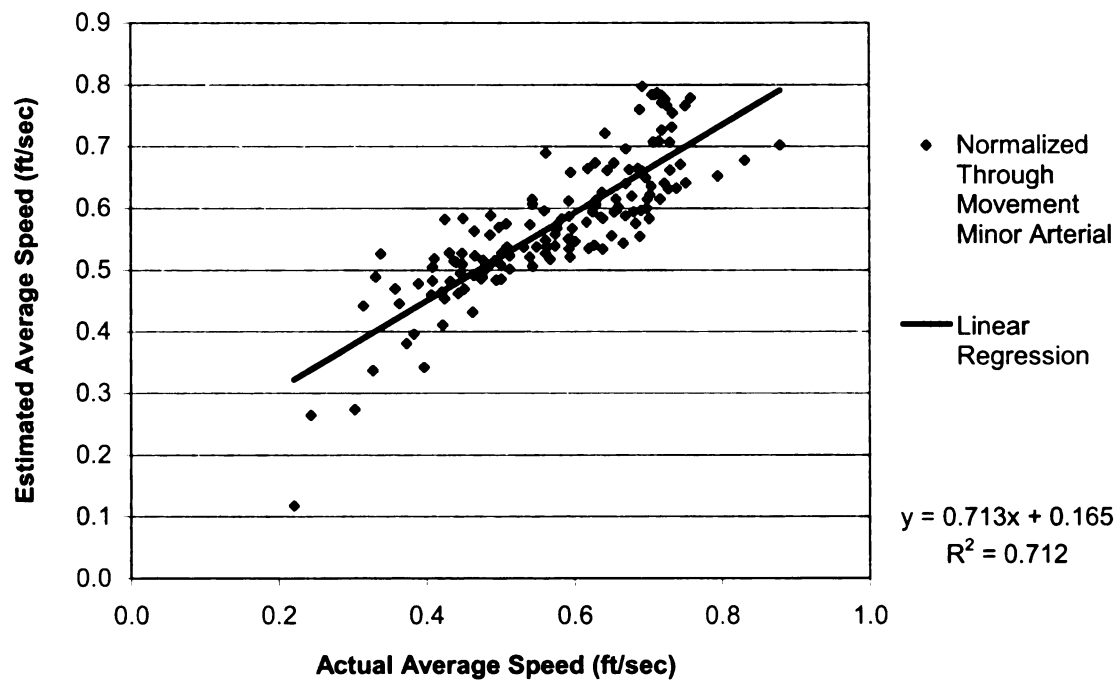


Figure 4.8 – Training Plot for Normalized Actual Average Speed versus Normalized Estimated Average Speed for Through Movement on Minor Arterials.

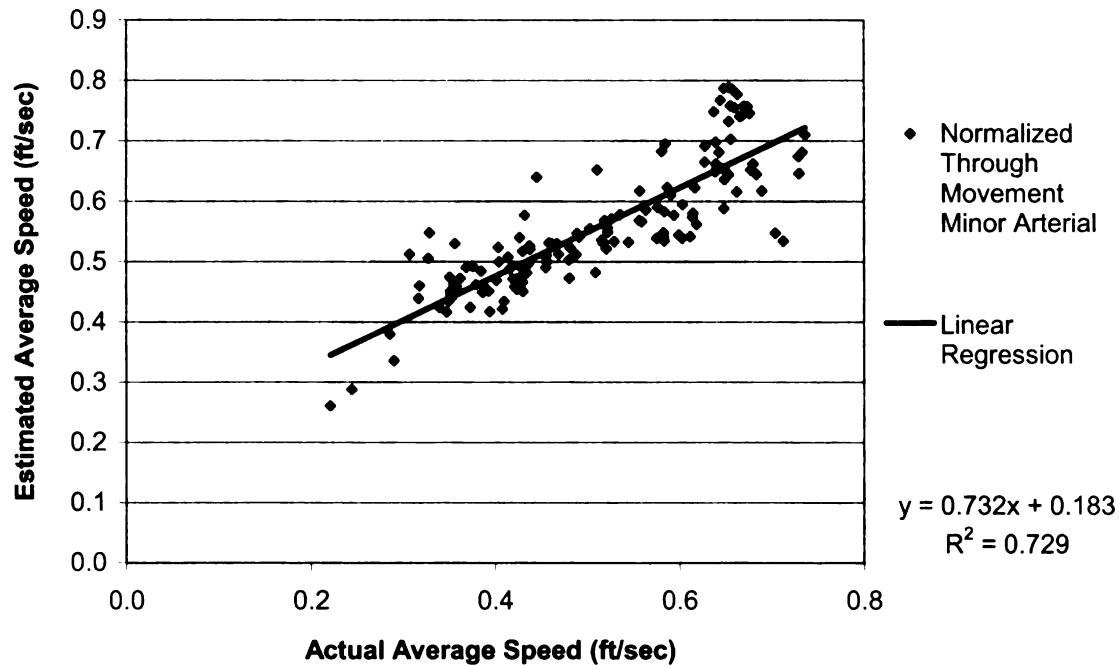


Figure 4.9 – Testing Plot for Normalized Actual Average Speed versus Normalized Estimated Average Speed for Through Movement on Minor Arterials.

The linear regression model for left-turn speed estimation on minor arterials is:

$$S_L = .453 + .387 LL - .843 Q_L + .268 G_L - .218 V_L$$

The plots of actual versus estimated average left-turn speed are shown in Figures 4.10 and 4.11 for the training and testing datasets, respectively. This model performs reasonably well, with an R^2 statistic of .728 for the training set. The performance of the model is validated in the testing set, with a similar distribution pattern and a R^2 statistic of .629.

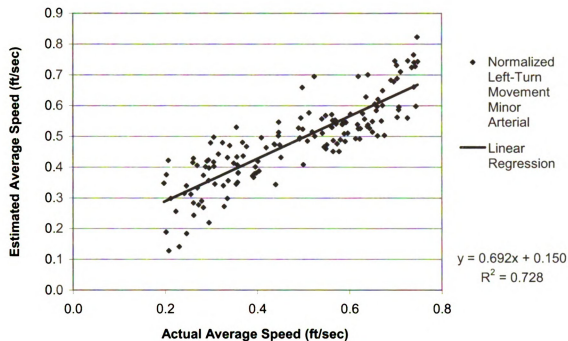


Figure 4.10 – Training Plot for Normalized Actual Average Speed versus Normalized Estimated Average Speed for Left-Turn Movement on Minor Arterials.

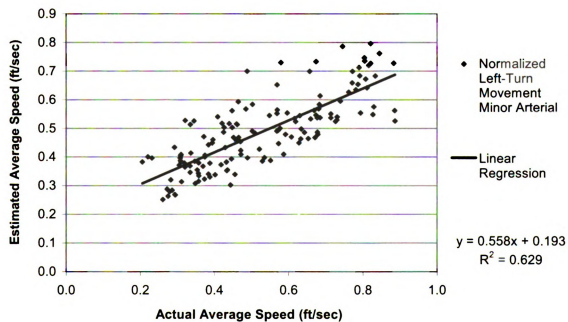


Figure 4.11 – Testing Plot for Normalized Actual Average Speed versus Normalized Estimated Average Speed for Left-Turn Movement on Minor Arterials.

The derivation of the speed estimation model for right-turns on minor arterials follows the same procedure as described for major arterials. The initial set of candidate variables results in poor R^2 statistics and significant derivations between the training and testing sets. Further exploration of the data pertaining to minor arterials reveals a strong correlation between average right-turn speed and average through movement speed. The resulting linear regression model for right-turn speed estimation on minor arterials is:

$$S_R = .028 + .526 S_T + .341 R - .209 V_X + .112 Off$$

This model is similar to the right-turn speed estimation model for major arterials, with the addition of explanatory variables corresponding to the red interval for the approach and the conflicting through volume on the crossing major arterial. These variables are likely correlated to right-turn speed on minor arterials because of the influence on right-turn-on-red movements. On major arterials heavier flows are experienced, and a heavier volume of through traffic may block right-turning vehicles from turning during the red interval more frequently than on minor arterials where flows are lighter. Thus, on minor arterials there may be an advanced opportunity to turn right-on-red, and these variables are included in the right-turn speed estimation model.

The plots of actual versus estimated average right-turn speed are shown in Figures 4.12 and 4.13 for the training and testing datasets, respectively. The performance of the model is less than desirable, with an R^2 statistic of .416 for the training set. Additional statistics are explored, including correlations between various stratifications of the candidate independent variables and right-turn speed. However, none of these measures reveal any

explanatory relationships or improvements in the model. The performance of the model is validated in the testing set, with a similar distribution pattern and a R^2 statistic of .316.

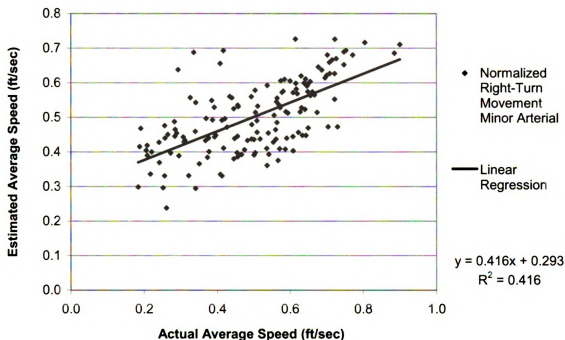


Figure 4.12 – Training Plot for Normalized Actual Average Speed versus Normalized Estimated Average Speed for Right-Turn Movement on Minor Arterials.

Although the predictive capability of right-turn speed estimation models for major and minor arterials is not as accurate as for the left-turn and through movement, the impact on travel time estimation is not yet clear. As previously stated, estimated average speed is only one of the input variables used in travel time estimation and prediction. Additionally, the overlying goal of this thesis is to create models that can accurately predict travel time for a route within an arterial network. Despite the inaccuracy of right-turn speed estimation models, the SSNN models may be able to overcome this deficiency in terms of overall travel time estimation and prediction capability.

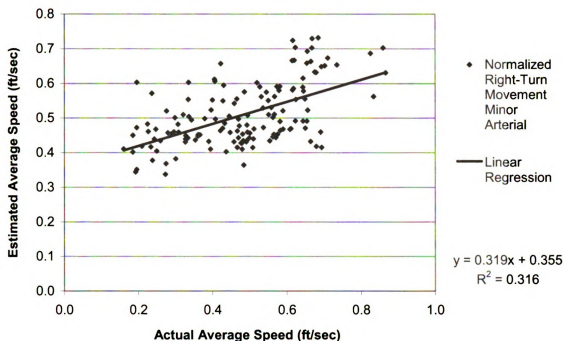


Figure 4.13 – Testing Plot for Normalized Actual Average Speed versus Normalized Estimated Average Speed for Right-Turn Movement on Minor Arterials.

The independent variables with the strongest correlation to the dependent variable are the same between the average speed estimation models for each of the left-turn, right-turn, and through movements. This supports the validity of the models in that the relationships between independent variables and through vehicle speed are similar throughout the network, and that the relationships observed are not arbitrary or descriptive of only certain links. This is a promising result leading into the development of SSNN models for the estimation and prediction of travel time.

Chapter 5

State-Space Neural Network Modeling Methodology

Traffic conditions in an arterial network are dynamic and constantly changing in time and space based on a variety of influences. Traffic control devices, traffic demand, weather, incidents, available capacity, and a number of other variable factors can impact the state of an arterial link. In 2006, Singh established that Artificial Neural Networks (ANN) are useful to model the dynamic relationship between traffic conditions and travel time. Singh developed a series of State-Space Neural Network (SSNN) models, which are a variation of ANN, to estimate and predict travel time for right-turn, left-turn, and through movements on arterial links. The results presented by Singh prove that the modeling framework developed is useful for the purpose of this thesis.

While these models were shown to be successful in the results presented by Singh (2007), the data used to develop the models did not account for variations in turning movements at intersection approaches. The operation of a signalized intersection is crucial in determining the state of the arterial links that feed the intersection. Turning movement patterns vary over time and between intersections in a typical arterial network. In order to develop SSNN models that are truly robust and applicable to the urban arterial environment, dynamic turning movement patterns must be incorporated into the modeling procedure. Variable turning movements are incorporated into the microscopic simulation used in this experiment as described in Chapter 3.

The dynamic relationship between travel time and the state of an arterial link is expected to be influenced due to the incorporation of variable turning movements. The success of the SSNN modeling framework in estimating and predicting travel time depends on the ability of the models to adapt to a more realistic situation where turning movement percentages are not constant.

5.1 State-Space Neural Networks

State-Space Neural Networks (SSNN) are a generic form of ANN that can be used to model dynamic non-linear systems, such as the state of traffic in an arterial network. SSNN modeling incorporates local feedback loops that allow the model to “learn” from variations in the input data over a series of iterations. Elman (1990) developed a general recurrent neural network framework consisting of an input layer, a hidden layer, a context layer, and an output layer, as shown in Figure 5.1.

In this framework, the dotted lines represent trainable connections whereby the appropriate weights between layers are learned. The solid line represents a non-trainable connection, which enables the context layer to store values from the hidden layer for the past time period. For dynamic systems, this context layer provides a built-in short-term memory for the model to learn from previous iterations.

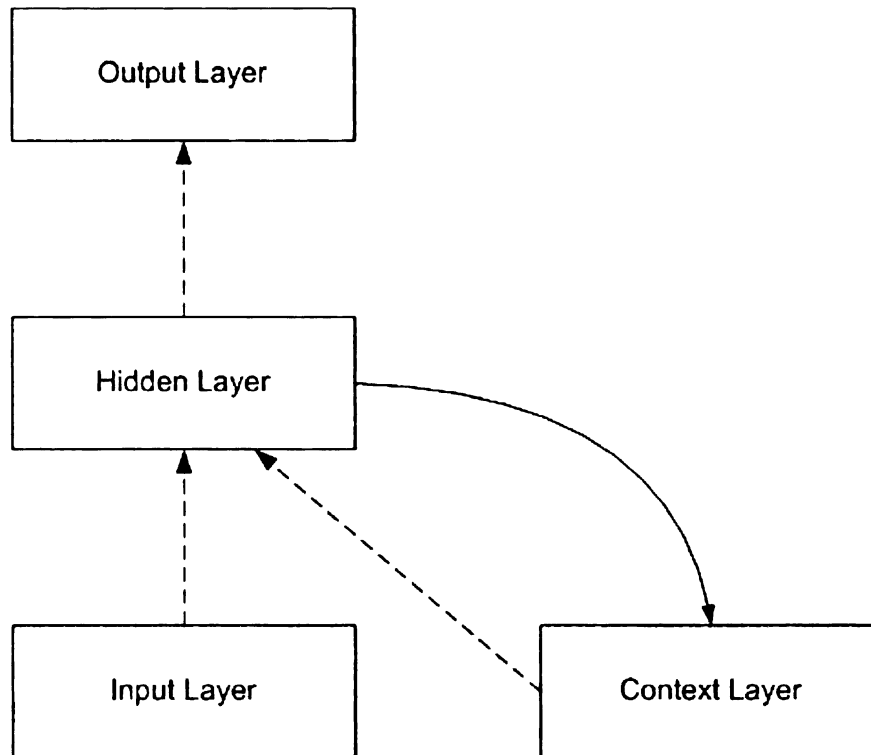


Figure 5.1 – Simple Neural Network Framework.

5.2 State-Space Neural Network Topology

Based on the general framework of the neural network model presented in Figure 5.1, SSNN models are developed for the purpose of estimating and predicting travel time on urban arterial links. Singh (2006) developed separate modeling frameworks for both travel time estimation and short-term prediction. This is necessary due to the time intervals considered in each case. The SSNN models are trained using data representing the state of several arterial links. Therefore, this topology will produce travel time estimations and predictions for links, and not routes. Such travel times are aggregated to estimate and predict travel time for arterials and arterial routes.

5.2.1 SSNN Topology for Travel Time Estimation

The SSNN model for travel time estimation consists of an input layer, a hidden layer, a context layer, and an output layer, following the structure of the Elman model. The input layer contains an input vector consisting of variables that influence travel time at the current departure time period t . This vector is designated as $U(t)$. The hidden layer represents the state of the system at time t , and is designated as $X(t)$. The hidden layer activates the nodes in the context layer in a single time step. The context layer serves as the short-term memory for the model, as the context layer represents the state of the system at time $t-1$. The output layer represents the average travel time estimated at time period t for the set of input variables. The SSNN topology for travel time estimation is shown in Figure 5.2.

5.2.2 SSNN Topology for Travel Time Prediction

The SSNN model for travel time prediction is similar to that of travel time estimation, except that the time period analyzed is different. The input layer contains an input vector consisting of variables that influence travel time at the current departure time period t , including the travel time estimated at time t . The hidden layer for travel time prediction represents the state of the system at time $t+1$, and the context layer represents the state of the system at time t . The output layer represents the average travel time at time period $t+1$, and is therefore a single step travel time prediction. The SSNN topology for travel time estimation is shown in Figure 5.3.

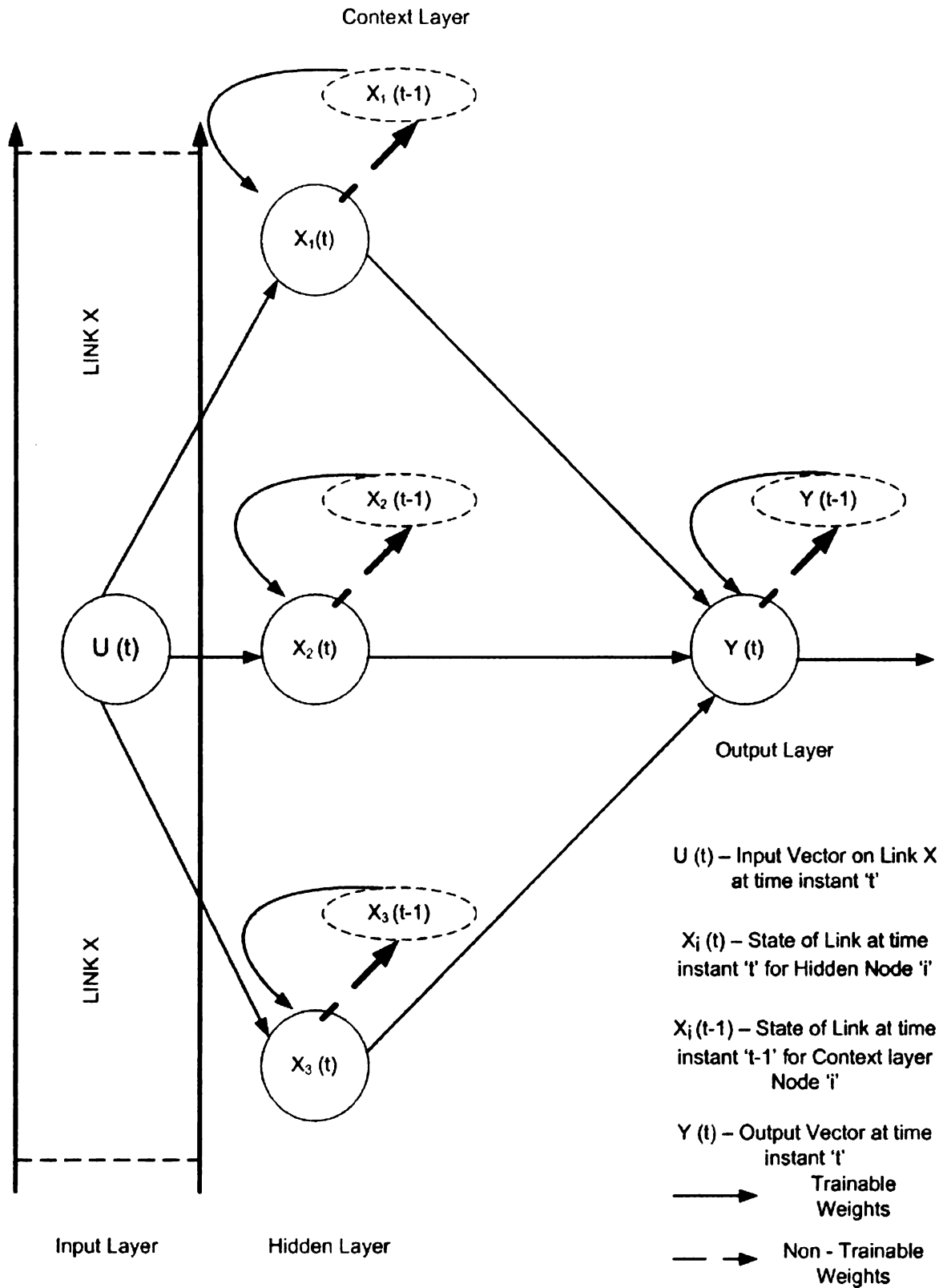


Figure 5.2 – State-Space Neural Network Topology for Travel Time Estimation.

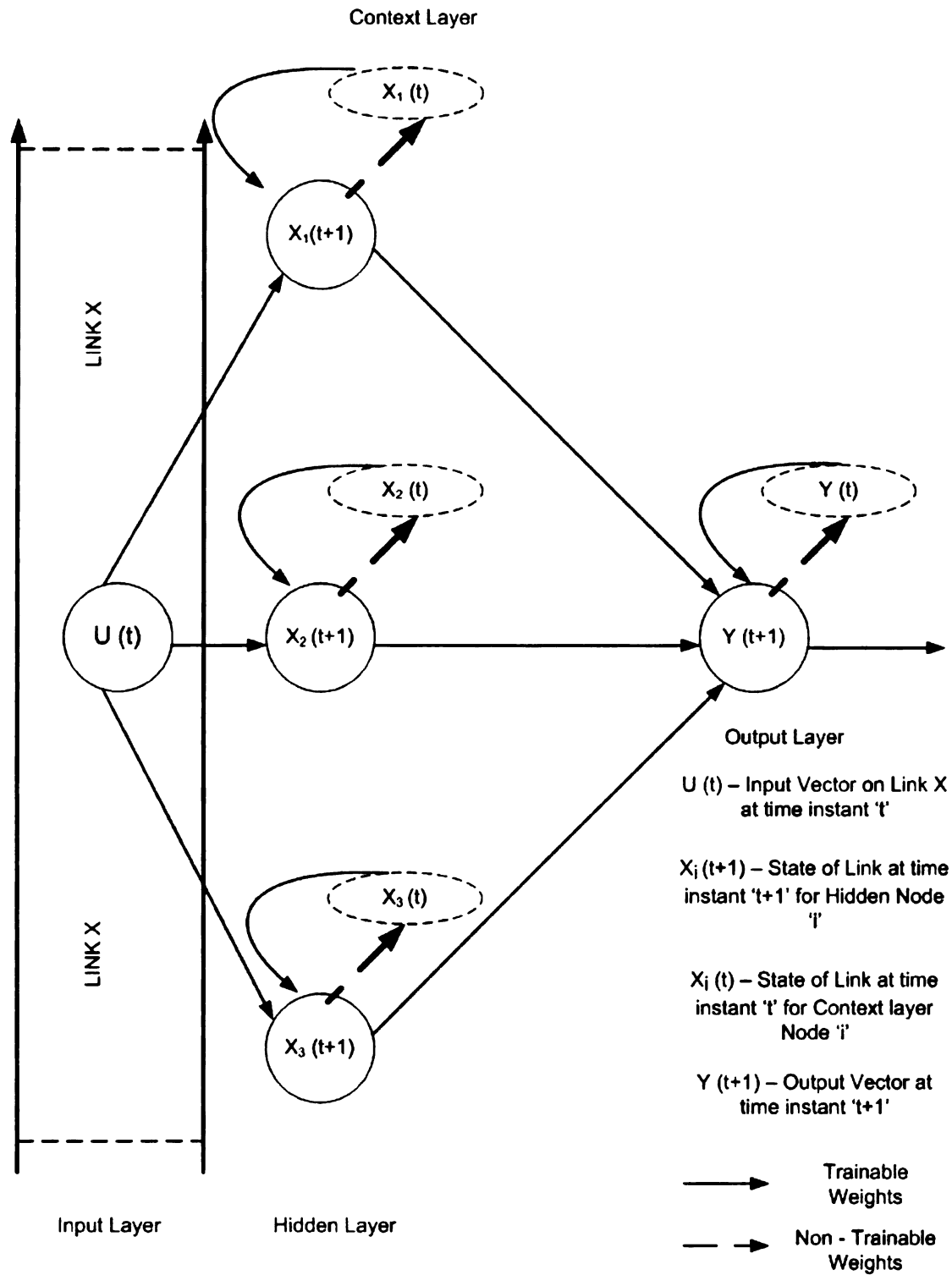


Figure 5.3 – State-Space Neural Network Topology for Travel Time Prediction.

The topology shown in Figure 5.2 and Figure 5.3 contains exactly 3 nodes in the hidden and context layers for both the travel time estimation and prediction models. The framework developed by Elman and shown in Figure 5.1 contains only one node, or neuron, in both the hidden and context layers. Rivals and Personnaz (1996) present that the state of the neural network elements can be computed using any number of hidden neurons depending on the complexity of the system.

Travel time estimation and prediction models are developed for right-turn, left-turn, and through movement travel time estimation and prediction. The topology defined in Figure 5.2 and 5.3 is a general representation of the framework that is applied for all three movements. As the complexity in travel time estimation and prediction between through and turning movements is expected to vary, the number of hidden neurons is also expected to differ. In order to determine the proper number of hidden nodes for the travel time estimation and prediction SSNN models, a range of 3 to 10 neurons is tested to determine the optimal state-space representation for each movement. For both the estimation and prediction models utilized in this thesis, the number of hidden neurons equals 4 for through movement, and 10 for right-turn and left-turn movements.

5.3 State-Space Neural Network Training and Testing

The SSNN models for travel time estimation and prediction for left-turn, right-turn, and through movements are replicated using MATLAB computing software, Version 7.0. The program code was written by Singh (2006) and has been modified for use in this thesis. The code was developed following the guidelines for learning rate, momentum

constant, and the number of hidden nodes documented by Haykin (1999). A generic version of the SSNN programming code is provided in Appendix A. For each model, the training dataset is fed to the network in a sequential pattern corresponding to the time intervals of the microscopic simulation. This allows the model to learn the temporal fluctuations in the variables that influence travel time.

The input layer of each SSNN model consists of a single node, which is defined by an input vector comprised of a set of explanatory variables. The input variables for this thesis are variables that influence traffic conditions on an arterial link, and that are easily collected using existing surveillance infrastructure. These variables are defined in Section 2.1 and include V_T , V_R , V_L , S_T , S_R , S_L , G_T , G_L , R , Off , Q_T , Q_L , and LL . The output layer of each SSNN model is travel time for either the current or one-step future time period. The specific input and output variables for each model are defined in Table 5.1 and 5.2.

Table 5.1 – Input and Output Variables for SSNN Travel Time Estimation Models.

SSNN Travel Time Estimation Models	Input Variables (current time period)	Output Variable (current time period)
SSNN-Thru	V_T , V_R , V_L , S_T , G_T , R , Off , Q_T , and LL .	TT_T
SSNN-Left	V_T , V_R , V_L , S_L , G_L , R , Off , Q_L , and LL .	TT_L
SSNN-Right	V_T , V_R , V_L , S_R , G_T , R , Off , Q_T , and LL .	TT_R

Table 5.2 – Input and Output Variables for SSNN Travel Time Prediction Models

SSNN Travel Time Prediction Models	Input Variables (current time period)	Output Variable (future time period)
SSNN-Thru	<i>Estimated TT_T, V_T, V_R, V_L, S_T, G_T, R, Off, Q_T, and LL.</i>	TT_T
SSNN-Left	<i>Estimated TT_L, V_T, V_R, V_L, S_L, G_L, R, Off, Q_L, and LL.</i>	TT_L
SSNN-Right	<i>Estimated TT_R, V_T, V_R, V_L, S_R, G_T, R, Off, Q_T, and LL.</i>	TT_R

As the training data are fed to the MATLAB neural network program, a training graph is plotted that details the performance of the model over a series of epochs, or iterations. A sample training plot is shown in Figure 5.4.

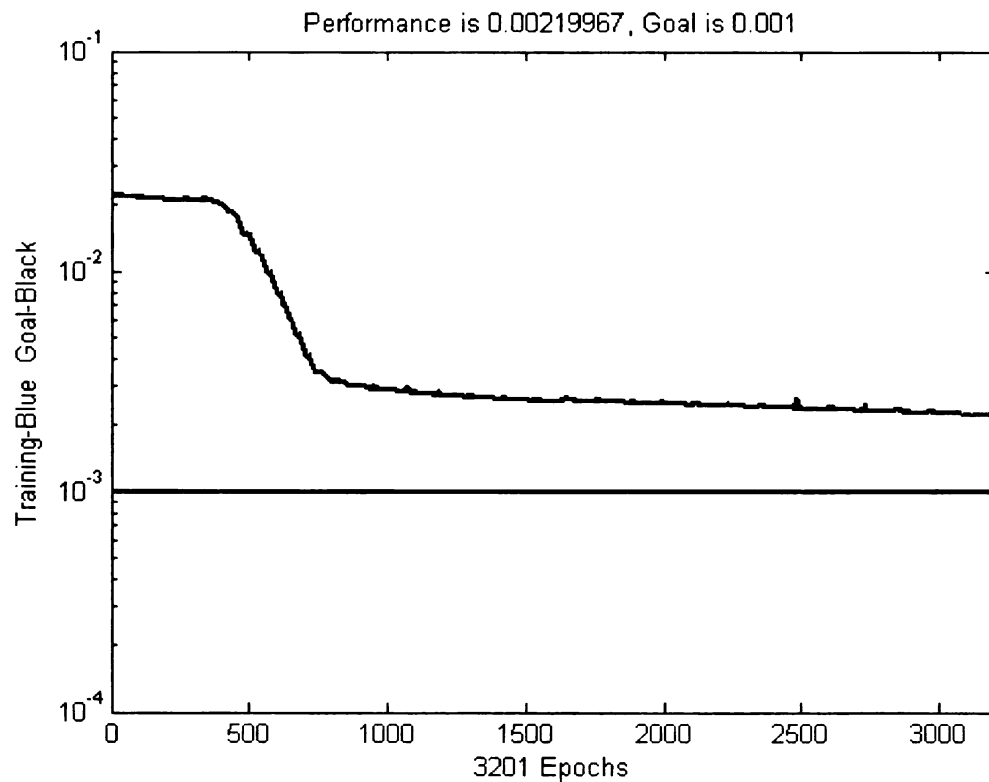


Figure 5.4 – Sample MATLAB Graphical Output for SSNN Training.

The performance of the model is evaluated based on the mean square error (MSE). As the performance converges on the specified objective error, the trainable weights converge on an optimal value. The testing dataset is then used to test the validity of the optimal weights determined in the training of the model.

5.4 Application of State-Space Neural Network Models to Travel Time Estimation and Prediction for Arterial Routes

The output data from the SSNN models represent the average travel time for a single arterial link given a set of input variables representing traffic conditions on that link during time period t . Advanced Traffic Management Systems (ATMS) and Advanced Traveler Information Systems (ATIS) function mainly on the ability to estimate and predict travel time along an arterial or arterial route within a network. Therefore, the results of arterial link travel time estimation and prediction must be able to be applied to arterial routes in order for the modeling procedure to fulfill the objectives of this thesis.

Following the definitions outlined in Section 2.1, an arterial route is comprised of a series of arterial links, and vehicles traversing such a route complete a series of specific through and/or turning movements from arterial link to arterial link. Therefore, the results of travel time estimation and prediction for a specific set of arterial links, corresponding to the appropriate vehicle movements, can be aggregated to estimate and predict travel time along a specified arterial route.

Two arterial routes are examined in this thesis to evaluate the predictive capability of the models developed for the purpose of this thesis. These routes are shown in Figure 5.5, as routes 16-25 and 16-3, and the results are discussed in Chapter 6.

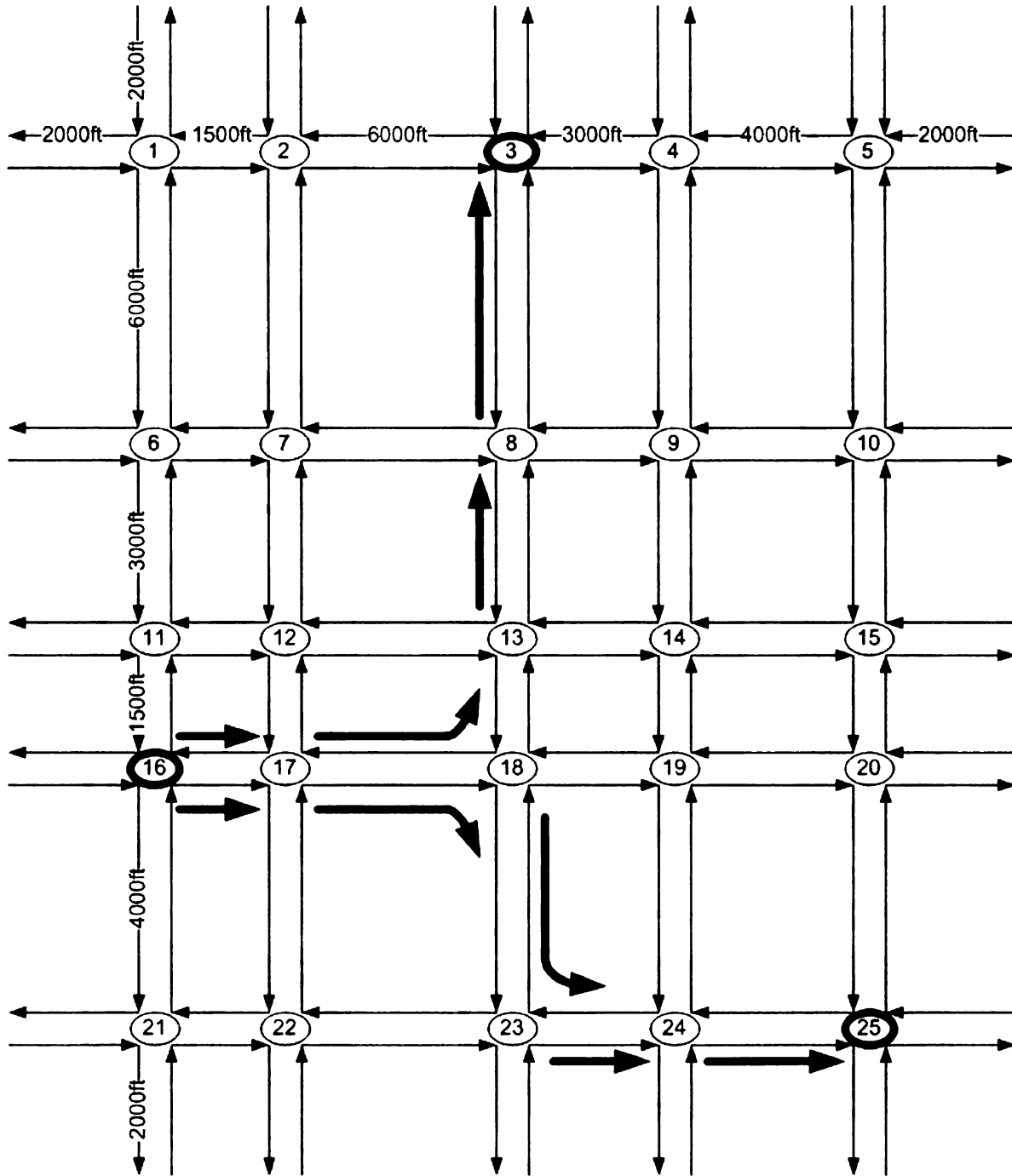


Figure 5.5 – Study Routes for the Evaluation of SSNN Model Performance.

Chapter 6

Results and Discussion

The performance of each State-Space Neural Network (SSNN) model is evaluated based on the ability of the model to accurately estimate or predict travel time for an arterial link. Travel time estimations and predictions produced with each SSNN model are compared to actual average travel times observed in the microscopic simulation trials. The performance of the SSNN models is evaluated corresponding to travel times for 16 arterial links. Additionally, the performance of the models in terms of travel time estimation and prediction for two sample arterial routes is analyzed. These results are presented in this chapter along with discussion of significant findings.

6.1 Measures of Effectiveness

The results of travel time estimation and prediction are expected to have some associated error in comparison to actual observed travel times. This error is measured in a number of ways, including Mean Absolute Error (MAE), Root Mean Square Error (RMSE), and Mean Absolute Percentage Error (MAPE). Additionally, estimated/predicted travel time is plotted versus actual travel time to analyze the relationship between them. The R-squared (R^2) statistic is calculated to evaluate the ability of each model to explain the variance in travel time on arterial links in the sample network (Kutner et al. 2004).

Mean Absolute Error (MAE)

The MAE statistic represents the average absolute value of the error between estimated/predicted and actual travel time for an arterial link for the duration of the study period. The value of error is calculated as the difference between estimated/predicted and actual travel times for each arterial link during a specific time interval t . The absolute value of the error is calculated and averaged for time period t_0 through t_n . The value of MAE is found for each arterial link and is specific to the magnitude and range of the average travel times in a particular study. Therefore, MAE is only used to evaluate the performance of the models in this study, and not for comparison with previous works.

Root Mean Square Error (RMSE)

The RMSE statistic represents the square root of the average squared error values for an arterial link for the duration of the study period. The value of error is calculated as the difference between estimated/predicted and actual travel times for each arterial link during a specific time interval t . The value of the error is squared and averaged for time period t_0 through t_n to calculate the Mean Square Error (MSE). The square root of the MSE is taken to determine the RMSE for each arterial link. Similar to MAE, RMSE is specific to the magnitude and range of the average travel times in a particular study, and is only used to evaluate the performance of the models in this thesis.

Mean Absolute Percentage Error (MAPE)

The MAPE statistic represents the proportion of the average value of error between estimated/predicted and actual travel times, and the actual average travel time. The value of error is calculated as the difference between estimated/predicted and actual travel times for each arterial link during a specific time interval t . The absolute value of the error is calculated and averaged for time period t_0 through t_n . The value of MAPE is the percentage of the average absolute error versus the actual average travel time for an arterial link. The MAPE statistic is a relative measure of the error associated with a prediction, and is used to compare the results of this thesis with the results presented by Singh (2006).

Square of the Correlation Coefficient (R^2)

The correlation coefficient, r , is a measure of the linear association between a dependent variable and a set of independent variables. The correlation coefficient can have a positive or negative value depending on the relationship between the response and explanatory variables, and defines the slope of the regression line. The square of the correlation coefficient, R^2 , is a measure of the ability of a set of independent variables to explain the observed variation in the dependent variable. The R^2 statistic ranges in value from 0.0 to 1.0, where a value of 1.0 signifies that all of the variation in the dependent variable is explained by the independent variables in the model.

For each travel time estimation/prediction model the estimated/predicted travel time is plotted versus the actual travel time and the R^2 statistic is calculated. In the ideal case the scatter plot follows a perfectly straight linear pattern and the R^2 statistic equals 1.0. As the objective of this thesis is to develop models that accurately estimate and predict travel time in comparison to actual travel times observed, the plotted travel time values should follow a linear pattern, and the R^2 statistic should be close to 1.0.

6.2 Travel Time Estimation on Arterial Links

Three separate models are developed for travel time estimation respective to right-turn, left-turn, and through movements on arterial links. These models are referred to as SSNN-Right, SSNN-Left, and SSNN-Through, respectively. The data contained in the training set corresponding to the input variables defined in Section 5.3 for each model are fed to the appropriate SSNN. The models learn the relationship between travel time and the states of an arterial link based on the training data, and are then applied to traffic conditions represented in the testing dataset. The resulting output from each model is the estimated travel time for the current time period t , for both the training and testing datasets. The estimated travel time will be used as an input variable for travel time prediction, and so the accuracy of these models must be explored.

6.2.1 Results of SSNN Travel Time Estimation Model for Through Movement

The results of travel time estimation for the through vehicle movement are presented in this section for both the training and testing datasets. The scatter plot of estimated average speed versus actual average speed for the training set is shown in Figure 6.1.

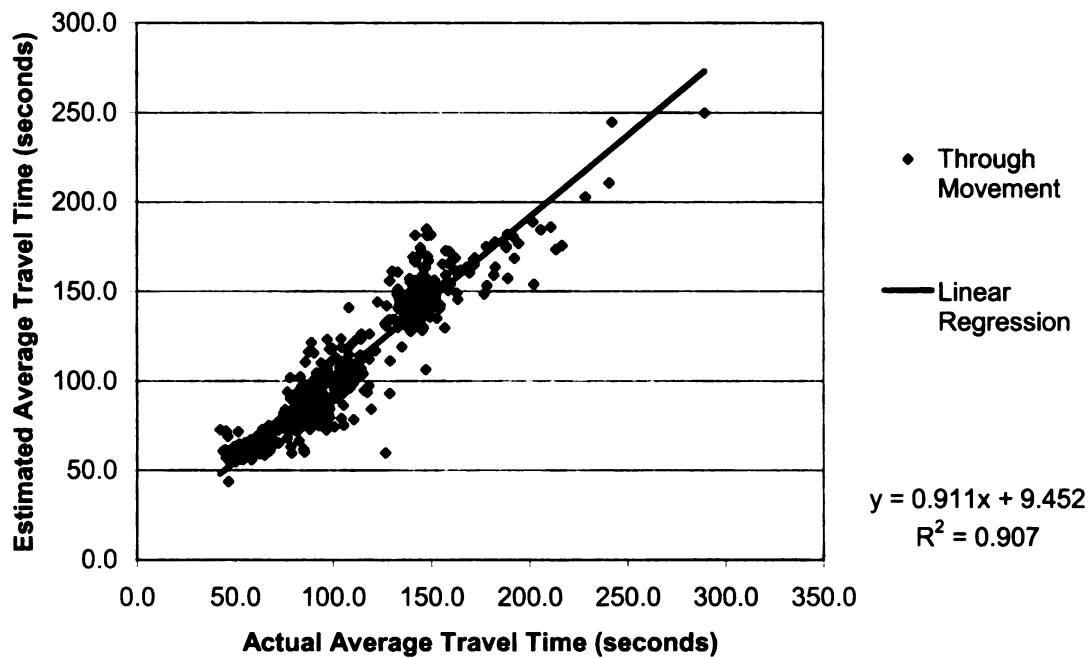


Figure 6.1 – Training Scatter Plot of Actual versus Estimated Travel Time for the Through Movement.

The R^2 statistic for the training set is .907, and a nearly linear relationship is observed. This suggests that the model has efficiently learned the patterns influencing travel time estimation for the through vehicle movement. The model is applied to the independent traffic conditions captured in the testing dataset to validate the model. The scatter plot of estimated average speed versus actual average speed for the testing set is shown in Figure

6.2

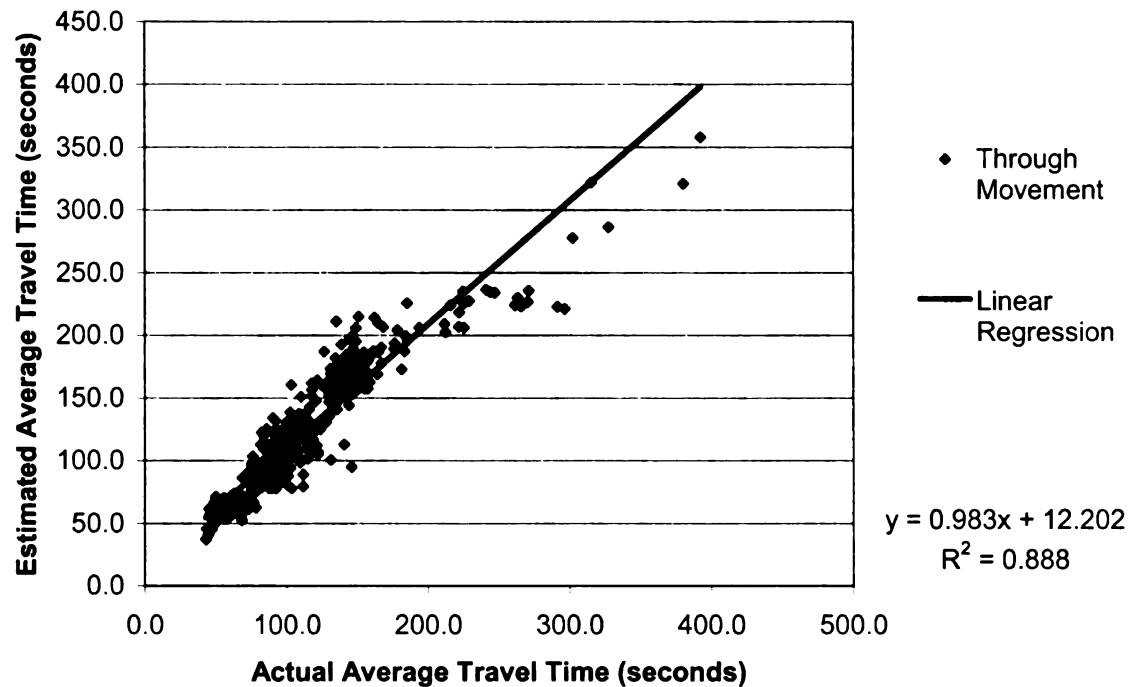


Figure 6.2 – Testing Scatter Plot of Actual versus Estimated Travel Time for the Through Movement.

The R^2 statistic for the testing set is .888. This shows that the model is able to perform in traffic conditions other than those used to train the model. Error statistics for the training and testing sets are also generated and are displayed in Table 6.1. The error statistics are slightly higher for the testing set travel time estimations. This implies that the SSNN-Through model for travel time estimation may have learned some patterns that are only present in the training dataset. Overall though, these statistics reveal that the model performs reasonably well, with a MAPE of 13.8 percent for the testing set. A closer analysis of the testing plot shows that as actual travel times increase, the model actually overestimates travel time slightly for the through movement, except for a small number of cases where the actual travel time exceeds 250.0 seconds.

Table 6.1 – Travel Time Estimation Error Statistics for the Through Movement.

	Arterial	MAE (seconds)	RMSE (seconds)	MAPE (%)
Training	<i>6-10</i>	10.2	14.4	9.9
	<i>16-20</i>	7.6	10.1	8.5
	<i>21-25</i>	6.8	9.0	7.5
	<i>3-23</i>	10.0	13.3	10.1
	<i>Total</i>	8.6	11.7	9.0
Testing	<i>6-10</i>	13.3	18.3	12.3
	<i>16-20</i>	13.6	17.7	12.8
	<i>21-25</i>	14.3	19.2	14.0
	<i>3-23</i>	17.5	22.9	16.0
	<i>Total</i>	14.7	19.5	13.8

6.2.2 Results of SSNN Travel Time Estimation Model for Left-Turn Movement

The results of travel time estimation for the left-turn movement are presented in this section for both the training and testing datasets. The scatter plot of estimated average speed versus actual average speed for the training set is shown in Figure 6.3. The R^2 statistic for the training set is .813, and the majority of points follow a linear pattern. More specifically, for actual travel times lesser than 200 seconds, most points are clustered near the regression line. Only for larger travel times, likely resulting from congested conditions, does the relationship between estimated and actual speed become slightly less linear.

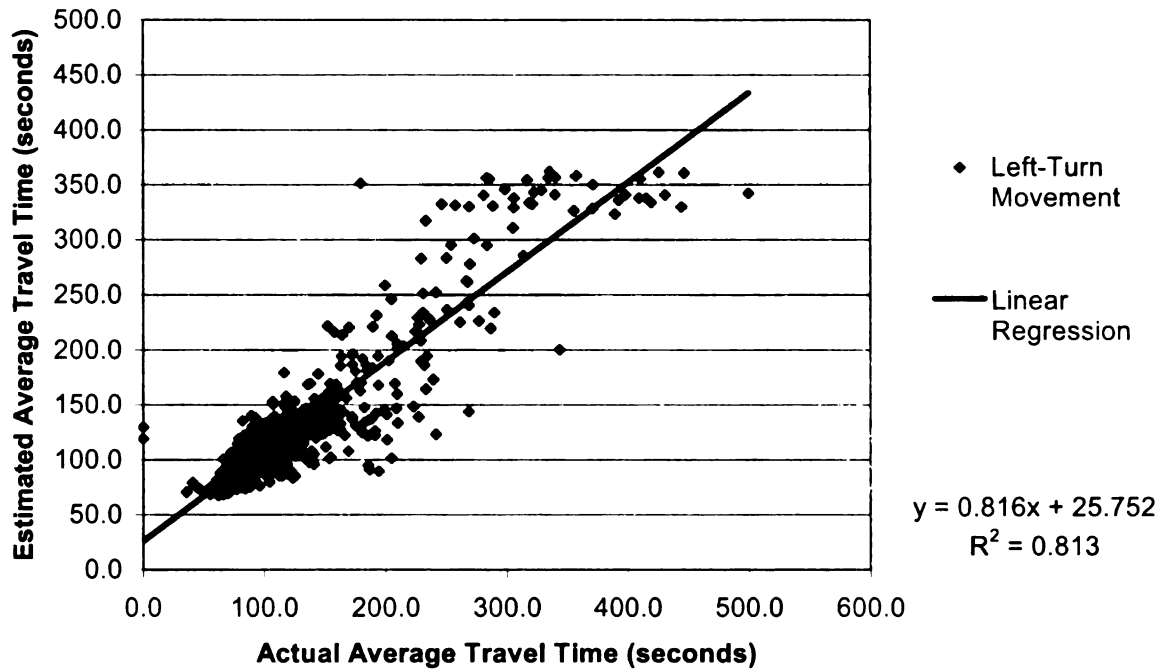


Figure 6.3 – Training Scatter Plot of Actual versus Estimated Travel Time for the Left-Turn Movement.

The model is applied to the independent traffic conditions captured in the testing dataset to validate the model. The scatter plot of estimated average speed versus actual average speed for the testing set is shown in Figure 6.4. The R^2 statistic for the testing set is .796, and the testing plot follows a similar pattern as the training plot. Error statistics for the training and testing sets are also generated and are displayed in Table 6.2.

The error statistics for the left-turn movement reveal similar information about the validity of the left-turn model as for the through movement estimation model. Overall, the model performs reasonably well, with a MAPE of 16.2 percent for the testing set.

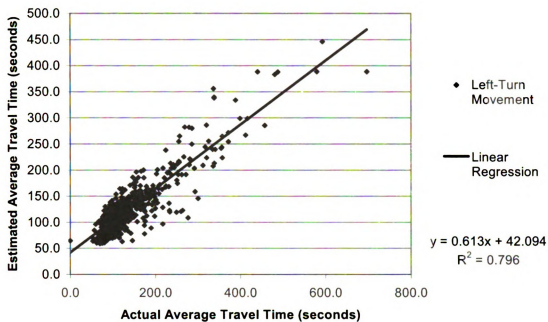


Figure 6.4 – Testing Scatter Plot of Actual versus Estimated Travel Time for the Left-Turn Movement.

Table 6.2 – Travel Time Estimation Error Statistics for the Left-Turn Movement.

	Arterial	MAE (seconds)	RMSE (seconds)	MAPE (%)
Training	6-10	26.1	38.0	16.3
	16-20	18.6	27.8	14.8
	21-25	19.2	25.6	14.6
	3-23	19.9	21.7	13.6
	Total	20.7	20.8	14.8
Testing	6-10	27.3	46.6	16.6
	16-20	22.2	34.9	15.3
	21-25	23.4	33.0	15.3
	3-23	28.7	44.8	17.6
	Total	25.4	39.8	16.2

6.2.3 Results of SSNN Travel Time Estimation Model for Right-Turn Movement

The results of travel time estimation for the right-turn movement are presented in this section for both the training and testing datasets. The scatter plot of estimated average speed versus actual average speed for the training set is shown in Figure 6.5.

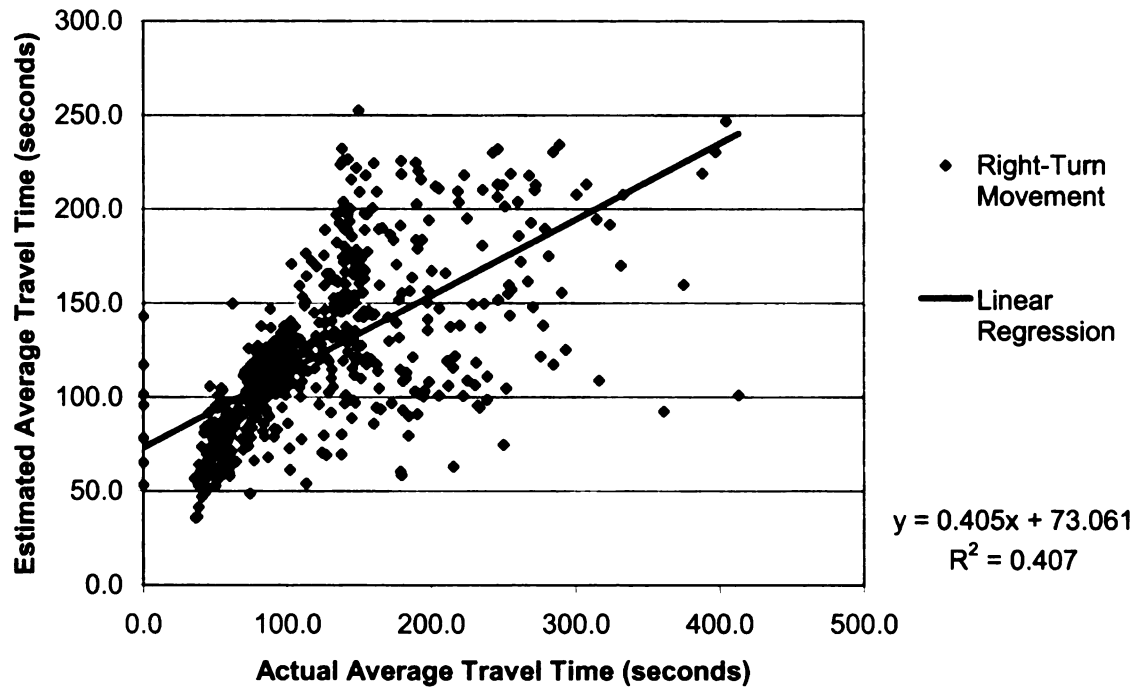


Figure 6.5 – Training Scatter Plot of Actual versus Estimated Travel Time for the Right-Turn Movement.

The R^2 statistic for the training set is .407, and the majority of points are spread in both directions from the regression line. A linear of cluster of points can be seen where the actual average travel time is between 50.0 and approximately 150.0. When the actual travel time increases beyond 150.0 seconds though, the SSNN model fails to accurately estimate travel time for the right-turn movement. A very similar pattern is observed in

the scatter plot of estimated average speed versus actual average speed for the testing set.

The testing scatter plot, with an R^2 statistic of .418 is shown in Figure 6.6.

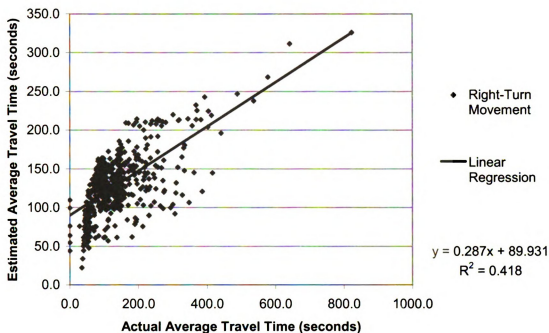


Figure 6.6 – Testing Scatter Plot of Actual versus Estimated Travel Time for the Right-Turn Movement.

Error statistics for the training and testing sets are generated for the right-turn estimation model and are displayed in Table 6.3. These statistics reveal significant errors in the travel time estimations derived from both the training and testing sets, with a MAPE between 30 and 40 percent. From these results it is obvious that the variability in right-turns between intersections and over time has a severe impact on the accuracy of right-turn speed estimation. An impact of this severity is not observed, though for left-turn speed estimation, where turning movements are also variable.

Table 6.3 – Travel Time Estimation Error Statistics for the Right-Turn Movement.

	Arterial	MAE (seconds)	RMSE (seconds)	MAPE (%)
Training	6-10	40.3	57.8	30.6
	16-20	30.1	39.9	27.9
	21-25	35.3	49.0	31.3
	3-23	44.8	61.7	31.6
	Total	37.62	52.1	30.3
Testing	6-10	45.0	64.8	39.06
	16-20	42.7	59.8	36.6
	21-25	45.9	59.5	43.7
	3-23	59.0	88.7	37.4
	Total	48.1	68.2	39.2

There are two distinct differences between left-turn and right-turn behaviors in the modeling procedure that likely result in more accurate travel time estimation for left-turning vehicles than for right-turning vehicles. First, the left-turn movement is accommodated in the microscopic simulation model with a dedicated left-turn bay at each intersection approach. Second, left-turns are served by a protected signal phase. As a result, the input variables corresponding to signal control and queue length are more directly connected to the average flow rate, and thus the average travel time for left-turning vehicles.

Right-turning vehicles share the rightmost travel lane with through moving vehicles. This creates an interaction between through and right-turning vehicles, as introduced in Section 4.3. Although the travel time for through movement should correlate closely with the travel time for the right-turn movement, the presence of right-turn-on-red movements changes the typical pattern of right-turn travel times. In the case of constant turning movement percentages, right-turn-on-red movements may be more consistent,

and have a lesser impact on average right-turn speed. When right-turn profiles are varied between intersections and over time, the right-turn travel time distribution becomes more unpredictable, and the SSNN model is unable to accurately capture the patterns between the state of the link and right-turn speed.

The SSNN models for travel time estimation developed by Singh (2006) were trained and tested based on data assuming constant turning movement percentages. The resulting MAPE statistics are shown in Table 6.4 in comparison with the MAPE results derived in this thesis under similar conditions, but incorporating turning movements that vary over time and space.

Table 6.4 – Mean Absolute Percentage Error Comparison Under Constant and Variable Turning Movement Percentage Conditions.

		Movement	Constant Turning %	Variable Turning %
MAPE (%)	Training	<i>Through</i>	7.6	9.0
		<i>Left-Turn</i>	7.5	14.8
		<i>Right-Turn</i>	8.4	30.3
	Testing	<i>Through</i>	7.3	13.9
		<i>Left-Turn</i>	8.6	16.2
		<i>Right-Turn</i>	14.0	39.2

The MAPE results between the two scenarios do differ slightly for the through movement. This is expected as turning vehicles, especially right-turning vehicles, do interact with through vehicles in a traffic stream, but do not significantly detract from the accuracy of travel time estimation for the through movement. The influence of variable

turning movement percentages is clearly seen though, in the MAPE statistics for left and right-turns. The left-turn MAPE is nearly double, and the right-turn MAPE is approximately triple in the presence of variable turning movement percentages. While it is unclear at this point how these findings impact travel time estimation and prediction for arterials and arterial routes, it is determined that variable turning movements significantly impact the overall accuracy of the SSNN models, especially for right-turn speed estimation.

6.3 Travel Time Prediction on Arterial Links

Three models are developed for travel time prediction respective to right-turn, left-turn, and through movements on arterial links. These models are separate from the models designed to estimate travel time, but the function is the same. The data contained in the training set corresponding to the input variables defined in Section 5.3 for travel time prediction are fed to the appropriate SSNN, including the estimated travel time for each movement. The models learn the relationship between travel time and the states of an arterial link based on the training data, and are then applied to traffic conditions represented in the testing dataset. The resulting output from each model is the predicted travel time for the one-step future time period $t+1$, for both the training and testing datasets.

6.3.1 Results of SSNN Travel Time Prediction Model for Through Movement

The results of travel time prediction for the through vehicle movement are presented in this section for both the training and testing datasets. The scatter plot of estimated average speed versus actual average speed for the training set is shown in Figure 6.7.

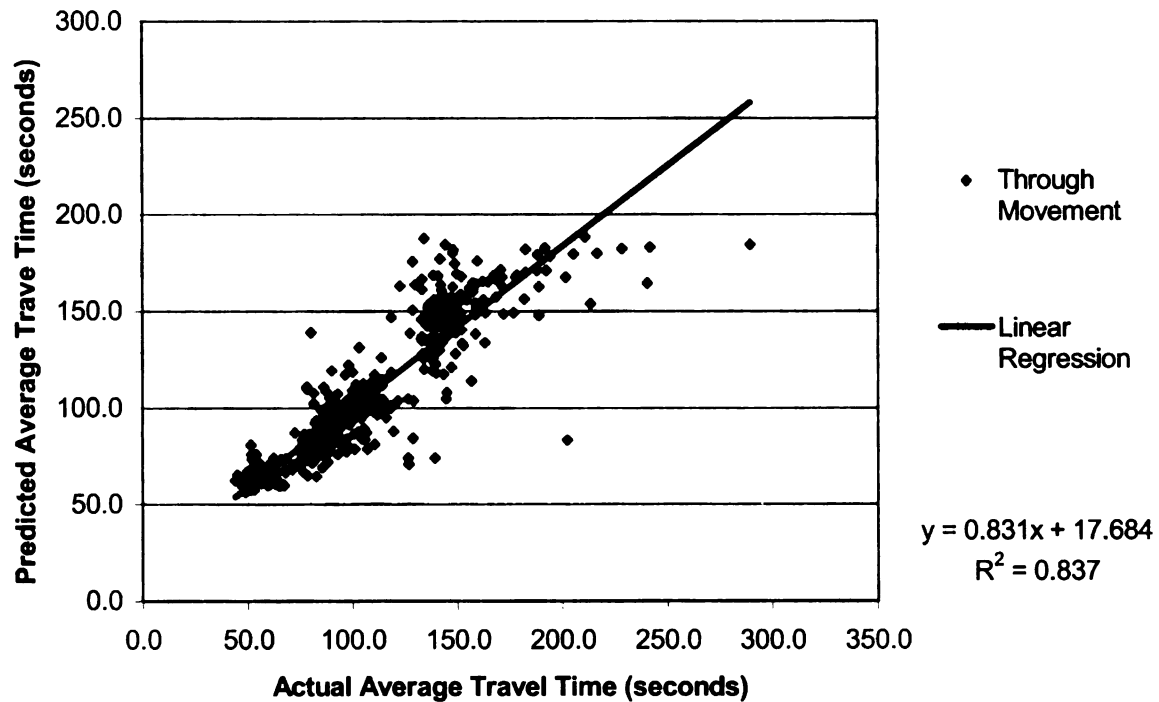


Figure 6.7 – Training Scatter Plot of Actual versus Predicted Travel Time for the Through Movement.

The R^2 statistic for the training set is .837, and a nearly linear relationship is observed. This suggests that the model has efficiently learned the patterns influencing travel time estimation for the through vehicle movement. There are two distinct point clusters that occur along the regression line. For actual average travel times above approximately 130 seconds, more variability is observed between the actual and predicted travel time. This

pattern is strongly correlated with the link length, where travel times below 130 seconds occur mainly on short links, while the majority of the points above 130 seconds occur on the longest links in the network. Although the model performs more accurately for shorter links, the overall performance is reasonable.

The model is applied to the independent traffic conditions captured in the testing dataset to validate the model. The scatter plot of predicted average speed versus actual average speed for the testing set is shown in Figure 6.8.

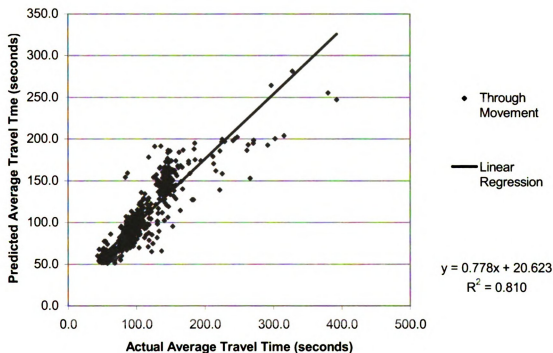


Figure 6.8 – Testing Scatter Plot of Actual versus Predicted Travel Time for the Through Movement.

The R^2 statistic for the testing set is .810. This shows that the model is able to perform in traffic conditions other than those used to train the model. Clustering is observed above and below approximately 130.0 seconds, but is not as severe as for the training set. Error

statistics for the training and testing sets are also generated and are displayed in Table 6.5.

Table 6.5 – Travel Time Prediction Error Statistics for the Through Movement.

	Arterial	MAE (seconds)	RMSE (seconds)	MAPE (%)
Training	<i>6-10</i>	11.6	17.9	10.9
	<i>16-20</i>	8.65	14.4	9.7
	<i>21-25</i>	7.5	11.2	8.2
	<i>3-23</i>	13.9	18.6	13.6
	<i>Average</i>	10.42	15.5	10.6
Testing	<i>6-10</i>	12.8	22.6	10.6
	<i>16-20</i>	10.5	17.5	9.4
	<i>21-25</i>	10.2	15.9	10.9
	<i>3-23</i>	17.2	27.1	13.2
	<i>Average</i>	12.7	20.8	11.0

The error statistics reveal that the model performs reasonably well, with a MAPE of 10.6 percent for the training set and 11.0 percent for the testing set. In order to validate this level of confidence in the performance of the SSNN-Through model, a detailed analysis of the accuracy of travel time predictions on each arterial link is necessary. The Absolute Percentage Error (APE) is plotted for each arterial link in 5-minute increments for both the training and testing datasets. Figure 6.9 and Figure 6.10 display APE data for major arterial 6-10.

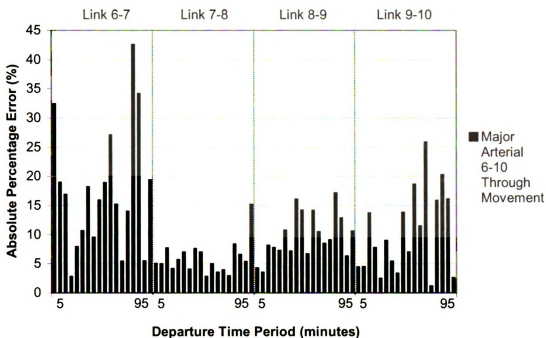


Figure 6.9 – Absolute Percentage Error of Through Movement Travel Time Prediction for Training Set Arterial 6-10.

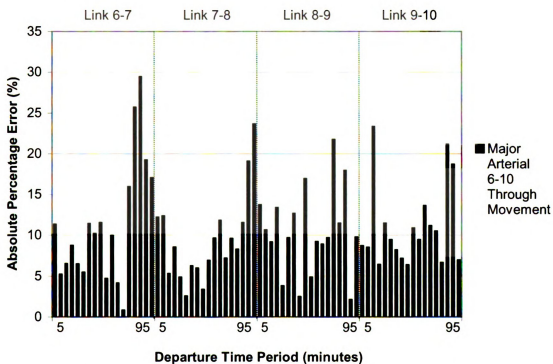


Figure 6.10 – Absolute Percentage Error of Through Movement Travel Time Prediction for Testing Set Arterial 6-10.

The APE for each link comprising arterial 6-10 is generally less than 10 percent for both the training and testing sets. However, there are some specific links and time increments for which the performance of the model is not as desirable. On arterial link 6-7 the APE is consistently in excess of 15 percent, and is as high as 43 percent. For most cases, this corresponds to an absolute error of 10 seconds or less. From time 80 minutes to 90 minutes though, this percentage equates to approximately one minute of error. If this level of error is experienced for the entire length of an arterial the predicted travel time may differ from the actual travel time by 5 minutes or more, which is not acceptable for ITS applications. On the other hand, it is possible that positive and negative errors may balance along the length of an arterial or arterial route, thus resulting in an acceptable overall level of error. The predicted versus actual travel time and the associated error for two particular routes is analyzed at the end of this chapter.

The through movement APE for major arterial 16-20 are shown in Figure 6.11 for the training set and Figure 6.12 for the testing set. Similar to arterial 6-10, the APE is generally less than 10 percent on each link, except for link 16-17 where travel time prediction errors ranging from 15 to 35 percent are consistently observed in the training dataset. This level of error is only experienced for three time intervals in the testing set, though. This may be due to the stochastic nature of arrivals in the microscopic simulation, where an intense concentration of vehicle arrivals at an intersection decreases signal operation level of service and therefore travel time predictability. Nonetheless, travel time prediction models must be able to operate reliably in a wide range of traffic conditions to be effective in ITS applications.

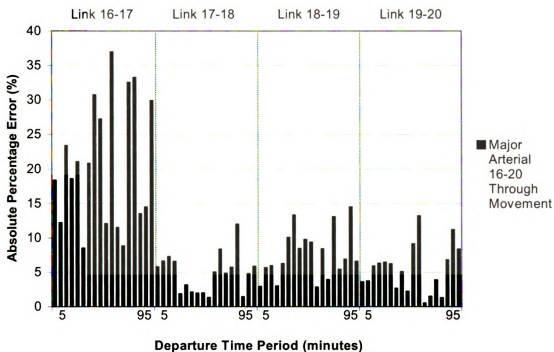


Figure 6.11 – Absolute Percentage Error of Through Movement Travel Time Prediction for Training Set Arterial 16-20.

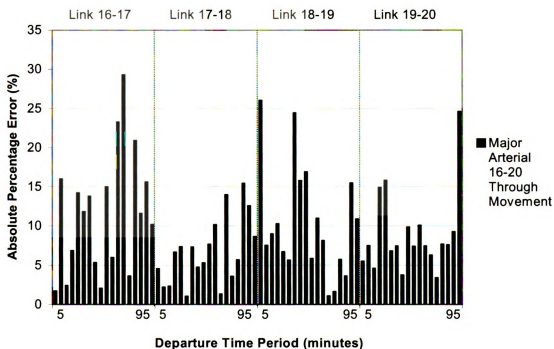


Figure 6.12 – Absolute Percentage Error of Through Movement Travel Time Prediction for Testing Set Arterial 16-20.

The APE is plotted for major arterial 21-25 in Figure 6.13 and Figure 6.14. Overall, travel time prediction is within 10 percent of the actual travel time for all links for both the training and testing datasets. There are isolated time intervals for which the APE is in excess of 20 percent. These intervals with a higher range of error are typically consecutive, and the accuracy of travel time prediction recovers in approximately 15 minutes. This trend is observed for other links in the network and corresponds to sudden peaks in travel time, which could be due to intersection blockage or other sudden loss in capacity. As the SSNN model learns patterns in traffic over one time step, a sudden increase in travel time is not effectively predicted by the model developed for the through movement. Incorporating multiple time steps into the learning process may improve the accuracy of these models. The relatively rapid recovery of the predictive capability of the model is promising though for real-world applications where unpredictable incidents often impact the flow of traffic.

The APE is plotted for arterial 3-23 in Figure 6.15 and Figure 6.16. The error in travel time prediction is generally higher for this minor arterial, with average percentage errors regularly observed between 10 and 15 percent. The patterns in the APE are similar to those described for the major arterials, and where APE exceeds 25 percent the accuracy of the model is shown to recover quickly.

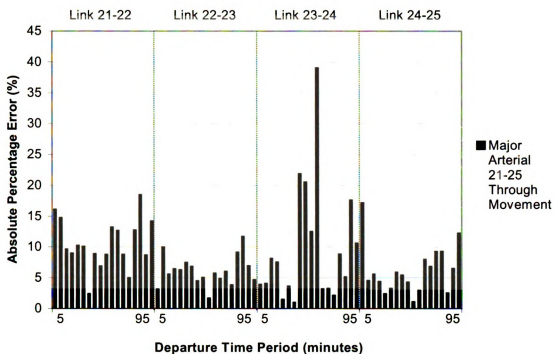


Figure 6.13 – Absolute Percentage Error of Through Movement Travel Time Prediction for Training Set Arterial 21-25.

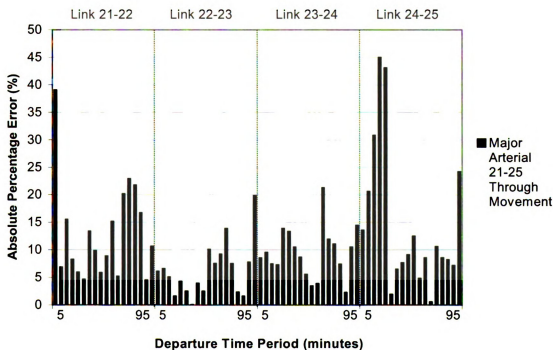


Figure 6.14 – Absolute Percentage Error of Through Movement Travel Time Prediction for Testing Set Arterial 21-25.

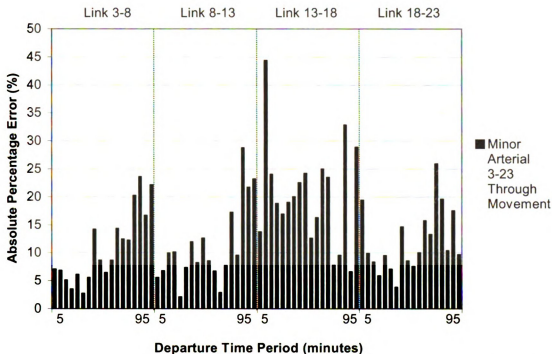


Figure 6.15 – Absolute Percentage Error of Through Movement Travel Time Prediction for Training Set Arterial 3-23.

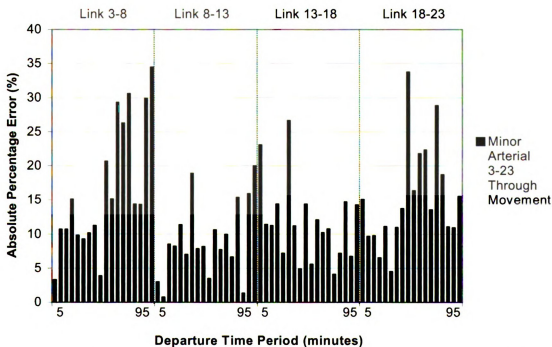


Figure 6.16 – Absolute Percentage Error of Through Movement Travel Time Prediction for Testing Set Arterial 3-23.

As previously mentioned there are time periods when the percentage error for travel time prediction is observed to spike, and then improve in a short period of time. Sudden breakdowns in traffic conditions may cause travel time to become more unpredictable using single time step prediction models and the variable types utilized in this thesis. For ITS applications, large discrepancies between actual travel times and those communicated to users and system administrators are not desirable. For this reason, the ability of the SSNN models to rapidly detect changing traffic conditions must be improved.

To further explore the ability of the SSNN-Thru model to learn and follow changing patterns in traffic conditions and accurately predict travel time, the actual travel time and predicted travel time are plotted together over time. These results for the testing set are shown for each arterial in Figures 6.17, 6.18, 6.19, and 6.20.

For each arterial link, the pattern of the predicted travel time closely follows the actual travel time. The SSNN-Through model successfully models the dynamic relationship between the state of an arterial link and travel time in the short-term future for the through movement. Although there are errors observed between the actual and predicted travel times, the model does show the ability to learn from changes in the input variables selected in this thesis. Significant errors in travel time prediction are typically isolated, and do not propagate through future time intervals. Further research to incorporate multiple time step learning of the SSNN model will likely advance the accuracy of travel time predictions observed here.

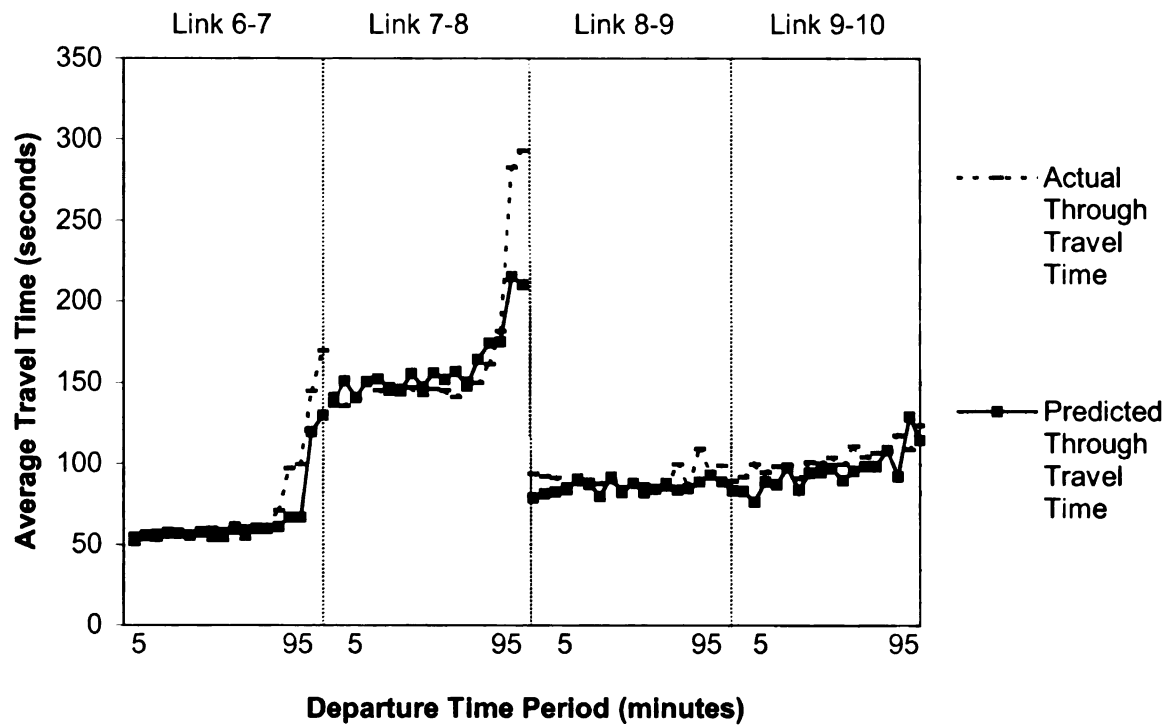


Figure 6.17 – Pattern of Actual versus Predicted Travel Time for Through Movement on Testing Set Arterial 6-10.

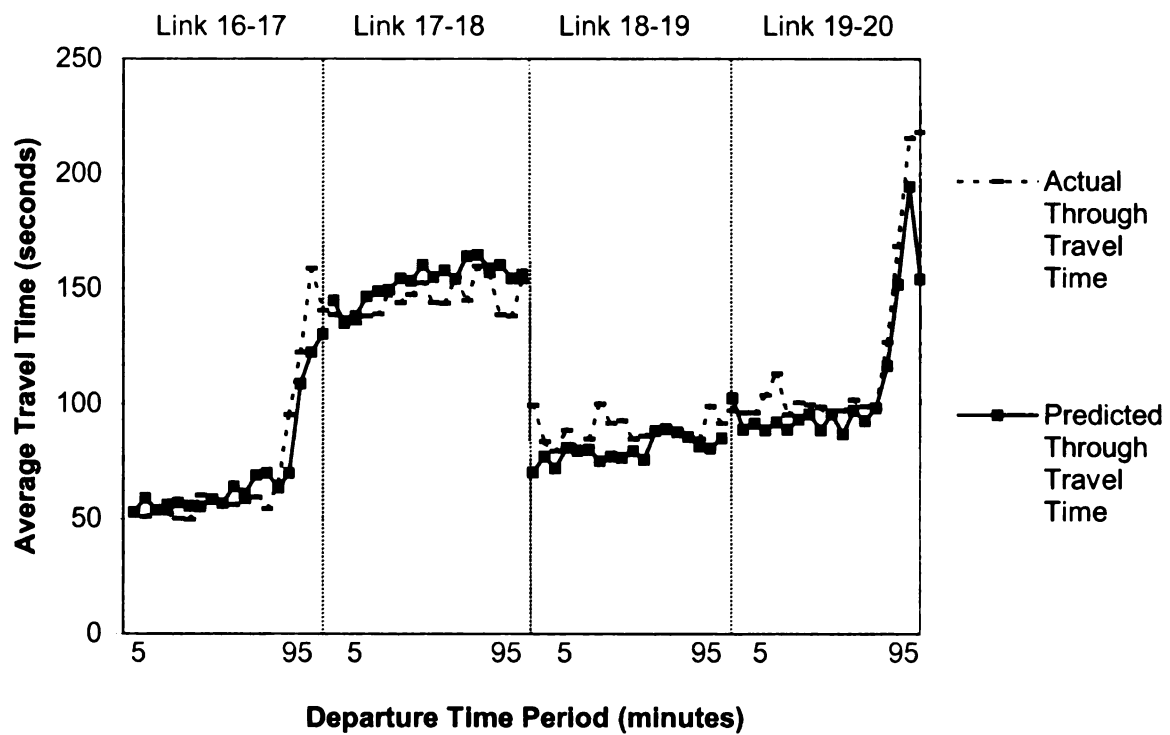


Figure 6.18 – Pattern of Actual versus Predicted Travel Time for Through Movement on Testing Set Arterial 16-20.

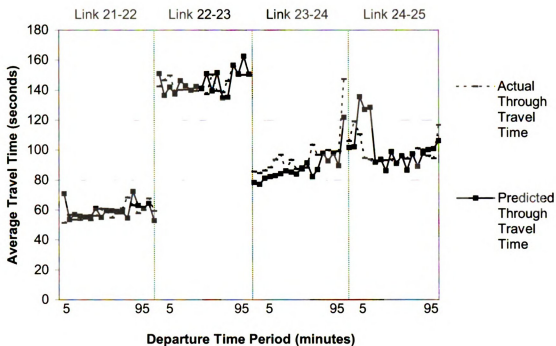


Figure 6.19 – Pattern of Actual versus Predicted Travel Time for Through Movement on Testing Set Arterial 21-25.

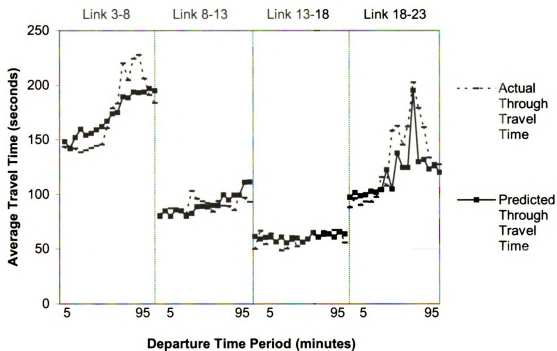


Figure 6.20 – Pattern of Actual versus Predicted Travel Time for Through Movement on Testing Set Arterial 3-23.

In conclusion of this section, the results observed for the accuracy of travel time prediction for the through movement are compared to the results obtained by Singh (2006) under the assumption of constant turning movement percentages. This comparison is shown in Table 6.6.

Table 6.6 – Mean Absolute Percentage Error Comparison for Through Movement Under Constant and Variable Turning Movement Percentage Conditions.

		Movement	Constant Turning %	Variable Turning %
MAPE (%)	Training	<i>Through</i>	9.0	10.6
	Testing	<i>Through</i>	8.8	11.0

Based on this comparison, the incorporation of variable turning movements into the modeling procedure does have a slight impact on the accuracy of travel time prediction for the through movement. Similar to the comparison of data from the training set, this increase in error can be expected due to the interaction of through and turning vehicles in a traffic stream.

Overall, it is concluded that the influence of variable turning movements is not significant in terms of travel time prediction for the through movement. For the length of an arterial, which is slightly less than 3 miles, travel time is predicted on average within 13 seconds of the actual travel time for vehicles making only a through movement. This is a promising result for the future use of this model in Intelligent Transportation System (ITS) applications.

6.3.2 Results of SSNN Travel Time Prediction Model for Left-Turn Movement

The results of travel time prediction for the left-turn movement are presented in this section for both the training and testing datasets. The scatter plot of estimated average speed versus actual average speed for the training set is shown in Figure 6.21.

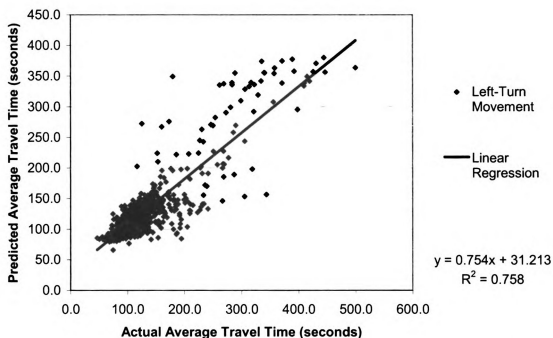


Figure 6.21 – Training Scatter Plot of Actual versus Predicted Travel Time for the Left-Turn Movement.

The R^2 statistic for the training set is .758, which is less accurate the results obtained for the through movement. There is a cluster of points observed for cases corresponding to an actual average travel time of less than 200.0 seconds. For these cases the travel time for the left-turn movement is predicted with more accuracy than for cases where the

actual travel time exceeds 200.0 seconds. In the latter circumstance, the relationship between predicted and actual travel time is more dispersed and less linear.

The model is applied to the independent traffic conditions captured in the testing dataset to validate the performance of the model. The scatter plot of predicted average speed versus actual average speed for the testing set is shown in Figure 6.22.

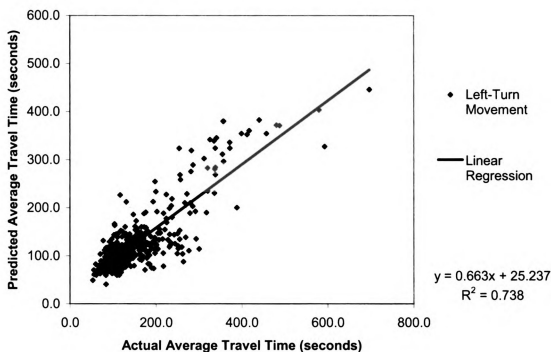


Figure 6.22 – Testing Scatter Plot of Actual versus Predicted Travel Time for the Left-Turn Movement.

The R^2 statistic for the testing set is .738. This is similar to the accuracy observed for the training set, and shows that the model is equally as accurate in traffic conditions other than those used to train the model. Clustering is again observed for actual travel times below 200 seconds, and the pattern of dispersion along the regression line is similar to that observed for the training dataset. Travel times in excess of 200 seconds are observed

for the left-turn movement on various link lengths, so increases in travel time can be attributed to congested conditions rather than simply the length of the link. Due to variations in the percentage of left-turn movements between intersections and over time, the SSNN model becomes less accurate as congestion builds on network links and actual travel times increase.

In order to further examine the accuracy of travel time prediction for the left-turn movement, error statistics for the training and testing sets are generated and are displayed in Table 6.7.

Table 6.7 – Travel Time Prediction Error Statistics for the Left-Turn Movement.

	Arterial	MAE (seconds)	RMSE (seconds)	MAPE (%)
Training	<i>6-10</i>	31.2	44.6	18.6
	<i>16-20</i>	22.9	32.8	17.8
	<i>21-25</i>	22.5	31.1	16.7
	<i>3-23</i>	24.0	33.3	17.5
	<i>Average</i>	25.2	35.5	17.6
Testing	<i>6-10</i>	36.1	55.2	20.9
	<i>16-20</i>	25.3	36.5	17.1
	<i>21-25</i>	31.2	45.3	19.6
	<i>3-23</i>	32.0	48.1	20.3
	<i>Average</i>	31.1	46.3	19.5

The error statistics reveal that the influence of variable turning movements is more severe for left-turn travel time prediction than is observed for the through movement. The SSNN-Left prediction model performs with a MAPE of 17.6 percent for the training set and 19.5 percent for the testing set. This level of error is shown later in this chapter to impact the accuracy of travel time prediction for two routes within the arterial network.

The MAPE for each arterial is broken down by link in order to identify any patterns or specific predictions that may explain the error displayed in Table 6.7. The Absolute Percentage Error (APE) is plotted for each arterial link in 5-minute increments for both the training and testing datasets. Figure 6.23 and Figure 6.24 display APE data for major arterial 6-10.

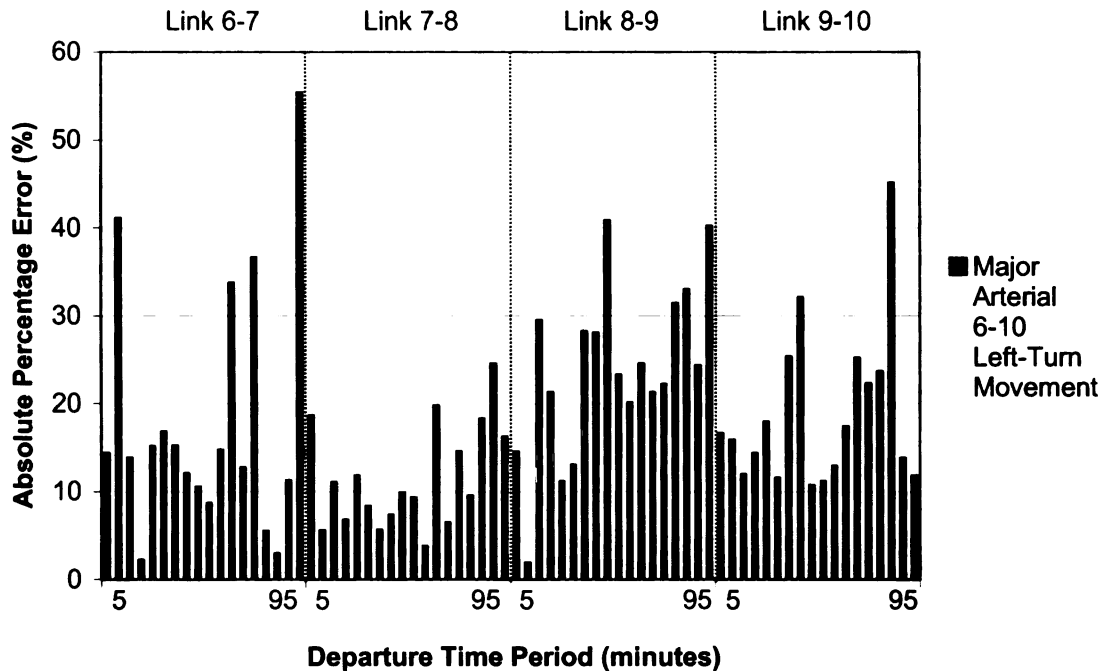


Figure 6.23 – Absolute Percentage Error of Left-Turn Movement Travel Time Prediction for Training Set Arterial 6-10.

The APE for each link comprising arterial 6-10 is generally between 10 percent and 20 percent for both the training and testing sets. However, the magnitude of error on each particular link changes between the training and testing sets. For example, on link 8-9 the APE exceeds 20 percent for all but two time intervals in the training set, while for links 6-7 and 7-8 the average error is closer to 10 percent. For the testing set, the APE for link 8-9 is typically below 15 percent, while the error for links 6-7 and 7-8 is

consistently in excess of 15 percent. This discrepancy in the error patterns between the training and testing sets implies that the patterns in traffic conditions learned to predict left-turn travel time in the training set do not apply in the same manner for the testing set. The variability in left-turn movements coupled with changing traffic conditions between datasets causes randomness in the accuracy of travel time predictions that is not desirable for ITS applications.

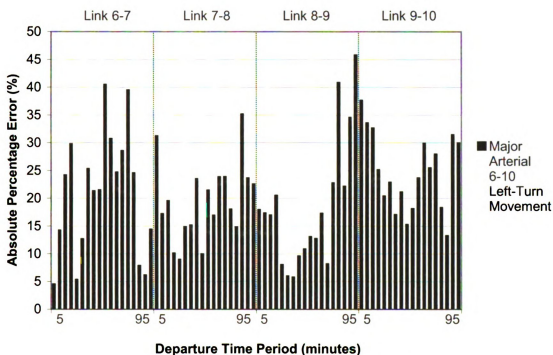


Figure 6.24 – Absolute Percentage Error of Left-Turn Movement Travel Time Prediction for Testing Set Arterial 6-10.

The APE is plotted for arterial 16-20 in Figures 6.25 and 6.26, for arterial 21-25 in Figures 6.27 and 6.28, and for arterial 3-23 in Figures 6.29 and 6.30. The APE is consistently near 20 percent for each link, and the same discrepancy between the training and testing sets as described for arterial 6-10 is observed for these arterials.

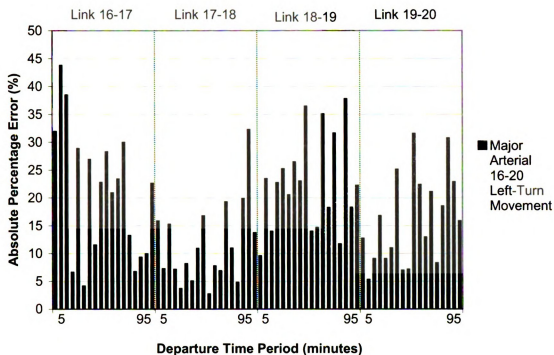


Figure 6.25 – Absolute Percentage Error of Left-Turn Movement Travel Time Prediction for Training Set Arterial 16-20.

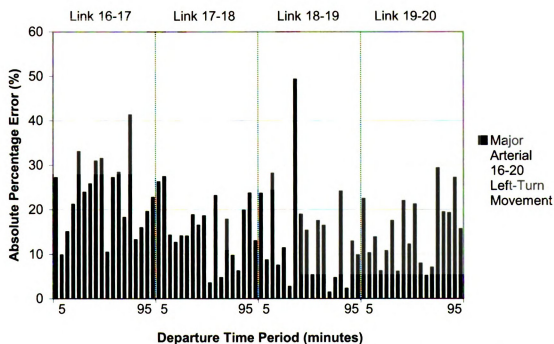


Figure 6.26 – Absolute Percentage Error of Left-Turn Movement Travel Time Prediction for Testing Set Arterial 16-20.

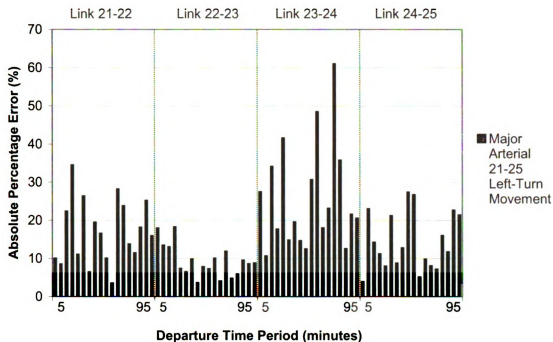


Figure 6.27 – Absolute Percentage Error of Left-Turn Movement Travel Time Prediction for Training Set Arterial 21-25.

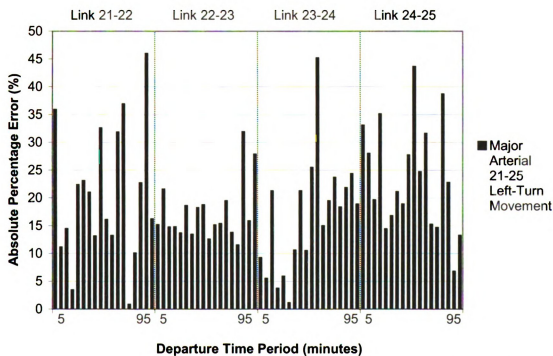


Figure 6.28 – Absolute Percentage Error of Left-Turn Movement Travel Time Prediction for Testing Set Arterial 21-25.

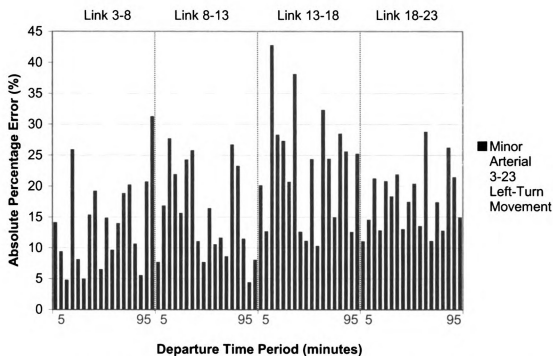


Figure 6.29 – Absolute Percentage Error of Left-Turn Movement Travel Time Prediction for Training Set Arterial 3-23.

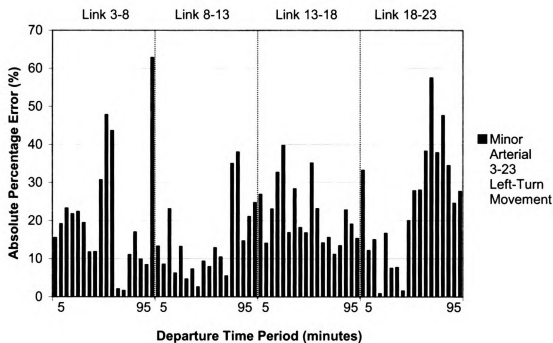


Figure 6.30 – Absolute Percentage Error of Left-Turn Movement Travel Time Prediction for Testing Set Arterial 3-23.

Inconsistencies in the errors observed between the training and testing sets imply that the learning of the SSNN-Left model is limited to the traffic conditions observed in the training set. The influence of variable turning movements and changing traffic conditions causes a variation in the accuracy of predictions made by the model. To further explore the ability of the SSNN-Left model to learn and follow changing patterns in traffic conditions and accurately predict travel time, the actual travel time and predicted travel time are plotted together over time. These results for the testing set are shown for each arterial in Figures 6.31, 6.32, 6.33, and 6.34.

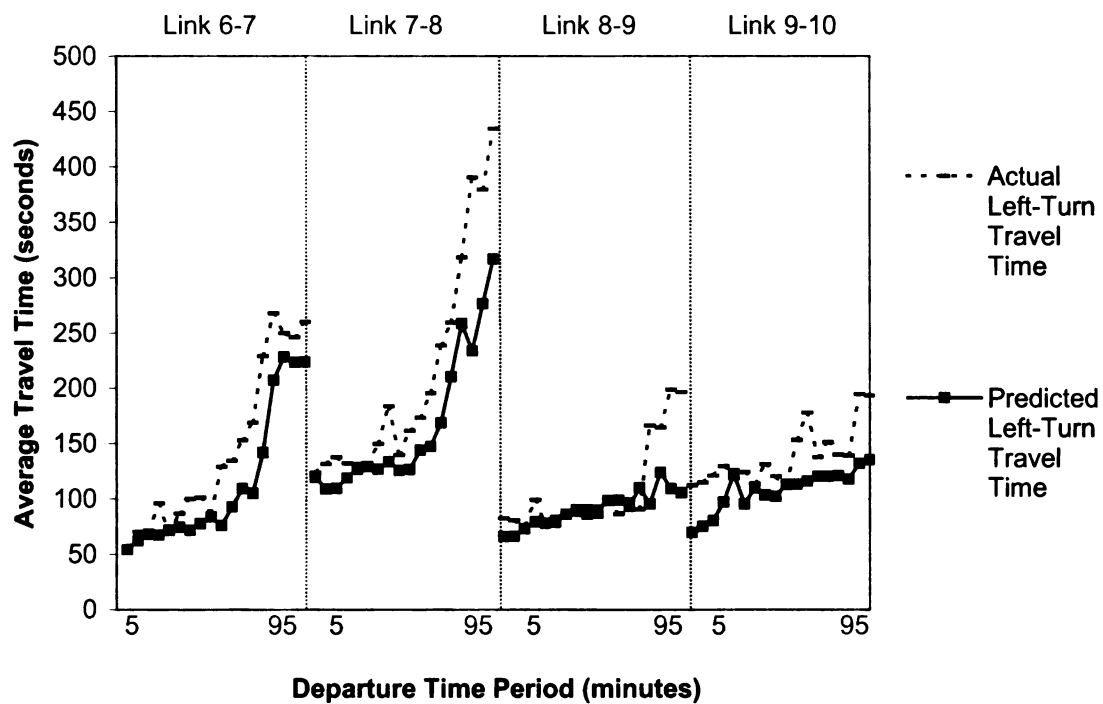


Figure 6.31 – Pattern of Actual versus Predicted Travel Time for Left-Turn Movement on Testing Set Arterial 6-10.

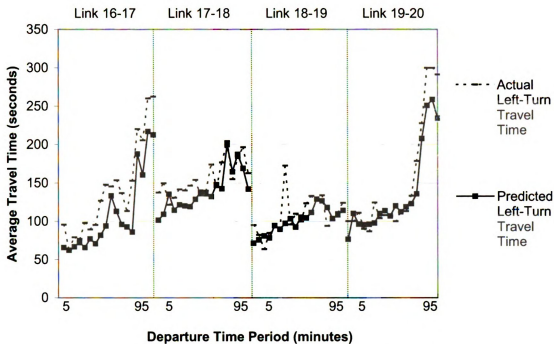


Figure 6.32 – Pattern of Actual versus Predicted Travel Time for Left-Turn Movement on Testing Set Arterial 16-20.

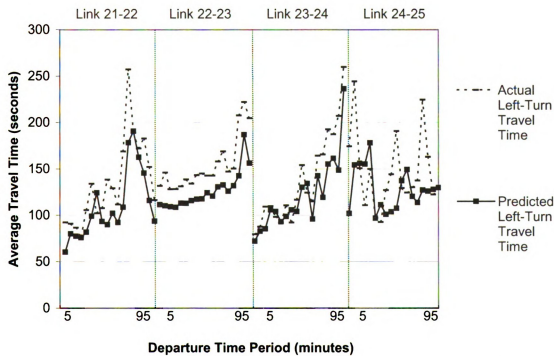


Figure 6.33 – Pattern of Actual versus Predicted Travel Time for Left-Turn Movement on Testing Set Arterial 21-25.

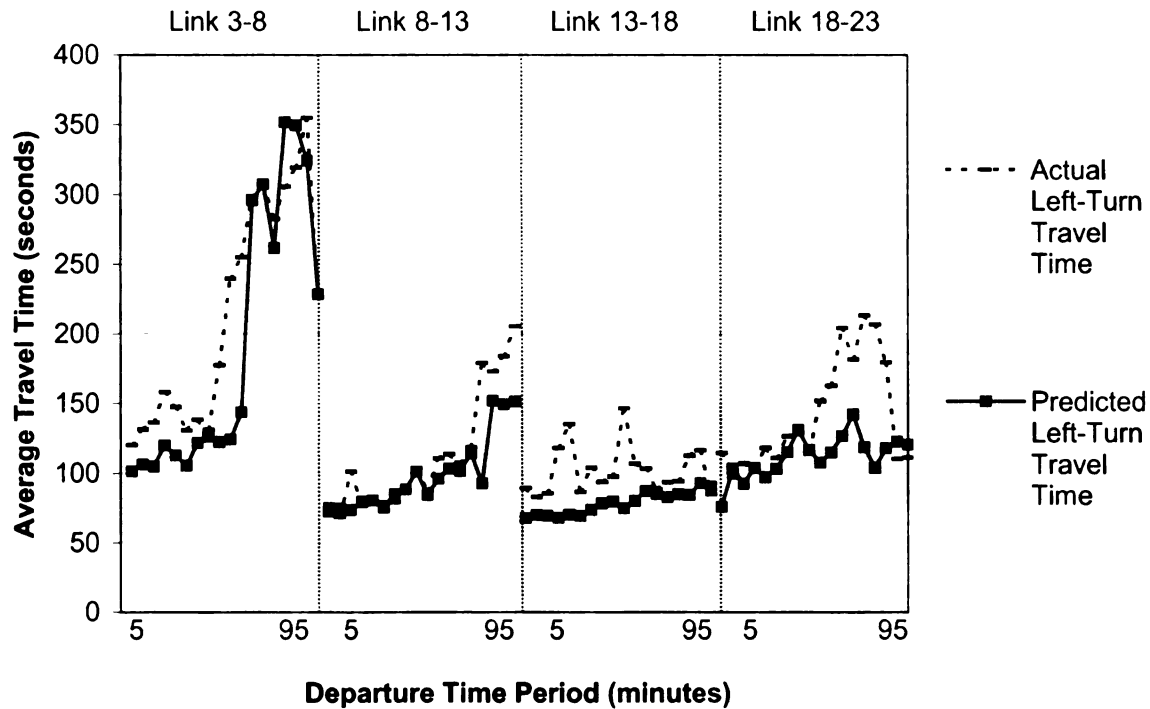


Figure 6.34 – Pattern of Actual versus Predicted Travel Time for Left-Turn Movement on Testing Set Arterial 3-23.

In many cases the predicted travel time is less than the actual travel time, such as on links 6-7, 7-8, 16-17, 21-22, 22-23, and 13-18. Despite the underestimation of travel time, the predicted travel time is in the same range and follows the same pattern as the actual travel time for most links. The cause for underestimation in many cases seems to be due to a delay in the predictive capability of the model. When actual travel time changes, the change in the prediction made by the model follows one or two time-steps later. This lag in the reaction of the model to changing traffic conditions is not desirable, and is the cause of much of the APE observed for the SSNN-Left travel time prediction model.

In conclusion of this section, the results observed for the accuracy of travel time prediction for the left-turn movement are compared to the results obtained by Singh

(2006) under the assumption of constant turning movement percentages. This comparison is shown in Table 6.8.

Table 6.8 – Mean Absolute Percentage Error Comparison for Left-Turn Movement Under Constant and Variable Turning Movement Percentage Conditions.

		Movement	Constant Turning %	Variable Turning %
MAPE (%)	Training	<i>Left-Turn</i>	7.3	17.6
	Testing	<i>Left-Turn</i>	8.8	19.5

Based on this comparison, the incorporation of variable turning movements into the modeling procedure has a significant impact on the accuracy of travel time prediction for the left-turn movement. The magnitude of the MAPE is increased 10 to 11 percent as compared to the results obtained assuming constant turning percentages. The variability in the left-turn movement influences the accuracy of travel time predictions under changing traffic conditions, and causes delay in the predictive capability of the model.

The success of Advanced Traffic Management Systems (ATMS) and Advanced Traveler Information Systems (ATIS) are dependent on the accuracy and reliability of the travel time prediction models that drive them. In order to be useful for such applications, the travel time prediction model must be able to adapt quickly and accurately to changing traffic conditions. The addition of multiple time-steps to the learning process of the model may improve the flexibility and reactive capability of the model.

6.3.3 Results of SSNN Travel Time Prediction Model for Right-Turn Movement

The results of travel time prediction for the right-turn movement are presented in this section for both the training and testing datasets. The scatter plot of estimated average speed versus actual average speed for the training set is shown in Figure 6.35.

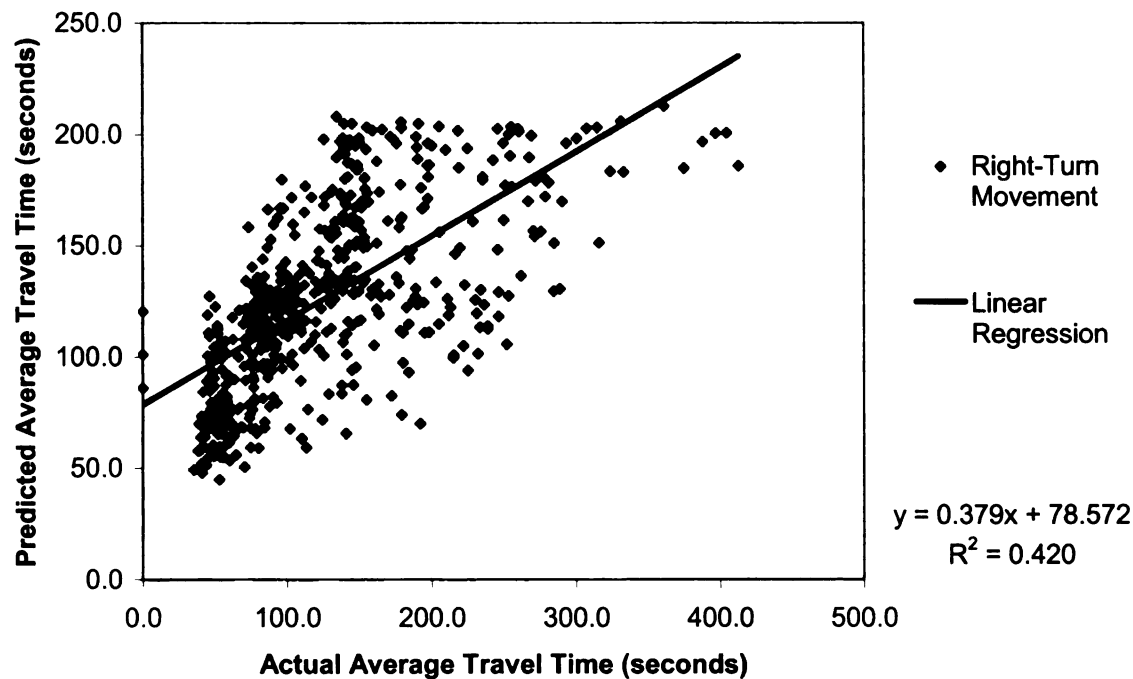


Figure 6.35 – Training Scatter Plot of Actual versus Predicted Travel Time for the Right-Turn Movement.

The R^2 statistic for the training set is .420, which indicates that the average travel time for the right-turn movement is not accurately predicted. The pattern in the dispersion of points is similar to that observed for travel time estimation for right-turns, where a linear pattern can be detected for actual travel times less than 150 seconds. For travel times in excess of 150 seconds, the SSNN model fails to accurately predict travel time for the right-turn movement. A very similar pattern is observed in the scatter plot of estimated

average speed versus actual average speed for the testing set. The testing scatter plot, with an R^2 statistic of .485 is shown in Figure 6.36.

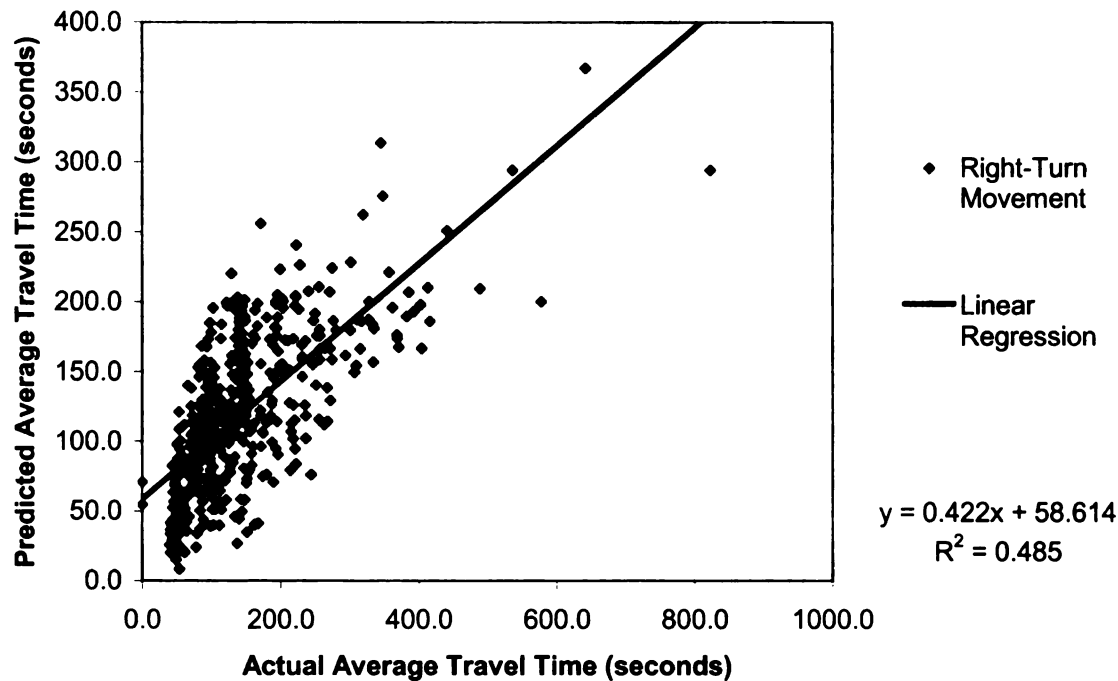


Figure 6.36 – Testing Scatter Plot of Actual versus Predicted Travel Time for the Right-Turn Movement.

The accuracy observed for the testing set is similar to that of the training set, and shows that the model performs equally in traffic conditions other than those used to train the model. Due to variations in the percentage of right-turn movements between intersections and over time though, the accuracy of travel time predictions is not sufficient to support ITS applications. In order to further examine the accuracy of travel time prediction for the right-turn movement, error statistics for the training and testing sets are generated and are displayed in Table 6.9.

Table 6.9 – Travel Time Prediction Error Statistics for the Right-Turn Movement.

	Arterial	MAE (seconds)	RMSE (seconds)	MAPE (%)
Training	<i>6-10</i>	42.4	58.1	34.8
	<i>16-20</i>	31.4	41.4	29.6
	<i>21-25</i>	35.6	48.6	31.5
	<i>3-23</i>	46.7	59.5	37.0
	<i>Average</i>	39.0	51.9	33.2
Testing	<i>6-10</i>	40.2	61.4	28.4
	<i>16-20</i>	40.8	57.2	30.7
	<i>21-25</i>	35.2	54.5	27.8
	<i>3-23</i>	57.3	88.3	34.6
	<i>Average</i>	43.4	65.4	30.4

These statistics reveal significant errors in the travel time predictions derived from both the training and testing sets, with a MAPE of approximately 30 percent. As is stated in the discussion of travel time estimation for right-turns, it is obvious that the variability in right-turns between intersections and over time has a severe impact on the accuracy of right-turn travel time prediction.

Right-turn-on-red maneuvers add to the complexity of travel time prediction for this movement, especially for this experiment where right-turning vehicles share the rightmost lane with through vehicles. During the red interval the presence of only one through vehicle in queue may potentially block vehicles from turning right-on-red, thus increasing travel time for those vehicles. On the other hand, right-turning vehicles that are not blocked by a through vehicle in the rightmost lane experience decreased travel time as they are allowed to progress during the red interval. In congested conditions the complexity of this situation increases due to the volume of crossing traffic, and travel time becomes more unpredictable.

The MAPE for each arterial is broken down by link in order to identify any patterns or specific predictions that may explain significant level of error in travel time prediction for the right-turn movement. The Absolute Percentage Error (APE) is plotted for each arterial link in 5-minute increments for both the training and testing datasets. Figure 6.37 and Figure 6.38 display APE data for major arterial 6-10.

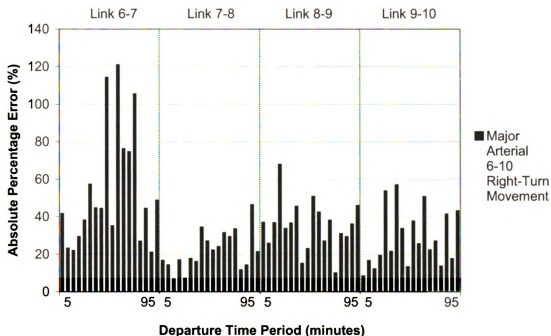


Figure 6.37 – Absolute Percentage Error of Right-Turn Movement Travel Time Prediction for Training Set Arterial 6-10.

The APE for each link comprising arterial 6-10 is at or in excess of 20 percent during most time intervals and on all links for both the training and testing sets. No significant pattern is observed in the APE for this arterial, and the model performs poorly in general for right-turn travel time prediction. The variability in turning movement percentages causes absolute percentage errors in excess of 50 percent in some cases, and in one case the error exceeds the travel time. This level of accuracy is obviously not suitable for

ATMS and ATIS applications, where user confidence in the travel time predicted is highly important.

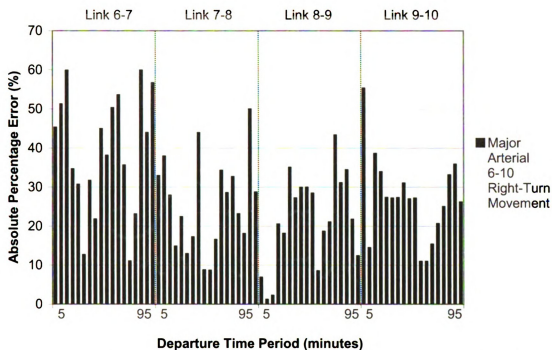


Figure 6.38 – Absolute Percentage Error of Right-Turn Movement Travel Time Prediction for Testing Set Arterial 6-10.

The APE is plotted for arterial 16-20 in Figures 6.39 and 6.40, for arterial 21-25 in Figures 6.41 and 6.42, and for arterial 3-23 in Figures 6.43 and 6.44. The APE is consistently in excess of 20 percent for each link, with an average error near 30 percent. The impact of the errors presented in this section are prevalent in the results for travel time prediction for arterial routes, and are discussed in more detail in Section 7.4.

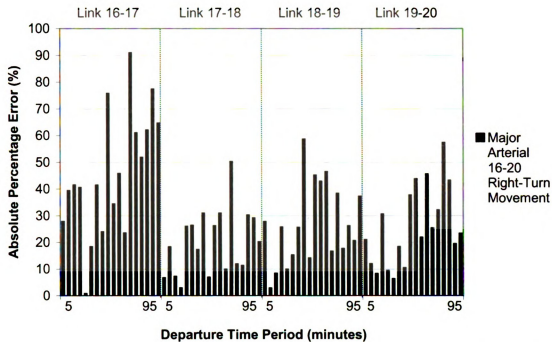


Figure 6.39 – Absolute Percentage Error of Right-Turn Movement Travel Time Prediction for Training Set Arterial 16-20.

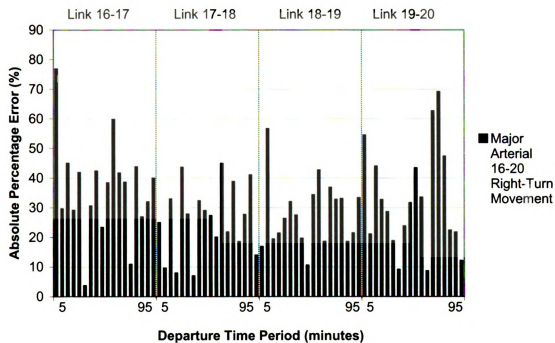


Figure 6.40 – Absolute Percentage Error of Right-Turn Movement Travel Time Prediction for Testing Set Arterial 16-20.

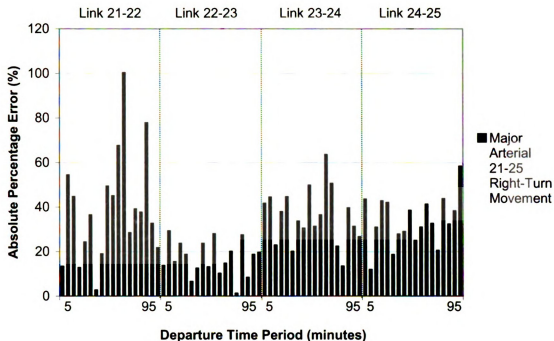


Figure 6.41 – Absolute Percentage Error of Right-Turn Movement Travel Time Prediction for Training Set Arterial 21-25.

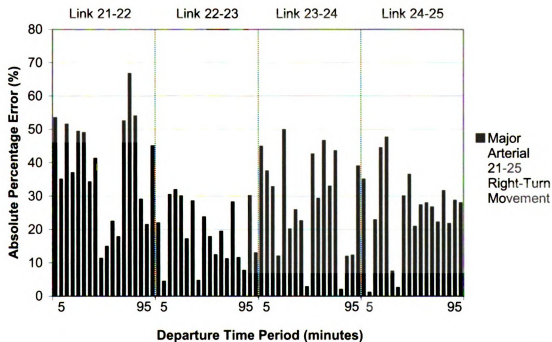


Figure 6.42 – Absolute Percentage Error of Right-Turn Movement Travel Time Prediction for Testing Set Arterial 21-25.

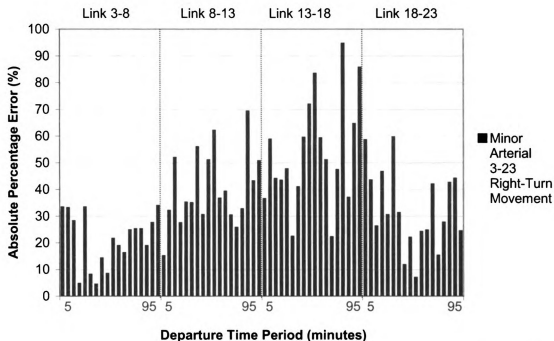


Figure 6.43 – Absolute Percentage Error of Right-Turn Movement Travel Time Prediction for Training Set Arterial 3-23.

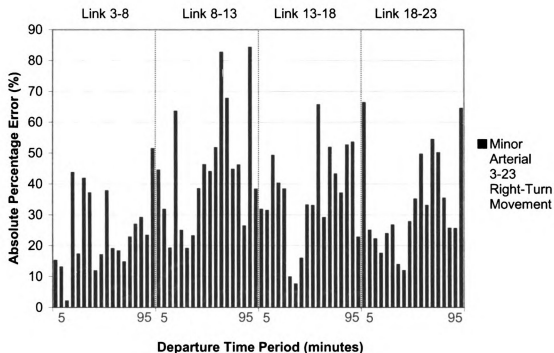


Figure 6.44 – Absolute Percentage Error of Right-Turn Movement Travel Time Prediction for Testing Set Arterial 3-23.

The high level of error associated with travel time prediction for the SSNN-Right model is due to the influence of variable turning movements between intersections and over time. The model does not show the capability to accurately learn the patterns in traffic conditions that are connected to changes in travel time for the right-turn movement. To further explore the performance of the SSNN-Right model, the actual travel time and predicted travel time are plotted together over time. These results for the testing set are shown for each arterial in Figures 6.45, 6.46, 6.47, and 6.48.

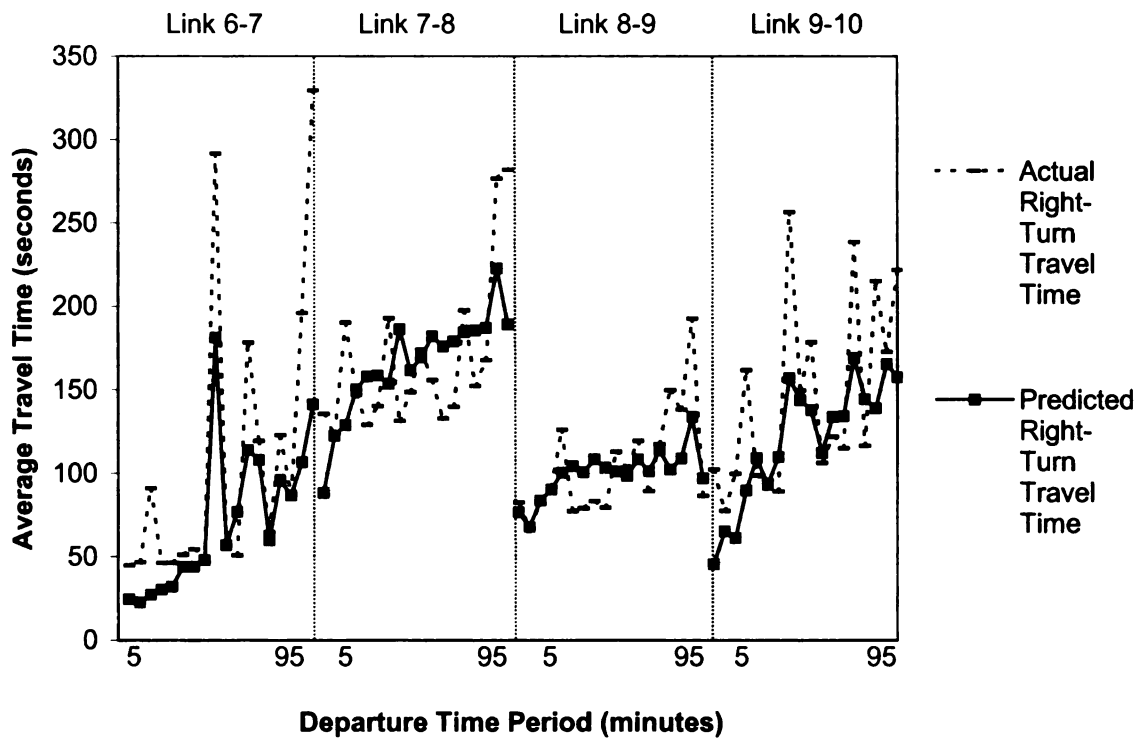


Figure 6.45 – Pattern of Actual versus Predicted Travel Time for Right-Turn Movement on Testing Set Arterial 6-10.

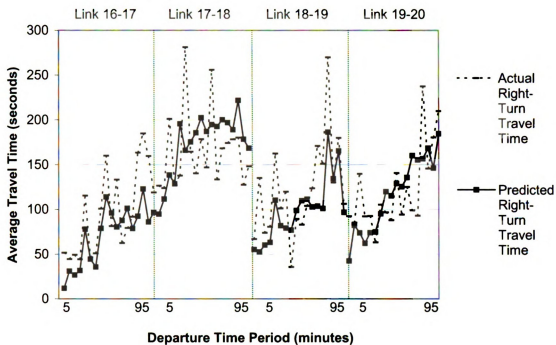


Figure 6.46 – Pattern of Actual versus Predicted Travel Time for Right-Turn Movement on Testing Set Arterial 16-20.

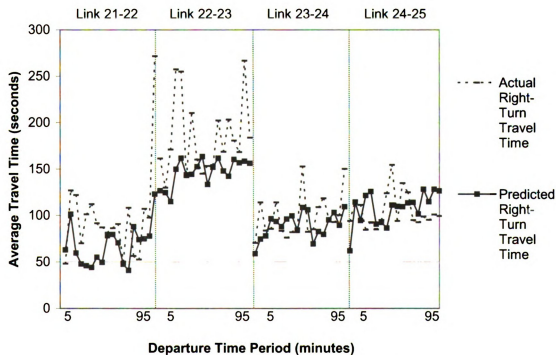


Figure 6.47 – Pattern of Actual versus Predicted Travel Time for Right-Turn Movement on Testing Set Arterial 21-25.

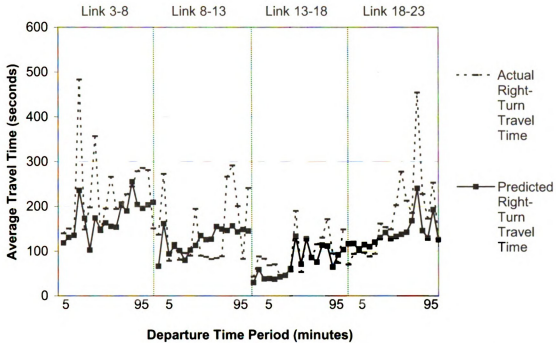


Figure 6.48 – Pattern of Actual versus Predicted Travel Time for Right-Turn Movement on Testing Set Arterial 3-23.

Across each arterial for which right-turn travel time is measured, drastic variations are observed with sharp increases and decreases in actual travel time. The variability of turning movements along with permitted right-turn-on-red and interference from through vehicles causes a highly unpredictable scenario for right-turn travel time. For each arterial link, the pattern of predicted travel time does follow that of the actual travel time in a general sense. However, when sudden changes occur in the actual average travel time, the model is not able to respond adequately. As a result, the actual travel time oscillates higher and lower while the predicted travel time maintains a more uniform slope, with minor oscillations. This is especially seen on arterial 16-20.

In order to improve the predictive capability of the SSNN-Right model, multiple time-steps must be incorporated into the memory of the model. This will allow the model to

store more information regarding the change in travel time due to sudden changes in the state of the arterial link. The model developed in this thesis is unable to react to rapid changes in traffic conditions that are seemingly inherent with right-turn movements under the conditions of the network implemented. The influence of variable turning movements is severe for right-turn travel time prediction, and this influence carries into the accuracy of travel time prediction for arterial routes.

An additional measure that may improve the performance of the SSNN-Right model may be to decrease the duration of the time-step from 5 minutes to 1 minute. This would improve the temporal resolution of the model, and may capture more of the variations observed in right-turn travel time. It is possible that the aggregation of data in 5-minute intervals causes an averaging effect in which finite causes of change in right-turn travel time are lost.

In conclusion of this section, the results observed for the accuracy of travel time prediction for the right-turn movement are compared to the results obtained by Singh (2006) under the assumption of constant turning movement percentages. This comparison is shown in Table 6.8.

Table 6.10 – Mean Absolute Percentage Error Comparison for Right-Turn Movement Under Constant and Variable Turning Movement Percentage Conditions.

		Movement	Constant Turning %	Variable Turning %
MAPE (%)	Training	<i>Left-Turn</i>	9.6	33.2
	Testing	<i>Left-Turn</i>	15.9	30.4

Based on this comparison, the incorporation of variable turning movements is obviously detrimental to the performance of the travel time prediction model for the right-turn movement. The magnitude of the MAPE is 2 to 3 times greater than for the results obtained assuming constant turning percentages. Actual average travel time for the right-turn movement changes rapidly and frequently due to the variability in traffic conditions, and the SSNN model is unable to predict these changes accurately based on the condition of each arterial link in the current time period. The addition of multiple time-steps to the learning process of the model may improve the flexibility and reactive capability of the model. Additional research is needed to identify traffic related variables that better model the dynamic changes in right-turn travel time.

6.4 Travel Time Prediction on Arterial Routes

The performance of travel time estimation and prediction models is examined in great detail in reference to arterial links. The state of traffic on each link influences the travel time on that link, and in congested conditions can impact the travel time on adjoining links. Travel time on an arterial link is the fundamental unit that contributes to the overall travel time along an arterial or arterial route, so the accuracy of the models presented in this thesis are analyzed first at the most fundamental level. In terms of real-world applications though, the utility of travel time estimation and prediction models is in determining the travel time along a route within the network of study. In general, system

users want to know how long it will take to get from origin to destination, not how long it will take to get from intersection to intersection along the way.

In order to analyze the performance of the SSNN-Through, SSNN-Left, and SSNN-Right models in reference to an arterial route, two routes are selected within the network as defined in Figure 5.5 of Section 5.4. The appropriate model is applied to predict the travel time for each arterial link depending on the movement at the downstream intersection approach, and the results are aggregated for the length of the route.

6.4.1 Results of SSNN Travel Time Prediction Models for Arterial Route 16-25

In Figure 6.49 the actual and predicted average travel time for route 16-25 are plotted over time for the duration of the study period. The travel times shown represent the time to traverse the route when departing during the current time interval.

Overall, the predicted travel time follows closely with the pattern of the actual average travel time, especially from a departure time period of 55 to 90 minutes. There are two prominent peaks in the actual travel time that are not well predicted by the SSNN models. In order to gain a better understanding of the cause of the error at departure times of 15 minutes and 30 minutes, a detailed plot of actual versus predicted travel time is generated respective to each link comprising the route. This plot is displayed in Figure 7.50.

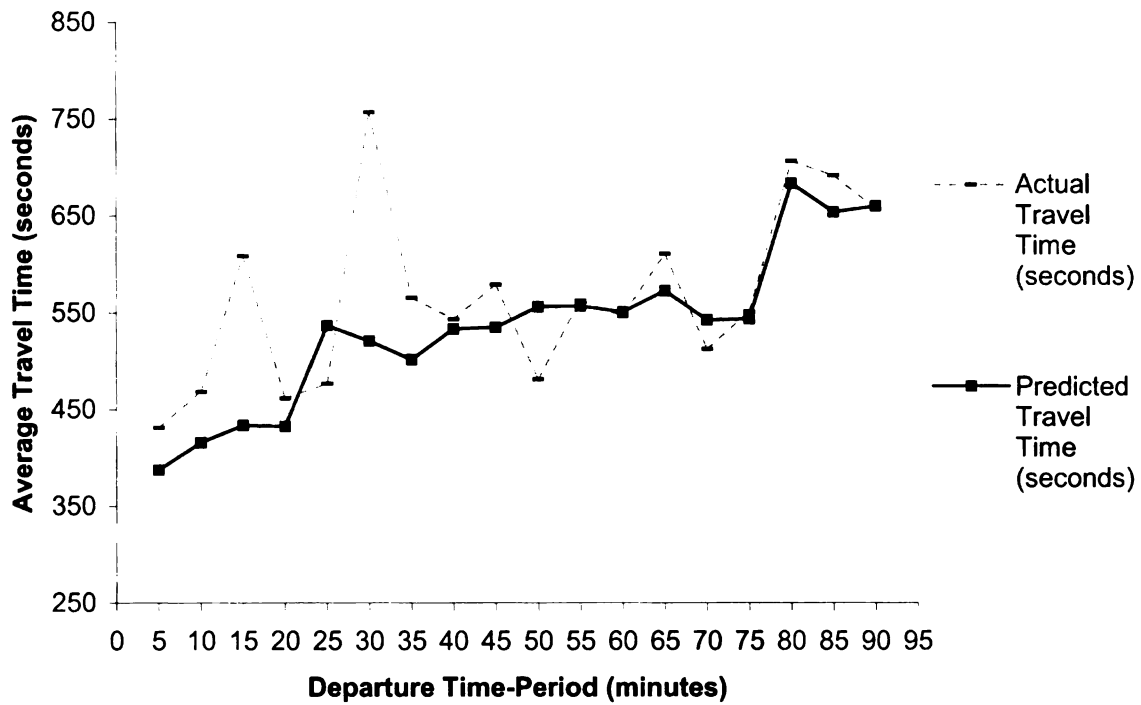


Figure 6.49 – Pattern of Actual versus Predicted Travel Time for Arterial Route 16-25.

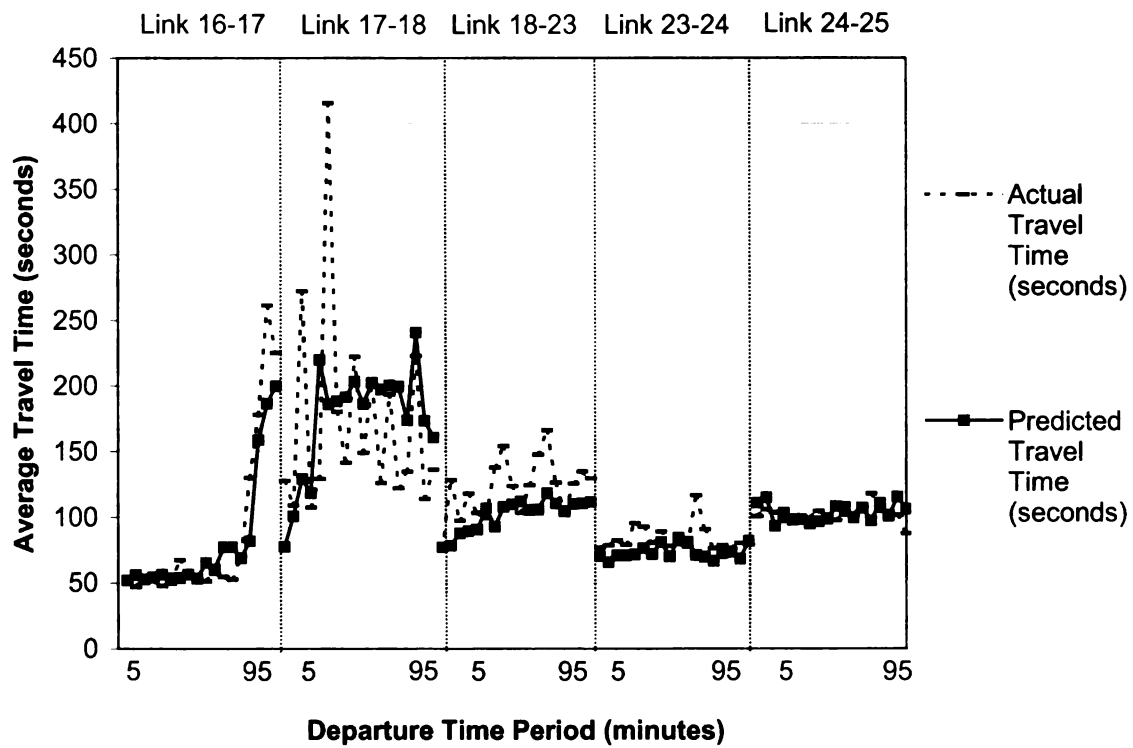


Figure 6.50 – Pattern of Actual versus Predicted Travel Time for Arterial Route 16-25.

In general for each arterial link the predicted travel time follows closely with the actual travel time. This is especially true for links 16-17, 23-24, and 24-25. These links are defined by a through movement along the route, so it is logical following the results observed for the SSNN-Through model that travel time prediction remains accurate for these links. Link 18-23 is defined by a left-turn movement on this route, and the results here follow the general observations for the SSNN-Left travel time prediction model in that the predicted travel time is slightly lower and lags behind changes in the actual travel time. A right-turn movement defines link 17-18, and the actual travel time oscillates while the predicted travel time steadily follows the general pattern with significant error. Moreover, the peaks in the actual travel time observed for link 17-18 correspond to departure times of 15 minutes and 30 minutes. These spikes in actual travel time for the right-turn movement on arterial link 17-18 cause the spikes observed for these departure times in Figure 6.49. Therefore, the error in the travel time prediction for route 16-25 is caused primarily by the error in right-turn travel time prediction.

In analyzing travel time in terms of arterial links significant percentage errors are observed for the left-turn and right-turn prediction models tested in this thesis. More importantly, the error observed in right-turn travel time prediction is seen to propagate into the accuracy of travel time prediction for an arterial route. Despite average errors in excess of 30 percent for the right-turn movement, the mean absolute percentage error for the predicted travel time along route 16-25 is only 8.9 percent. A breakdown in the percentage error for the route by departure time is shown in Figure 6.51.

Given that the average actual travel time for this route is approximately 9.5 minutes, the average error in travel time prediction is 50.5 seconds. For an arterial link that is

approximately 3.5 miles in length, an error in travel time prediction of less than one minute is promising for the application of SSNN prediction models for Intelligent Transportation System applications.

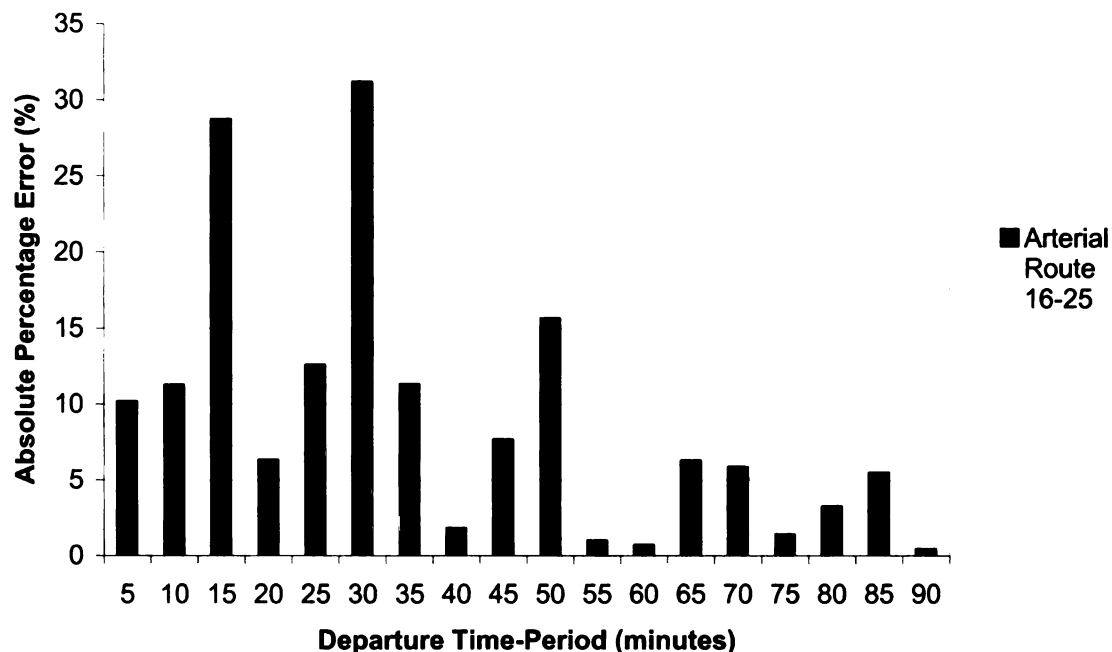


Figure 6.51 – Absolute Percentage Error of Travel Time Prediction for Arterial Route 16-25.

6.4.2 Results of SSNN Travel Time Prediction Models for Arterial Route 16-3

In Figure 6.52 the actual and predicted average travel times for route 16-3 are plotted over time for the duration of the study period. Route 16-3 does not contain any right-turn movements, and there are no significant discrepancies observed between the actual and predicted travel times for the route. The model accurately follows the changes in travel time over the duration of the study period; however, underestimates the travel time as the volume of traffic in the network builds and the actual average travel time increases.

The cause for the underestimation in travel time is seen in Figure 6.53 where the model does not respond to a sudden increase in the actual travel time on link 8-3.

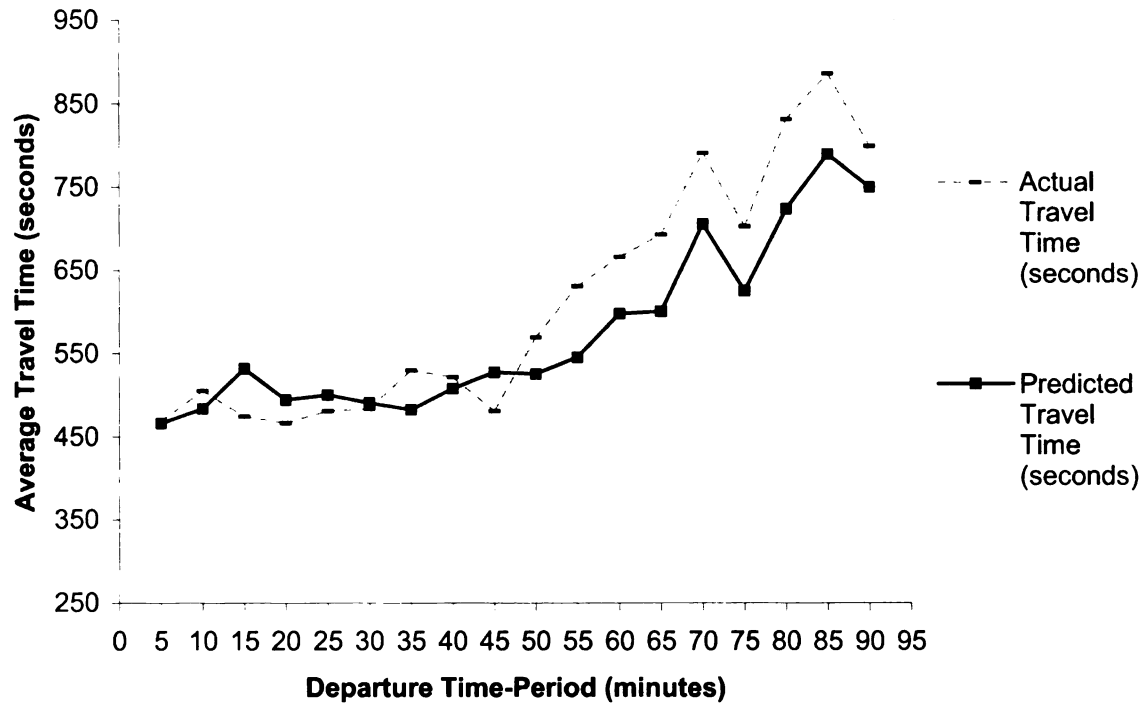


Figure 6.52 – Pattern of Actual versus Predicted Travel Time for Arterial Route 16-3.

The overall MAPE of travel time predictions for arterial route 16-3 is 8.1 percent, which is slightly lower than for arterial route 16-25. This is a positive result that shows the capability of the model to predict travel time equally well on multiple routes. The average percentage error is shown for the route by departure time in Figure 6.54.

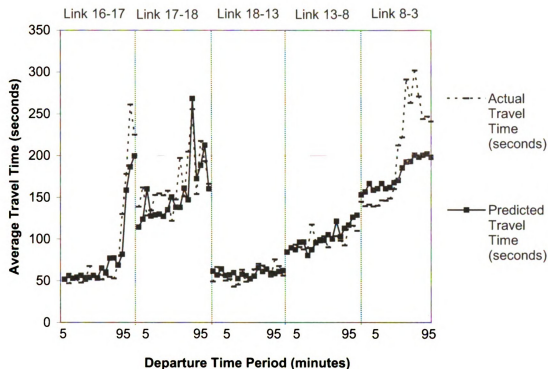


Figure 6.53 – Pattern of Actual versus Predicted Travel Time for Arterial Route 16-3.

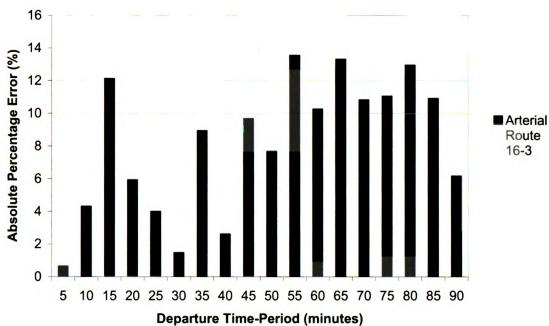


Figure 6.54 – Absolute Percentage Error of Travel Time Prediction for Arterial Route 16-3.

6.4.3 Results of SSNN Travel Time Prediction Models for Arterial Route 15-2

The routes discussed in thus far in this chapter are routes that are comprised of arterial links that are part of the datasets used to train and test the SSNN models. These models have proven here to be accurate within a 10 percent average error in predicting travel time over the length of a route. It is important however, to validate the accuracy of these models on a route that is unique and separate from those used to train the SSNN models. Figure 6.55 depicts arterial route 15-2, which contains a series of through, left-turn, and right-turn movements across a set of arterial links that have not been utilized in the model development procedure.

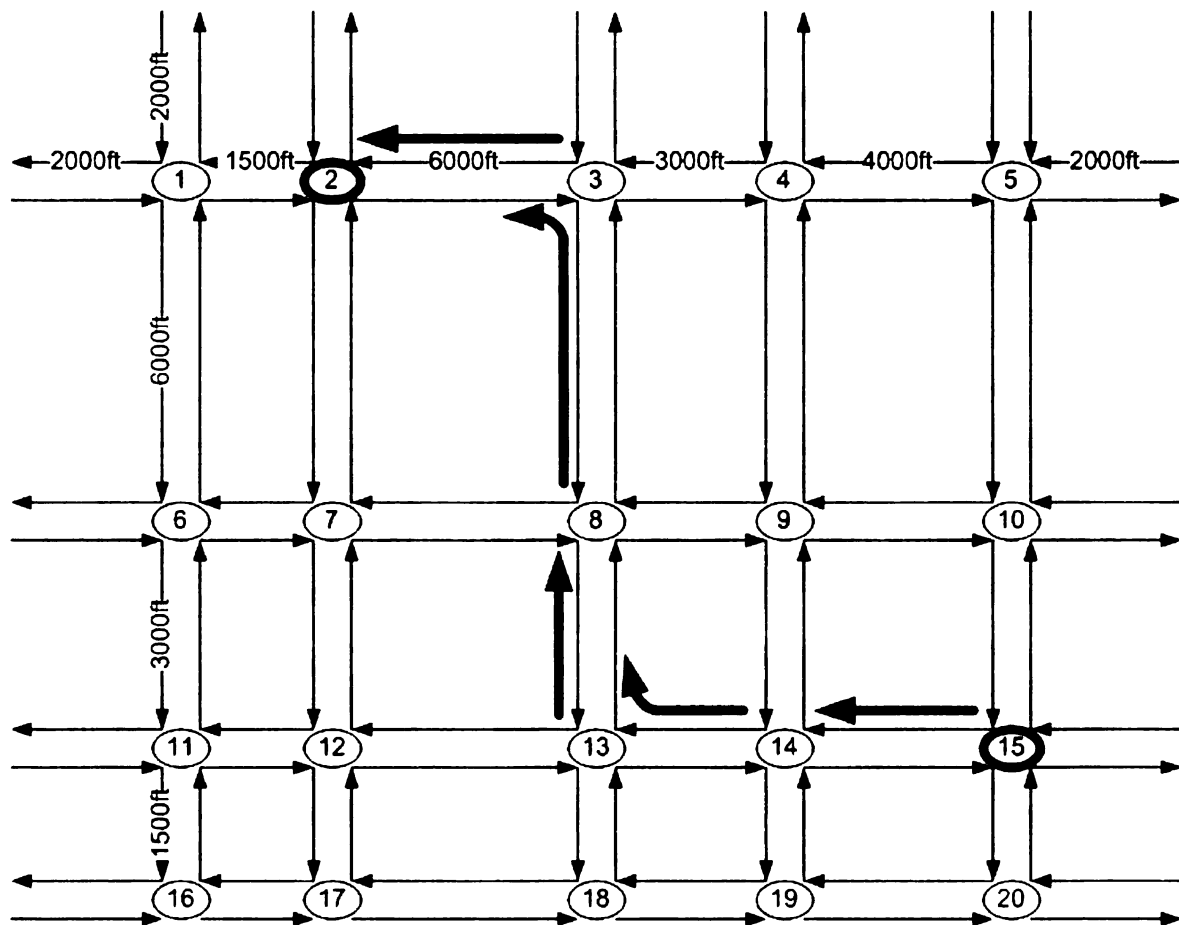


Figure 6.55 – Unique Route for the Validation of SSNN Model Performance.

In Figure 6.56 the actual and predicted average travel times for route 15-2 are plotted over time for the duration of the study period.

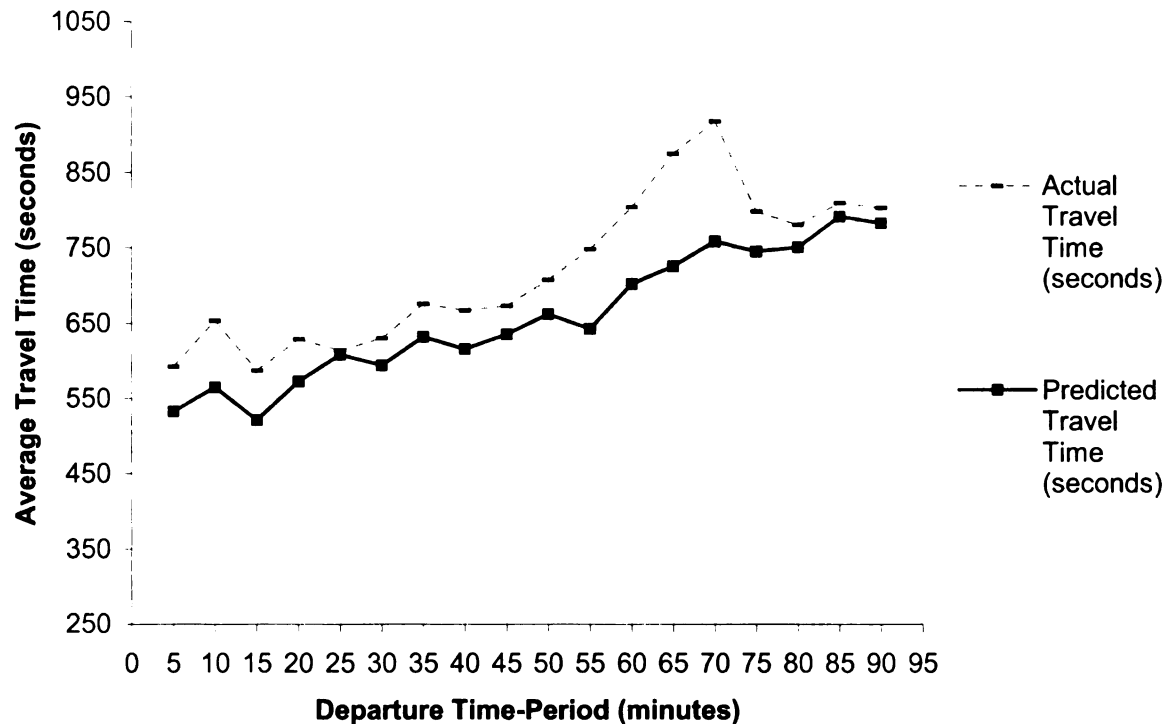


Figure 6.56 – Pattern of Actual versus Predicted Travel Time for Arterial Route 15-2.

For route 15-2 a very similar pattern is observed as for route 16-3, where the predicted travel time increases parallel with the increase of actual travel time. For all cases though, the travel time prediction is below the actual travel time. At a departure time of 70 seconds, the error in travel time estimation for this route is nearly 3 minutes. A more detailed plot of the travel time on each link comprising this arterial route is shown in Figure 5.57. Again, for the link defined by the right-turn movement, link 15-14, the errors in travel time prediction are significant. The difference between predicted and actual travel time for the right-turn movement on link 15-14 causes the error in travel time prediction for the route as a whole.

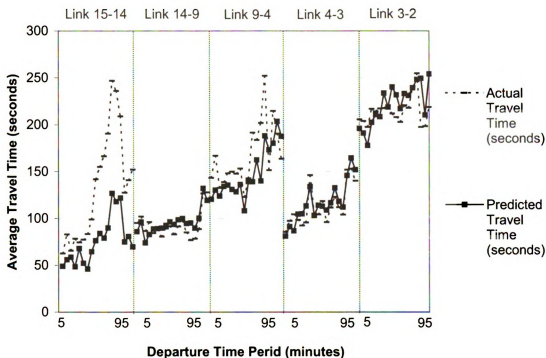


Figure 6.57 – Pattern of Actual versus Predicted Travel Time for Arterial Route 15-2.

Overall, the predicted travel time has a MAPE of 8.5%. It can be concluded that the performance of the SSNN models is validated, as the accuracy of travel time predictions is similar for this case where all arterial links comprising the route are unique to the training and testing datasets used to train the models. However, improvements in the modeling topology are needed to further improve the operation of the models for reliable implementation in ITS technologies, especially in the case of right-turn travel time prediction. The average percentage error is shown for the route by departure time in Figure 6.58.

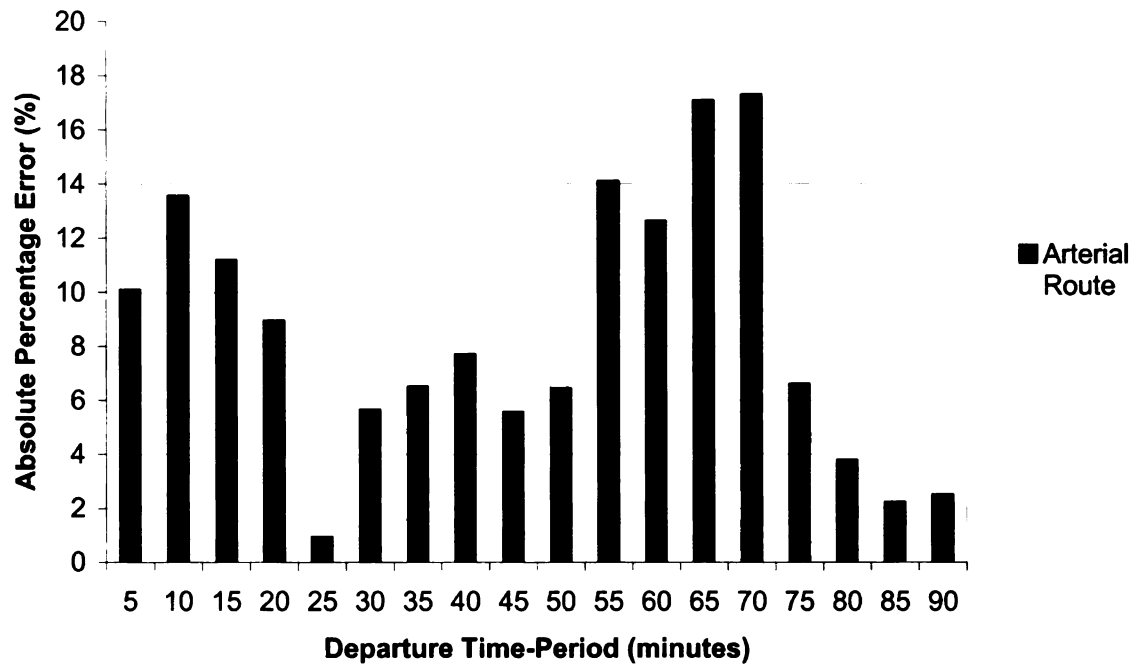


Figure 6.58 – Absolute Percentage Error of Travel Time Prediction for Arterial Route

15-2.

Chapter 7

Conclusions and Future Research

Travel time estimation and prediction are important components of Intelligent Transportation Systems (ITS) applications that communicate travel conditions to system users and administrators. The objective of this thesis is to develop State-Space Neural Network (SSNN) models that accurately estimate and predict travel time for links and routes in a signalized urban arterial network. The research presented is an advancement of the work completed by Singh (2006) to develop such models.

The modeling procedure incorporated in this thesis involves the introduction of variable turning movement percentages to the training and testing of various SSNN models. The operation of signalized intersections in an arterial network is a fundamental determinant of the state of the network. Therefore, it is paramount to consider variations in vehicle turning movements over time and space within the network. The results discussed present findings regarding the accuracy of the models and the influence of variable turning movement percentages on travel time estimation and prediction.

7.1 Key Findings and Conclusions

The significant findings from this research on the influence of variable turning movements on travel time estimation and prediction are as follows:

1. Traffic operations in a signalized urban arterial network are complex and dynamic. Travel time estimation and prediction must be done using modeling techniques that are capable of learning the dynamic relationship between travel time and the state of an arterial link. State-Space Neural Networks have been proven to be effective in capturing non-linear spatiotemporal changes in traffic conditions.
2. Three SSNN models are developed for travel time estimation respective to right-turn, left-turn, and through vehicle movements on arterial links. Three SSNN models for travel time prediction are developed following the same framework including an input layer, a hidden layer, a context layer, and an output layer. The context layer provides short-term memory for the models to learn the dynamic relationship between traffic conditions and travel times for each movement.
3. Travel time estimation and prediction models should be driven by input variables that are easily collected in the field using existing surveillance infrastructure. The findings of this thesis prove that variables such as queue length, average speed, and flow rate are beneficial in travel time estimation and prediction.
4. Data used to train and test SSNN models for travel time estimation and prediction must replicate realistic conditions in an urban arterial environment. Turning movement profiles are not constant within urban arterial networks, and so simulations used to generate traffic related data should incorporate variable turning movements.

5. Variable turning movement percentages have a significant influence on the variability of traffic conditions, and therefore the accuracy of travel time estimation and prediction models.
6. The Mean Absolute Percentage Error (MAPE) for travel times estimated and predicted using the SSNN model framework developed ranges from 9.0 percent for the through movement to 39.1 percent for the right-turn movement. The influence of variable turning movements degrades right-turn travel time predictability such that the right-turn models are not adequate for ITS applications.
7. The MAPE for three arterial routes, including one route that is independent of the datasets used to train and test the SSNN models is between 8.0 and 9.0 percent. Significant positive and negative errors in travel time prediction for arterial links cancel out in some cases over the length of an arterial route. Despite the positive results obtained for arterial route travel time prediction, the errors in link travel time prediction have a significant impact on the reliability of the SSNN models.
8. The pattern of predicted travel times follows that of the actual travel time over the duration of the study period for the through movement. The pattern of predicted travel times for the left-turn movement lags one to two time-steps behind changes in the actual average travel time. This often results in travel time predictions that are lower than the actual travel time. Actual travel times for the right-turn movement are less uniform and more unpredictable. The performance of travel time prediction models for the right-turn movement often does not accurately capture changes in actual travel time.

7.2 Limitations

The limitations of the modeling approach presented in this thesis are as follows:

1. The proposed methodology does not explicitly account for non-recurring traffic influences such as weather and incidents. The SSNN models must be able to adapt to these occurrences in order to be successful in widespread deployment.
2. The travel time estimation and prediction models proposed are developed based on data generated from a microscopic simulation that are not calibrated with actual field data. The implementation of these models in a field test is necessary to evaluate the readiness of the model for real world ITS applications.
3. Vehicles completing a left-turn movement must share the rightmost lane with through moving traffic. The interaction between vehicles coupled with possible right-turn on red movements causes increased variability in actual travel time for right-turns. The intersections in the simulation network do not have right-turn only lanes, which may significantly alter the predictability of right-turn travel time.
4. The intersection control scheme utilized in the microscopic simulation network includes pre-timed signal control only. The variability of actuated signal control is not accounted for, but may be realistic for modern urban arterial networks.

7.3 Scope of Future Research

Based on the findings and limitations of the work presented in this thesis, the following points are recommended to further the success of research in this area:

1. The factors that influence right-turn speed must be better understood and modeled. Research is necessary to determine the impact of right-turn on red permission on right-turn travel time. Additionally, the impact of right-turn only lanes should be investigated.
2. Additional research should be performed to identify additional candidate variables that may improve the accuracy of the SSNN models. There may be additional variables that can easily be collected in the field that are not included in this thesis.
3. State-Space Neural Network models must be advanced to incorporate multiple-step learning. This may improve the ability of the SSNN models to sense and react to rapid changes in traffic conditions.
4. The time-step resolution of the SSNN models should be further researched. Models with a shorter time-step and higher resolution may better capture the variability in travel time caused by variable turning movements.
5. The impact of actuated signal control should be investigated for the accuracy of travel time estimation and prediction models.

APPENDIX

The Appendix presents the MATLAB code for State-Space Neural Network Model. This code is written for travel time prediction of thru movement on arterials. Similar code can be used for other SSNN models changing the parameters.

```
%%%%%%%%%%%%%%%%%%%%%%%%%%%%%%%%%%%%%%%%%%%%%%%%%%%%%%%%%%
display('Prediction of TT Thru');
load traininout.m ;                               %loading input file

P = traininout(:,:);

P = rot90(P,1);

ptr3 = P( 2:10,:);ptr3 = con2seq(ptr3);           % link input
ttr3 = P(1,:);ttr3= con2seq(ttr3);                 % output

for i = 1:576

ptr{1,i} = ptr3{1,i};

end

for i = 1:576

ttr{1,i} = ttr3{1,i};

end

% Loading up State Space Neural Network called here as net1

disp('Loading up network ...');

load net1;

net1 = init(net1);                               % Initializing the network
```

```

% Training Parameters

net1.adaptParam.epochs = 20000;

net1.adaptParam.goal = 0.001;

net1.adaptParam.max_fail = 10000 ;    % Five Validations to check when error rises

net1.adaptParam.mem_reduc = 1;    % Full Jacobian Calculated, no memory restrictions

net1.adaptParam.min_grad = 1e-10;

net1.adaptParam.mu = 0.9;

net1.adaptParam.mu_dec = 0.001;

net1.adaptParam.mu_inc = 10;

net1.adaptParam.mu_max = 1e10;

net1.adaptParam.show = 100;

net1.adaptParam.time = inf;

net1.adaptParam.lr = 0.1;                % Learning Rate

net1.performFcn = 'mse';                % Performance = 'Mean Square Error'

% Training

disp('Training ...');

[net1,tr]= adapt(net1,ptr,ttr);

save net1.MAT net1 ;

%Conversion of ttr to concurrent matrix

ttr = seq2con(ttr);

% Results - Network Training

a2 = sim(net1,ptr);

a2 = seq2con(a2);

```

```

figure(2)

title('Regression Analysis of Training Results: Travel Time Thru'); hold on

[m,b,r] = postreg(a2{1,1},ttr{1,1}); hold off

perftgr1 = mse(a2{1,1} - ttr{1,1})

perftgr2 = mae(a2{1,1} - ttr{1,1})

% Testing the network

load testinout.m;                                %loading testing file

Q = testinout(:,:);

Q = rot90(Q,1);

test3 = Q(2:10,:); test3 = con2seq(test3);

for i = 1:576

test.P{1,i} = test3{1,i};

end

testT3 = Q(1,:);testT3 = con2seq(testT3);

for i = 1:576

test.T{1,i} = testT3{1,i};

end

test.T = seq2con(test.T);

% Results - Network Testing

a3 = sim(net1,test.P);

a3 = seq2con(a3);

figure(5)

title('Regression Analysis of Testing Results: Travel Time Thru'); hold on

```

```

[m,b,r] = postreg(a3{1,1},test.T{1,1}); hold off

perfst1 = mse(a3{1,1} - test.T{1,1})

perfst2 = mae(a3{1,1} - test.T{1,1})

format short;

disp('Network Architecture');

disp('Number of Layers');

disp(net1.numlayers+1);

nneurons = 7;

slayer = size(net1.layers);

for i=1:slayer(1,1)

nneurons=[nneurons net1.layers{i}.size];

end

% forming training and testing output files to save

trgoutttthru = a2{1}';

testoutttthru = a3{1}';

save trgoutttthru.dat trgoutttthru -ASCII -DOUBLE -TABS;           % saving output

in .dat files.

save testoutttthru.dat testoutttthru -ASCII -DOUBLE -TABS;

%%%%%%%%%

```


REFERENCES

- Cambridge Systematics. 2005. *Final Report: Traffic Congestion and Reliability, Trends and Advanced Strategies for Congestion Mitigation*. Cambridge, MA.
- Chen, C., Skabardonis, A., Varaiya, P. 2003. *A System for Displaying Travel Times on Changeable Message Signs*. Transportation Research Board 83rd Annual Meeting. Washington, D.C. January 2004.
- Chen, C., Skabardonis, A., Varaiya, P. 2002. *Travel Time as a Measure of Service*. Transportation Research Board 82nd Annual Meeting. Washington, D.C. January 2003.
- Coifman, B. 2002. Estimating Travel Times and Vehicle Trajectories on Freeways Using Dual Loop Detectors. *Transportation Research, Part A. Policy and Practice*. Vol. 36A, no. 4. p. 351-364.
- Elman, J. 1990. Finding Structure in Time. *Cognitive Science*, Vol. 14, pp. 179-211.
- Haykin, S. *Neural Networks: A Comprehensive Foundation*. 1999. Prentice-Hall, Upper Saddle River, N.J.
- ITS Joint Program Office. 2005. *Tracking the Deployment of the Integrated Metropolitan Intelligent Transportation Systems Infrastructure in the USA: FY2004*. Federal Highway Administration. Washington, D.C.
- Kantowitz, B., Hanowski, R., and Kantowitz, S. 1997. Driver Acceptance of Unreliable Traffic Information in Familiar and Unfamiliar Settings. *Human Factors*. Vol. 39. no. 2. p. 164-177.
- Kutner, M.H., Nachtsheim, C.J., Neter, J. 2004. *Applied Linear Regression Models*. McGraw-Hill/Irwin. New York. USA.
- Lin, W., Kulkarni, A., and Mirchandani, P. 2003. *Arterial Travel Time Estimation for Advanced Traveler Information Systems*. Transportation Research Board 82nd Annual Meeting. Washington, D.C. January 2003.
- Liu, H., van Zuylen, H., van Lint, H., Salomons, M. 2006. Predicting Urban Arterial Travel Time with State-Space Neural Networks and Kalman Filters. *Transportation Research Record*. Vol. 1968. p. 99-108.
- Mark, C. D., and Sadek, A.W. 2004. Learning Systems for Predicting Experiential Travel Times in the Presence of Incidents: Insights and Lessons Learned. In *Transportation Research Record: Journal of the Transportation Research Board*, No. 1879, TRB, National Research Council, Washington, D.C., pp. 51-58.

- May, A. 1990. *Traffic Flow Fundamentals*. Prentice Hall. Englewood Cliffs, NJ.
- Mineta, N. 2006. *National Strategy to Reduce Congestion On America's Transportation Network*. United States Department of Transportation. Washington, D.C.
- Park, D., and Rilett, L. 1999. Forecasting Freeway Link Travel Times with a Multilayer Feedforward Neural Network. *Computer-Aided Civil and Infrastructure Engineering*. Vol. 14. p. 357-367.
- Planug Transport Verkehr (PTV). 2005. VISSIM 4.10 User Manual. Germany.
- Quin, Xiao. 2006. *Traffic Flow Modeling with Real-Time Data for On-Line Network Traffic Estimation and Prediction*. Diss. University of Maryland, College Park, MD. UMI, 2006. 3495.
- Rivals, I., Personnaz, L. 1996. Black-Box Modeling with State-Space Neural Networks. In *Neural Adaptive Control Technology*, R.Zbikowski and K.J. Hunt eds., World Scientific, pp. 237-264.
- Roess, R., Prassas, E., McShane, W. 2004. Traffic Engineering, Third Edition. Pearson Prentice Hall. Upper Saddle River, NJ.
- Schrank, D., Lomax, T. 2005. The 2005 Urban Mobility Report. Texas Transportation Institute, The Texas A&M University System. <http://mobility.tamu.edu>.
- Singh, A. and Abu-Lebdeh, G. 2007. *State Space Neural Networks for Travel Time Predictions in Signalized Networks*. Proceedings of the 86th Annual Transportation Research Board Meeting, DC.
- Singh, A. and Abu-Lebdeh, G. 2006. Conditional Independence Graph-based State-Space Neural Network Modeling for Short-Term Travel Time Prediction on Urban Arterials. *Artificial Neural Networks in Engineering (ANNIE)*, Vol. 16. pp. 419-424.
- Sisiopiku, V.P., Roupail, N.M, and Santiago, A. 1994. Analysis of Correlation between Arterial Travel Time and Detector Data from Simulation and Field Studies. In *Transportation Research Record: Journal of the Transportation Research Board*, No. 1457, TRB, National Research Council, Washington, D.C., pp. 166-173.
- Transportation Research Board. 2000. *Highway Capacity Manual*. National Academy of Sciences. Washington, D.C.
- van Lint, J.W.C. 2004. Reliable Travel Time Prediction for Freeways. PhD Thesis. Delft University Press, Delft, The Netherlands.

van Lint, J.W.C., Hoogendoorn, S.P., and Van Zuylen, H.J. 2002. Freeway Travel Time Prediction with State-Space Neural Networks: Modeling State-Space Dynamics with Recurrent Neural Networks. In *Transportation Research Record: Journal of the Transportation Research Board*, No. 1811, TRB, National Research Council, Washington, D.C., pp. 30-39.

Wiedemann, R. 1974. Simulation des Straßenverkehrsflusses. Technical report, Institut für Verkehrswesen. Universität Karlsruhe, Karlsruhe, Germany.

MICHIGAN STATE UNIVERSITY LIBRARIES



3 1293 02956 2026